Author:
Kozlowski, Michal

Title:
Robust and Efficient Residential Indoor Localisation for Healthcare

Robust and Efficient Residential Indoor Localisation for Healthcare

By

MICHAŁ KOZŁOWSKI

Department of Electrical and Electronic Engineering
UNIVERSITY OF BRISTOL

A dissertation submitted to the University of Bristol in accordance with the requirements of the degree of DOCTOR OF PHILOSOPHY in the Faculty of Engineering.

JANUARY 2020

Abstract

This thesis contains a treatise on residential indoor localisation for pervasive health monitoring. Contained therein, are all of the aspects to consider, when developing an indoor positioning system. This work encompasses the evaluation of various popular sensor modalities, which are currently popular amongst the community. In addition, it considers the possible space for fusion combinations between said sensors, clearly displaying the current preferences of said community with respect to pressing application challenges, which include accuracy, efficiency and robustness. It also presents a novel dataset, which aims to address the lack of high resolution localisation data in the wider literature. The dataset comprises of a number of real residential houses, parametrised and prescribed using popular methods relating to Radio Frequency fingerprinting. Following this dataset, the thesis focuses on various issues pertaining to training and parametrisation, especially in relatively constrained spaces of residential abodes. It proposes a novel system which alleviates all of the above issues and provides an improvement on the overall data collection and training tasks, through Simultaneous Localisation and Mapping in the service of Radio Frequency fingerprinting.

The thesis then addresses the most important community challenges, by suggesting novel algorithms and methodologies aiming to mitigate their effects. In order to improve robustness and accuracy, a study is performed, which fuses Radio Frequency and Accelerometer data. Results demonstrate, that activity information is beneficial in face of network adversity, in addition to accuracy improvement and information about the well-being of the participant. The following study of adaptive sensor utilisation techniques through Reinforcement Learning, focuses on accuracy and efficiency of Wireless Sensor Networks. This work shows, that when presented with sensors of varying degree of efficiency, such as wearables and cameras, the system is able to perform weak training, over the lifetime of the infrastructure, whilst at the same time making the system energy aware. This helps the system to remain relatively maintenance free and unobtrusive for potential patients. Finally, in order to alleviate the issues concerning robustness and efficiency, this thesis will present an examination of efficient sensor selection methods in a Wireless Sensor Network environment. It confirms, that there exist a finite number of sensors which provide near-optimal service for indoor localisation. The results also suggest that data from real world measurements is best to benchmark this type of challenges, as opposed to toy examples. The thesis then summarises all of the above work, and provides indicators for possible future research avenues.

Dedication and acknowledgements

I would like to acknowledge a myriad of people who made this thesis possible. Due to lack of space, and for the sake of brevity, it pains me to say that I will have to constrain myself to a mere subset. First and foremost perhaps, I'd like to extend my thanks to my supervisory team, Robert Piechocki and Raúl Santos-Rodríguez, who provided much needed direction in the beginning and remained committed to this project throughout the last 4 years. Thanks also to Ian Craddock for the opportunity to become part of, and leave my mark at the Digital Health Engineering in Bristol. This work was supported by EPSRC and SPHERE IRC, grant number EP/K031910/1.

A massive thank you to the entire SPHERE IRC and Digital Health Engineering team, as varied as it was through the years. Shout-out to Ryan and Niall for enduring my countless, unrelenting questions and lending their ears in trying times, I really appreciate it. A separate thank you to Dallan, who helped shape me into an effective researcher. Could not have done it without your help!

A big, big thanks to my sister Kasia and her partner Jamie for helping me through some of the tough times, as well as always supporting me with reason and wisdom. You guys showed me what was possible with hard work and dedication. You are my MVPs.

Chciałem także podziękować reszcie brystolskiej trójcy doktorantów-muszkieterów, Marcie i Pawłowi, którzy razem ze mną nawigowali kwerendę i naukę, i bez których nie byłoby tego tekstu. Dzięki też wszystkim w naszej małej Poloni brystolskiej!

Podziękowania również należą się moim rodzicom i rodzinie, która zawsze mnie dopingowała i chciała żeby mi wyszło jak najlepiej. Bez was, nigdy nie udałoby mi się tego osiągnąć. Dziekuję wam bardzo, za motywację i pomoc!

I na sam koniec, bardzo szczere podziękowania dla mojej Natalii, która stała ze mną przez wszystkie te lata, oświetlając mi drogę i pozwalała zobaczyć dlaczego to wszystko robię.

To dla Ciebie.

AUTHOR'S DECLARATION

I declare that the work in this dissertation was carried out in accordance with the requirements of the University's Regulations and Code of Practice for Research Degree Programmes and that it has not been submitted for any other academic award. Except where indicated by specific reference in the text, the work is the candidate's own work. Work done in collaboration with, or with the assistance of, others, is indicated as such. Any views expressed in the dissertation are those of the author.

SIGNED: ..... DATE: .....

Table of Contents

List of Tables

List of Figures

Figure **Page**

List of Symbols and Abbreviations

Abbreviations

AMF Ambient Magnetic Field

ANN Artificial Neural Networks

AoA Angle-of-Arrival

AOD Angle-of-Departure

AP Access Point

AWGN Additive White Gaussian Noise

BF Brute Force

BLE Bluetooth Low Energy

CCD Charge Coupled Devices

CMOS Complementary Metal-Oxide-Semiconductor

CSI Channel State Information

DNN Deep Neural Networks

DoF Degrees of Freedom

DR Dead Reckoning

EKF Exteded Kalman Filter

EM Electro-magnetic

ES Environmental Sensors

FOV Field of View

GBF Greedy Brute Force

H4LO Helmet for Localisation Optimisation

HMM Hidden Markov Model

HRL High Resolution Localisation

IMU Inertial Measurement Unit

INS Inertial Navigation Systems

IoT Internet-of-Things

IPS Indoor Positioning Systems

k-NN k-Nearest Neighbours

KF Kalman Filter

KL Kullback-Leibler

KL-MI Kullback-Leibler - Mutual Information

LDA Linear Discriminant Analysis

LED Light Emitting Diode

LiDAR Light Detection and Ranging

LoS Line-of-Sight

MDP Markov Decision Process

MEMS Micro-Electro-Mechanical Systems

MI Mutual Information

MIMO Multiple-Input Multiple-Output

MMIMO Massive Multiple-Input Multiple-Output

mRMR Minimum-Redundancy Maximum-Relevance

NLoS Non-Loss-of-Sight

NTP Network Time Protocol

PCB Printed Circuit Board

PDR Pedestrian Dead Reckoning

PF Particle Filter

PIR Pyroelectric Infrared

QDA Quadratic Discriminant Analysis

RF Radio Frequency

RFID Radio Frequency Identification

RGB-D Red Green Blue - Depth

RL Reinforcement Learning

RPi Raspberry Pi

RSS Received Signal Strength

RSSI Received Signal Strength Indicator

SARSA State-Action-Reward-State-Action

SLAM Simultaneous Localisation and Mapping

SMC Sequential Monte Carlo

SURF Speeded Up Robust Features

TDoA Time-Difference-of-Arrival

ToA Time-of-Arrival

TR Time Reversal

UAV Unmanned Aerial Vehicle

UWB Ultra Wide-band

VLC Visible Light Communication

VLP Visual Light Positioning

VR Virtual Reality

WSN Wireless Sensor Networks

Symbols

α Learning rate

π^* Optimal policy

$\dot{\boldsymbol{x}}$ Kalman state vector

$\hat{\boldsymbol{L}}$ Vector of estimated location states

$\boldsymbol{B}$ Kalman input matrix

$\boldsymbol{C}$ Set of all LiDAR scans

$\boldsymbol{c}$ Specific Discrete scan

$\boldsymbol{F}$ Kalman state matrix

$\boldsymbol{H}$ Kalman observations

$\boldsymbol{L}$ Vector of groundtruth location states

$\boldsymbol{L}^*$ Vector of shortest path length

$\boldsymbol{M}$ Map

$\boldsymbol{r}$ Specific discrete location

$\boldsymbol{u}$ Kalman control input

$\boldsymbol{v}$ Kalman process noise

$\boldsymbol{z}$ Kalman output vector

ϵ ϵ-Greedy selection parameter

Γ Weak oracle labels

γ Discount factor

$\hat{l}$ Single estimated location state

λ Hidden Markov Model parameters

$\mathscr{L}$ Likelihood

$\mathscr{O}$ Arbitrary sensor observations

$\mathscr{X}_{\sigma}$ Zero-mean Gaussian Random Variable with Standard Deviation σ

ω Kalman measurement noise

ϕ Transformation in $theta$

ψ Performance dependent reward boost

τ Softmax temperature parameter

Ξ Sequence of states

ξ Transformation vector

A MDP Action space

Acc Sampled accelerometer features

B Arbitrary Sensor subset

b Reference Distance [m]

d Number of dimensions

F,D Arbitrary random variables

f,d Arbitrary normal distributions

i Node index

l Single groundtruth location state

P MDP Transition kernel

Pa Node parents

PL	Measured Path Loss Signal Strength [dBm]
Q	State-Action value matrix
R	Reward function
S	MDP State space
V	Arbitrary Sensor superset
v	Log-odd probability of occupancy
w_x	Transformation in x
w_y	Transformation in y
x	Arbitrary Bayesian node
z	Arbitrary observation
a	Specific action from MDP action space
B_X	Magnetic Field T
F_W	Lorenz Force
G	Set of AP Sensors
I	Current A
K	Number of time bins
k	AP index
L	Total number of discretised states
l	Discretised state
N	Size of time window
n	Number of experiment repetitions
q	Total number of packets
r	Number of valid packets

RSS Sampled RSS

s Specific state from MDP state space

W_Z Length of the Wire m

Y Inferred activity

CHAPTER 1

INTRODUCTION

Due to the steadily improving performance and decreasing cost of wearable devices, the innovative use of various on- and off-body sensors, along with novel methods for their networking, has become widely prevalent. In the domain of pervasive health monitoring, the space of sensor-driven applications is vast [46, 154, 155, 210, 225]. Some examples include pervasive sensor networks [225] bespoke sociometric wearables, [154] and IoT-specific applications [46]. The utilisation of numerous sensors, either exclusively or in unison, serves to monitor the health status of patients from their own comfort zone [46, 225]. Amongst the many healthcare-centric applications of wireless sensor networks, indoor localisation has been cited as an important indicator of recovery in patients [206]. The tracking and positioning of patients in their own abode can provide valuable information for clinicians, which would be difficult to obtain, even under constant hospital care. More importantly however, the patients are able to return to their homes, alleviating the burden on the health service, and depending on the case, minimising the risk of post-procedural complications stemming from the hospital environment.

In this thesis, the challenge of indoor localisation is approached from the perspective of sensor networks for residential environments. The scope covered by this work ranges from system training and deployment through robustification and efficiency to network streamlining. All of the above is constrained by the question of whether Indoor Positioning Systems (IPS) can be robustified cheaply, reliably and without overhead, by utilising diverse sensor modalities in a novel way. We aim to identify the possible shortcomings

associated with residential localisation and propose numerous improvements to said networks and their governing algorithms, all underpinned by the context of pervasive health and recovery monitoring.

1.1 Problem Statement

Indoor localisation is frequently addressed in wireless networking literature. There exist numerous implementations dedicated to tracking and positioning a participant in an indoor environment [24, 73, 157, 230]. Each implementation uses a unique combination of sensors and state-of-the-art algorithms, in order to estimate position in Euclidean space. This is done, either by training an automated model which later provides a prediction, so called fingerprinting, or by calculating the position of the participant outright, based on previous estimate route and the current sensor reading.

The application space of localisation systems is broad. Examples of few such applications range from, but are not limited to, residential abodes [24], commercial shopping malls [216], industrial halls and factories [94], hospitals [83] and natural formations, such as underwater caves [131]. In this thesis, the main function of the localisation system is to estimate the location of occupants of residential abodes as part of their recovery efforts and general monitoring of their well-being.

1.1.1 Motivating Example

Consider an example of a patient exhibiting signs of early-onset dementia. An immediate symptom of this disease includes a decrease in overall cognitive function [211]. Early-onset implies its emergence in people below 65 years of age. In addition to a cause for major concern for the sufferer, diagnosis of early-onset dementia can also yield far-ranging societal consequences, as they are still within the working age bracket of the population. This illness would prevent them from leading a 'normal' life and would instead force them to rely on either the health service or their close relatives for care. As time progresses, the cognitive function of the sufferer would rapidly diminish [211].

Clinicians can utilise indoor localisation technology to obtain information about the progression of the illness, while simultaneously analysing the same data to care for their patients [22, 206]. Studying patterns of indoor navigation was found to be a good metric to use, when inferring or determining health status in patients, as it can provide information about the patient's habits and their inconsistencies. This is especially true

if the patient has been involved in a longitudinal monitoring study, where long-term patterns are analysed and extracted. By recognising these patterns in learned behaviour from various sensor sources, the anomalies can be quickly uncovered and flagged for further analysis [22]. This can directly notify the clinician of the progress of the illness and help choose the appropriate treatment measures.

Localisation can also be used as a quick alert system, especially when coupled with various other sensor modalities [22]. With decreasing cognitive function, the patient would additionally exhibit confusion, forgetfulness and inattention [211]. In an environment where the patient is well cared for, the consequences of these symptoms can be directly rectified by the carers. However, in the case where the patient is alone, these type of issues can have a dire outcome. With anything from gas stoves, heating and opening front doors, dementia sufferers remain at risk of injury, harm or outside adversity. Through pervasive health localisation and monitoring system, these problems can be alleviated, by either notifying a caregiver or acting to redress them directly.

These types of implementations would therefore help care for the patient by helping them to retain a degree of autonomy in their everyday life with developing dementia. However, in order to make this system viable, it would have conform to a number of design decisions. Most importantly, it would have to be tailored to fit an individual's nature, making it as unobtrusive as possible [225]. With recent advances in MEMS fabrication and cost, the sensors which are used for this type of monitoring are becoming increasingly more affordable. These sensors, when coupled with current interests and trends of machine learning and automation community, are already creating implementations of these systems at a cheap cost and proven reliability [43, 225].

Out of many possible infrastructures fit for a pervasive sensing system, the one that is conformant to the above design choices is a Wireless Sensor Network (WSN). In this thesis we consider an implementation which relies on Received Signal Strength (RSS) indication, as a measure of relative 'distance' between network nodes. There exists a body of literature dedicated to this particular sensing domain [11, 24, 30, 195]. In terms of WSNs, the nodes are usually referred to as Access Points (AP), which, normally, remain undisturbed over the lifetime of the system. The participant carries a transmitter node on their body, which registers the signal strength as they move through the environment. The relative difference in signal strength from numerous Access Points as seen in different positions in the environment, is then used to perform a position estimation task [30, 100]. Figure 1.1 shows how signal strength, from a single AP, can vary in different locations in the house.

Using Fig. 1.1 as example, consider how signal is able to propagate through a residential environment. The colour gradient specifies the signal strength. The blue square is the Access Point, using which the strength is measured. The black squares show the tessellated environment. Notice how the gradient decreases, approximately with distance.

1.1.2 Challenges

Whilst indoor positioning and navigation methods remain a very popular topic amongst researchers [11, 24, 100], the fundamental question of a reliable and accurate indoor positioning system in a GPS-denied environment has not been fully addressed yet. There exist implementations spanning from purely inertia-driven, such as Pedestrian Dead Reckoning (PDR) [213], through to intricate infrastructures of various sensors, such as radio, inertia and ambient magnetic fields strength devices working in unison [26]. This relatively broad range of applications and implementations is, in part, due to an equally large application space in which these systems are used. The systems relying on WSN are also known to be subject to a variety of trade-offs. These are summarised below:

- Wireless Sensor Networks can experience gaps in service, rendering network nodes inoperable. This can happen due to noise, environment obstacles or outside adversity.

- Approaches which utilise popular machine learning models, whilst very popular, are notoriously difficult to train. This can be shown in Figure 1.2, where the author is pictured wearing specialised labelling hardware. Additionally, without periodic re-training, they remain susceptible to environment dynamicity causing performance degradation.

- Sensors generate inherent noise. In order to reduce this noise, corresponding increase in power is needed. The trade-off between noise and accuracy is particularly evident in low-power applications.

- Many implementations reporting very good results rely on elaborate infrastructures, which in turn draw considerable power. This is especially true when these systems are deployed to last over long periods of time.

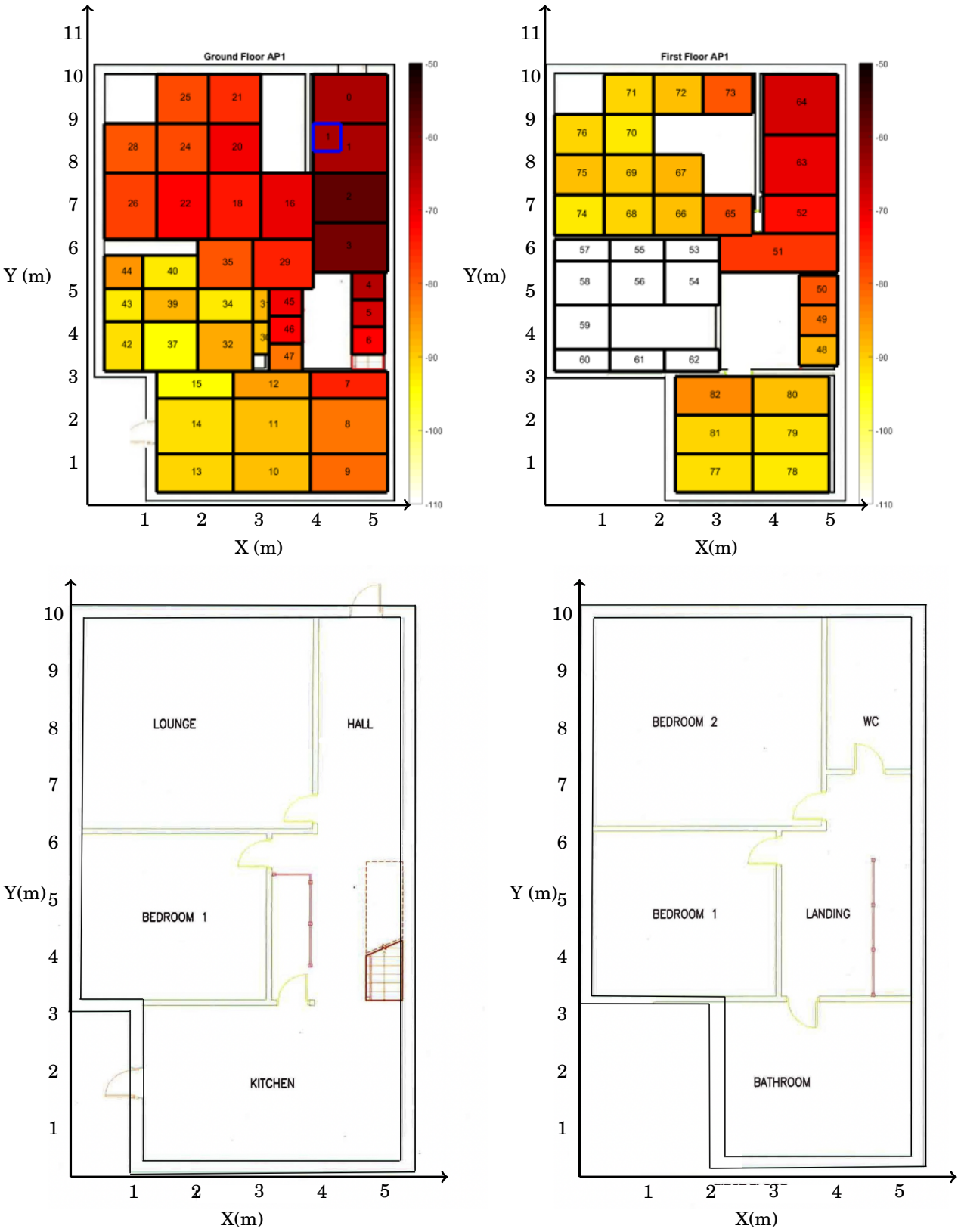

Figure 1.1: Above: Example of a resulting RSS heat map in a two-storey house discretised into states. **Below**: Corresponding floor plan.

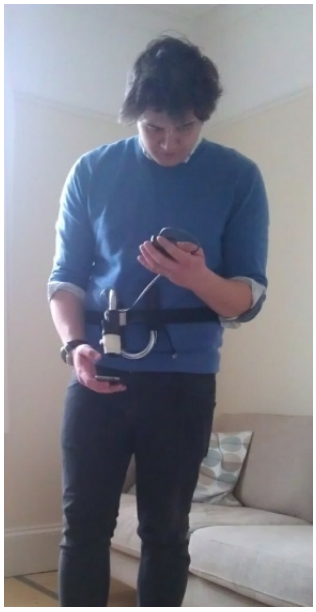

Figure 1.2: Author during data collection.

- Some of the systems found in literature can be considered obtrusive and unrealistic in terms of their implementation, depending instead on sterile conditions of a laboratory [21, 241].
- The costs associated with the system deployment are often omitted from localisation literature. These costs can be related to labour, energy consumption or simply the commercial cost of the hardware.

Through novel utilisation techniques of various sensors available in a specially adapted pervasive sensor network, this thesis aims to address the above shortcomings. Firstly, we identify the gaps in literature of sensor-driven indoor localisation and their fusion. We then evaluate existing datasets, and provide our own localisation set for residential indoor localisation using cheap, off-the-shelf hardware. We also consider the use of specially adapted hardware as well as state-of-the-art optimisation techniques as a way of reducing the overhead associated with training. Finally, we aim to reduce the dependence on single sensor modalities through fusion, and make the system energy-aware as to cut down on the power expenditure over the system's lifetime.

1.2 Thesis Outline and Contributions

The thesis is outlined as follows:

In Chapter 2 we give a detailed overview of the state-of-the-art methods, popular within the current literature. We consider various sensor modalities, and their fusion, in the service of indoor localisation. The importance of accurate and efficient location estimation and tracking is widely understood. Robustification of indoor localisation systems is an important consideration, especially if a given system's design necessitates steady performance under adverse conditions. However, localisation-specific sensor choices, utilisation and fusion methods are seldom reviewed. Localisation is largely case-specific and as such, the taxonomy of sensors used by the community is broad. The intent of this review is to take account of this taxonomy and to provide a wider understanding of the current state-of-the-art methods. In addition, we outline the popular fusion and integration techniques and discuss how their combinations can help in various environments. We scrutinise the sensor choice under a number of metrics, such as energy efficiency, resilience and ease of deployment.

Then, in Chapter 3, we consider the novel data collected as part of this thesis. Firstly, we outline the infrastructure and system which makes the collection possible. This infrastructure was thoroughly tested by the author. We present the raw data, as produced directly from the type of sensors included in this infrastructure. Then, we present a pervasive indoor localisation dataset collection, performed in a number of different residential abodes around Bristol. This particular dataset considers Received Signal Strength and accelerometer sensor readings, with high resolution location and activity labels. This dataset serves as the foundation for the analysis and algorithms within this thesis. This chapter also takes account of the encountered challenges and problems, which render this type of collection arduous.

Chapter 5 aims to compliment the above methods through novel data collection hardware. Learning from the challenges posed by fingerprinting, we consider a low-cost system designed to cut down on the labour by utilising an off-the-shelf Light Detection and Ranging device. This system performs Simultaneous Localisation and Mapping, providing the user with an accurate pose estimation and map of the environment. The high-resolution location estimation can then be used to train a localisation scheme where Received Signal Strength data is acquired from a wearable device. We examine the usefulness of this method by relating it to the camera-based fingerprinting methods from previous work by testing both ground-truthing approaches using a novel dataset. We find that the new algorithm is comparable in performance, whilst removing the need for time-consuming labour associated with with registering the participant location.

Continuing in Chapter 6, we outline methods of robustification and resilience of

the localisation performance. The study proposes a method, whereby semantic information about the location is learned from an additional source. This method deals with the question of robust indoor localisation prediction by extracting additional activity information available from a wrist worn acceleration sensor. A number of different fusion models are considered, before choosing and validating the model which provides highest improvement in accuracy and robustness over the baseline example. Then, we consider the energy-awareness of wireless sensor networks, by finding an optimal sensor utilisation scheme. It achieves this by utilising other sensors available in the environment. These other sensors provide weak labels, which are then used to employ the State-Action-Reward-State-Action algorithm and train the model over time.

Chapter 7 shows the need for optimal sensor selection, from the perspective of indoor localisation. Deriving the location of participating individuals using these sensors is the key to determining their behavioural patterns and, in-turn, their health. There is, however, a limit on the amount of salient information that these sensors can provide. In the case of residential indoor localisation using Received Signal Strength, there exists a saturation point, where any additional sources of information will not provide any meaningful information. In this chapter, we present a sensor selection method based Kullback-Leibler divergence and compare it to a variety of state-of-the-art algorithms. We motivate this problem by considering the variations of signal in a 2-dimensional Wireless Sensor Network-based state space. First, we confirm the findings using a simulated environment, before validating the methods on measurement data from four residential dwellings. We also highlight how each algorithm performs using additional contextual sensors, with algorithms outlined in previous chapters. This chapter proves that our novel methods are able to provide improvement to the localisation accuracy and that the sensor networks in different environments and with distinct coverages reach saturation using comparable amount of nodes.

Finally, we conclude the thesis in Chapter 8 and provide investigation avenues for future research. We scrutinise our contributions as part of a wider localisation literature. The purpose of this summary is to provide a viable starting point to the reader, and to solidify the contributions made by this thesis in the perspective of the community. We do this by addressing the challenges set out in this Chapter, paying close attention to the extent of how much the contributions of this thesis provided a solution to said challenges, and how much work remains.

1.3 Publications and Submissions

1.3.1 Publications

Michał Kozłowski, Niall Twomey, Dallan Byrne, James Pope, Raúl Santos-Rodríguez and Robert Piechocki:
'H4LO: Automation Platform for Efficient RF Fingerprinting using SLAM-derived Map and Poses'
in IET Radar, Sonar and Navigation (In Print)

Michał Kozłowski, Raúl Santos-Rodríguez, Robert Piechocki:
Sensor Modalities and Fusion for Robust Indoor Localisation
in EAI Endorsed Transactions on Ambient Systems (Dec. 2019)

Michał Kozłowski, Ryan McConville, Raúl Santos-Rodríguez and Robert Piechocki:
'Energy Efficiency in Reinforcement Learning for Wireless Sensor Networks'
in ECML-PKDD, Green Data Mining (Sept. 2018)

Dallan Byrne, **Michał Kozłowski**, Raúl Santos-Rodríguez, Robert Piechocki and Ian Craddock:
'Residential Wearable RSSI and Accelerometer Measurements with Detailed Location Annotations'
in Scientific Data Vol. 5, Springer, Nature (Aug. 2018)

Michał Kozłowski, Dallan Byrne, Raúl Santos-Rodríguez and Robert Piechocki:
'Data Fusion for Robust Indoor Localisation in Digital Health'
in IEEE WCNCW IoT-Health (Apr. 2018)

James Pope, Ryan McConville, **Michał Kozłowski**, Xenofon Fafoutis, Raúl Santos-Rodríguez, Robert Piechocki and Ian Craddock:
'SPHERE-in-a-Box: Practical and Scalable EurValve Activity Monitoring Smart Home Kit'
in IEEE LCNW (Oct. 2017)

Przemyslaw Woznowski, Allison Burrows, Tom Diethe, Xenofon Fafoutis, Jake Hall, Sion Hannuna, Massimo Camplani, Niall Twomey **Michał Kozłowski**, Bo Tan, Ni Zhu, Atis

Elsts, Antonis Vafeas, Adeline Paiement, Lili Tao, Majid Mirmehdi, Tilo Burghardt, Dima Damen, Peter Flach, Robert Piechocki, Ian Craddock, George Oikonomou: *'SPHERE: A Sensor Platform for HEalthcare in a Residential Environment' in Designing, Developing, and Facilitating Smart Cities, Springer, Cham* (Dec. 2016)

1.4 Datasets and Open Source Software

'Residential Wearable RSSI and Accelerometer Measurements with Detailed Location Annotations' available at: https://figshare.com/s/cf2868fe78deaa6c82e4

'H4LO: Automation Platform for Efficient RF Fingerprinting using SLAM-derived Map and Poses' available at:
https://github.com/mkoz71/h4lo$_{f}ingerprint_{a}utomation_{s}ystem$

'Energy Efficiency in Reinforcement Learning for Wireless Sensor Networks' available at:
https://github.com/mkoz71/Energy-Efficiency-in-Reinforcement-Learning

CHAPTER 2

BACKGROUND AND PRELIMINARIES

The primary aim of this chapter is to provide in-depth motivation for residential indoor localisation for the remainder of the thesis. This chapter has been published in [102]. However, we aim to extend the review beyond the confines of residential localisation, and into more broad application spectrum, as to show the true urgency of a viable indoor positioning system, which is easily generalisable and compact. Additionally, we aim to use this chapter to describe the fundamental algorithms which will be used throughout the thesis. These algorithms include the basic structure prediction and modelling methods which have been extensively employed here. We will also discuss the various fusion methodologies and outline their theory in detail. At the heart of every successful implementation of an IPS lies effective sensor data utilisation and analysis. In this chapter, we aim to provide a taxonomy of more and less popular sensing modalities currently preferred by the experts in the field. These sensors are used to achieve target tracking and localisation, either on their own, or in unison with other modalities.

First, we review every sensor and its internal operation, exhaustively examining the literature pertaining to each. Then, the modalities will be scrutinised against an evaluation framework, in order to provide the reader with an overview of their suitability. Later, we provide an extensive review of the typical fusion combinations, which can be found in the literature, paying close attention to the objective which that fusion serves. Specifically, we explore fusion for robustness, accuracy and energy efficiency. Using these formulations of various techniques, we additionally provide the outline of the preliminary

theory which underpins this entire thesis.

2.1 Motivation

Indoor localisation has been regularly cited as an important ambition of many fields in both, academia and industry. The use cases include pervasive health monitoring [24, 100], targeted advertising [12], factory vehicle tracking [92] and robotics [26, 119], amongst others. However, implementations of localisation methods and algorithms differ, depending on the need, deployment methods, available utilities, resources and sensors [73, 239].

Whilst the survey literature pertaining to localisation systems and methods is large [73, 230, 239], there exists very little in the way of localisation-centric sensor utilisation. This encompasses the use of bespoke [55] or off-the-shelf [24, 160] sensors, specifically for the use of location estimation, robustification and optimisation. This area is extensive [33, 49, 76, 110, 187, 198], yet very often bundled along with localisation technology surveys, without subsequent scrutiny. We aim to close this gap, by reviewing sensors, their fusion and utilisation as applied to localisation, in contrast to localisation methods, technologies and implementations themselves.

Most of the existing localisation surveys include technology-specific reviews [42, 73, 121, 239]. They concentrate upon the methods and algorithms related to indoor localisation [42, 121], techniques and technologies [239]. Some work also addresses localisation from the perspective of the device itself, such as smart-phones [230]. Xiao et al. study [230] is the most closely related work to our proposed examination. The main difference is, that instead of reviewing the devices as sensor clusters, we review the sensor modalities themselves. We also offer a more comprehensive review of fusion methods and provide exhaustive examples for each case.

The main contribution of this chapter is the inventorisation of the popular types of sensors used to provide location estimation and their respective advantages and disadvantages. We also provide the detailed description of their fusion methods with respect to their benefits and drawbacks. Finally, we show how these sensors are likely to fare in the future, paying close attention to the current community preference and trends surrounding each modality.

In Section 2.2 we outline the problem of localisation and provide a brief synopsis of the review process, concentrating on the most important indoor localisation-centric challenges found in literature. We then outline the evaluation criteria in Section 2.3.

Then, in Section 2.4, we consider various sensors which are used in the service of localisation. In Section 2.5 we outline how the sensor fusion is performed, and review the state-of-the-art literature pertaining to effective sensor fusion and combination methods. Finally, we conclude in Section 2.6.

2.2 Underlying Objective of Indoor Localisation

There exist various interpretations of positioning, navigation and tracking under the umbrella term *indoor localisation*. For example, Van Haute et al. [206] stipulates that tracking and positioning are not comparable. Whereas positioning implies establishing the location of an agent, either at real time or offline, tracking would involve performing localisation based on previous known location data, effectively storing the entire navigational history of an agent. This carries an additional risk of privacy intrusion, as the historical data would expose an agent's habits and previous locations [206]. We intend to adopt a similar mindset in this chapter.

In addition to the above assertion, we consider it necessary to address a common misconception with regards to the semantic meaning of *indoor localisation*. A catch-all term, it grew to signify localisation inside, regardless of whether the environment is accessible by doors or not. In this thesis, we understand indoor localisation to be an epitome of technologies and implementations for localisation in an *enclosed environment*. Examples of few such environments range from, but are not limited to, residential abodes [24], commercial shopping malls [216], industrial halls and factories [94], hospitals [83] and natural formations, such as underwater caves [131]. Here we consider sensor combinations stemming from the necessities imposed by these environments.

Simply put, an agent traversing an enclosed environment is being localised if its location, position or navigational history is estimated with respect to their previous position or performed actions. This is normally estimated in 2- or 3-dimensional space. The agent is assumed to be able to access the entirety of the surveyed environment. The model, or algorithm, performing the estimation also has access to the description of said environment as well as the features explaining the agent's actions. In the domain of sensor-driven estimation, agent's actions and locations are described through the use of sensors, which the agent either bears on itself or is subjected to, when travelling.

Localisation task can be further explained through an example. Consider a wheeled robot moving along the corridor. Being able to access every area in that corridor, it is allowed to move freely across the environment. The corridor resides inside a building

where GPS-based services fail to provide a viable position. In order to localise itself, the robot intermittently takes pictures of the surroundings as it moves. In order to perform effective exploration, the robot is programmed to favour the unexplored locations over explored ones. It realises this by comparing the photos of the immediate surroundings to the collected library of pictures. As it drives along, the output from its wheels give it the approximate location, as seen from previous location, so called Dead Reckoning (DR). Moving freely through the corridor, it visits all possible locations and creates a map, with respect to the DR location it estimated and approximate locations of the taken pictures.

Simultaneous Localisation and Mapping (SLAM) is just one of the open problems in localisation literature, but it clearly and succinctly explains the challenge. In a perfect, noiseless world, the robot would be able to localise itself based on the DR alone. Then, by using the pictures, it would map out the environment, effectively solving the problem, by providing a map, and a vector of locations it visited. However, due to various conditions it is subjected to, noiseless localisation is so far unattainable. Its wheels will drift, adding noisy readings to the model. Camera pictures can be subjected to occlusion and lighting effects, making direct comparison difficult. The environment itself can also be dynamic, which adds to the complexity of the problem, as, in the case of this example, the photogrammetric features used by the robot can be shifted, moved or otherwise removed from the corridor.

The motivation of using various sensor modalities, and their fusion, stems from the above mentioned issues. So far, there is no one definite way of performing localisation, as various sensors present different advantages and disadvantages. Whilst camera is known as a very accurate tool for feature extraction, it does so at the cost of high dimensionality and complexity of the data it collects. There exist modalities, which reduce the need for such high dimensionality, but in turn provide coarser location estimation. This implies that leveraging computational cost and estimation potential, across all modalities is, at the present moment, key to a successful implementation of an IPS in GPS-denied settings.

2.3 Evaluation Criteria

The existing surveys of current localisation literature usually scrutinise the research through the use of a evaluation framework. Here we list the most popular criteria established either through literature [42, 73, 121, 239] or the author's own experience. This list is not exhaustive and is only provided to encapsulate the issues faced by the

present-day implementations.

2.3.1 Accuracy

The most prevalent of metrics regarding localisation. Accuracy is usually calculated as Euclidean distance in 2D or 3D space [127]. Formal example is provided in Eq. 4.2. While effective, this metric is not infallible - there exist sensors and systems where a direct comparison of location accuracy (alternatively accuracy error) would not capture all necessary information required to examine any two given sensing systems. This point also considers whether certain sensors make it possible to scale the system to include more than one tracking node at a time.

2.3.2 Noise resilience

Sensing, in any form, will suffer from noise. This noise can be inherent in the sensing modality [116], environment [222], can be introduced during the manufacturing process[21, 151], or as a consequence of other factors, such as striving for improved energy efficiency [54]. Resilience of a sensor can also dictate whether drift and quantisation affect the location estimation and whether dependence on other sensor modalities can reduce it.

2.3.3 Cost

The costs associated with specific sensors are varied. These can be simple hardware costs, upkeep costs, deployment costs or maintenance costs. Hardware and upkeep costs encompass the initial expense of creating the infrastructure. Deployment and maintenance costs are related, in that they describe the value of labour associated with aforementioned tasks. Since different sensors will be comprised of different concessions regarding their performance and operation, they will all enjoy various advantages unique to their topology.

2.3.4 Energy efficiency

Efficiency has been cited as an important aspiration of a sensor-based system [53]. Deploying any system will come at a cost of establishing a number of trade-offs. Energy is often traded for accuracy/resilience to noise, as they tend to be mutually exclusive [170]. It is also important to recognise how easy is it to control the energy expenditure as

part of a positioning system, and also whether the sensors make the system adaptable for energy-aware operation.

2.3.5 Popularity

The systems present within the literature rarely exhibit the same taxonomy of sensors, share the same evaluation environment or training methods. There exist implementations of positioning systems which consider various sensor modalities, and various fusion combinations. As it was mentioned above, currently, localisation relies on objective-specific sensor fusion as to ensure appropriate redundancy during its operation. The trends in literature are also greatly influenced by the relative costs and availability of hardware.

2.4 Sensor Modalities for Indoor Localisation

2.4.1 Inertial sensors

Inertial sensors use the relative change in their frame of reference to provide an output. They are commonly employed in motion tracking [37] and detection systems [58]. In relation to robotic or human localisation and tracking, they mostly comprise of Micro-Electro-Mechanical Systems (MEMS) accelerometers and gyroscopes, embedded within Inertial Measurement Unit (IMU) chipsets [224].

Accelerometers calculate the acceleration in 3-dimensional space given by units in g or alternatively in m/s^2. Their electro-mechanical design is relatively simple [184] making them easy to produce. An example of the data they produce can be noted in Fig. 2.2. The manufacture of MEMS gyroscopes on the other hand, is much more involved [184]. This is due to the nature of the sensing paradigm they provide. By measuring the vibration of a proof mass relative to the axis (also known as Coriolis effect), they provide the angular rate of rotation, given by $°/s$. One other important difference between the two sensors is the power expenditure. Due to the method of operation, gyroscopes are known to draw more power (sometimes in orders of magnitude) when compared directly to accelerometers at the same sampling rates [124].

They are both, however, prominently used as part of Inertial Navigation Systems (INS) , which constitute the focus of many localisation-centric research enquiries. There is a large body of literature pertaining to inertial sensing for localisation [5, 21, 41, 73,

100, 133]. They are particularly popular as part of the Pedestrian Dead Reckoning (PDR) applications [21, 86, 243].

In an early implementations of PDR, the authors strived to complement the shortcomings presented by GPS systems by including a sensing module designed to perform pedometry [60, 91]. In 2005, Foxlin [60] presented a system dubbed NavShoe, where the accelerometer and gyroscope, along with a magnetometer, were mounted on foot-gear. The study then confirmed that the pedometry-based system can compliment a GPS. This was also one of the earliest papers to coin the phrase *Pedestrian Dead Reckoning*

As the manufacturing costs of MEMS devices reduced over years, their usage and the quality of their output has correspondingly increased. Lately, implementations feature smartphone devices which have these sensors readily embedded. One such study by Strozzi et al. [192] utilises a number of different hand held smartphones as a proxy to estimating step and its length. Similarly, Yin et al. [236] considers smartphone-based sensing, albeit as a tool for walking and running detection using accelerometers and gyroscopes embedded within.

While smartphones remain the favourite platform for sensing in many cases, there exist dedicated devices, so called wearables, which can provide acceleration and angular rotation from different parts of the body [13, 54]. Signatures from different sections of the human body were found to differ both, in the way they are exerted and their own estimation potential as per Bao et al. [13]. In our own study [100] we considered wrist-worn accelerometer as a complimentary source of information in indoor location estimation. This method aimed to robustify the localisation performance by assuming that humans have a tendency of performing similar tasks in similar places in a house.

This type of sensing is not without its challenges however, as there has also been some advances in residential user identification. McConville et al. [137] showed that due to uniqueness of each person's gait patterns, it is possible to recognise them directly from the inertial signals. The authors argued, that even though this was useful in pervasive health environments, it posed a significant privacy intrusion risk [137]. Off-body inertial sensor usage has also been investigated. Dang et al. [41] used different walking canes with attached IMUs to establish gait of the users, and consequently the distance travelled. This however relied on the participant using the cane with no abnormal deviations.

2.4.2 Ultrasonic and Acoustic Sensors

Ultrasound has also been explored for indoor localisation applications [75, 148, 165, 166, 245]. The basic implementation considers a number of speakers in the environment,

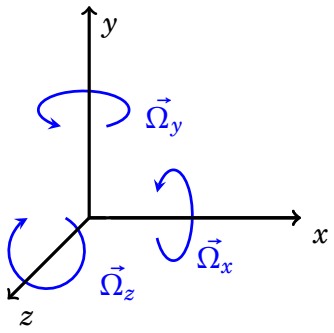

Figure 2.1: Domain of accelerometer (black) and gyroscope (blue) sensing.

which exert ultrasonic vibration [75] or frequency chirping [148]. The sensor designs themselves do not differ much from generic transducer-based microphones and speakers. In fact, this is done by using a piezo-ceramic or piezo-film transmitter, excited to generate a response at frequencies in [148] or over the human audible range [75], which is subsequently registered by a receiver.

The bulk of the localisation estimation is done through lateration schemes, such as Time-of-Arrival (ToA) [165, 167] and Time-Difference-of-Arrival (TDoA)[148, 156] or angulation, like Angle-of-Arrival (AoA) [166]. They can be further categorised into Active and Passive [148]. Due to their physical nature, the sound waves experience similar shortcomings as electro-magnetic (EM) waves, in that they are limited by the Line-of-Sight (LoS) conditions However, when not experiencing multi path fading effects and Non-Loss-of-Sight (NLoS) conditions, the localisation based on acoustic signal reportedly outperforms radio frequency (RF) based methods [148].

Early approaches, such as Cricket [165] used a combination of an ultrasound and RF to obtain a cheap localisation system. The experiments included static and mobile performance of the algorithm in an indoor office environment. This was late expanded into Cricket Compass [166] aimed at using angle of arrival in order to perform localisation.

More recently, Murakami et al. [148] used a smartphone-based mixture of active and passive signals. They were able to track the target along an open corridor. Qi et al. [167] used a number of ultrasonic receiver and transmitter modules in an Wireless Sensor Network environment. The aim was to establish a viable method for localisation under Non-Line-of-Sight conditions. This was tested by using a mobile robot, traversing in circles.

In their paper, Khyam et al. [96] used orthogonal ultrasonic chirping to utilise the wider part of the spectrum and facilitate multi-transmitter positioning in a passive

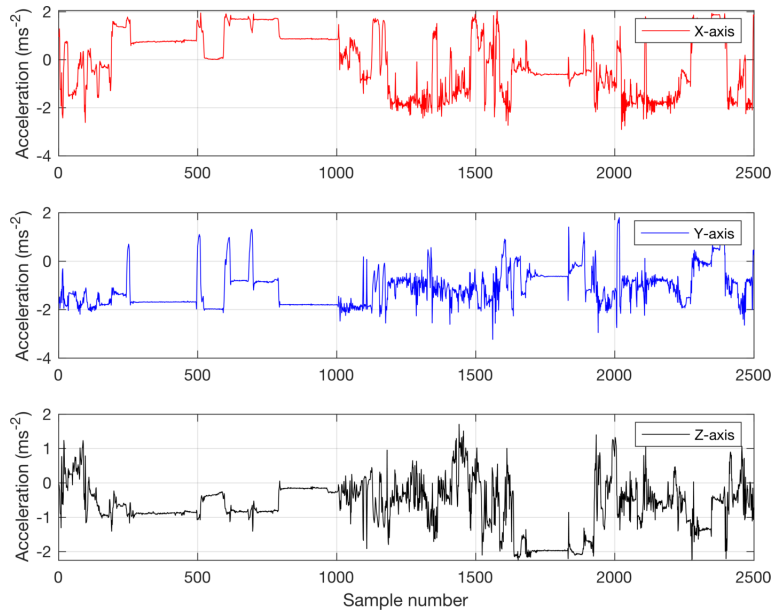

(a)

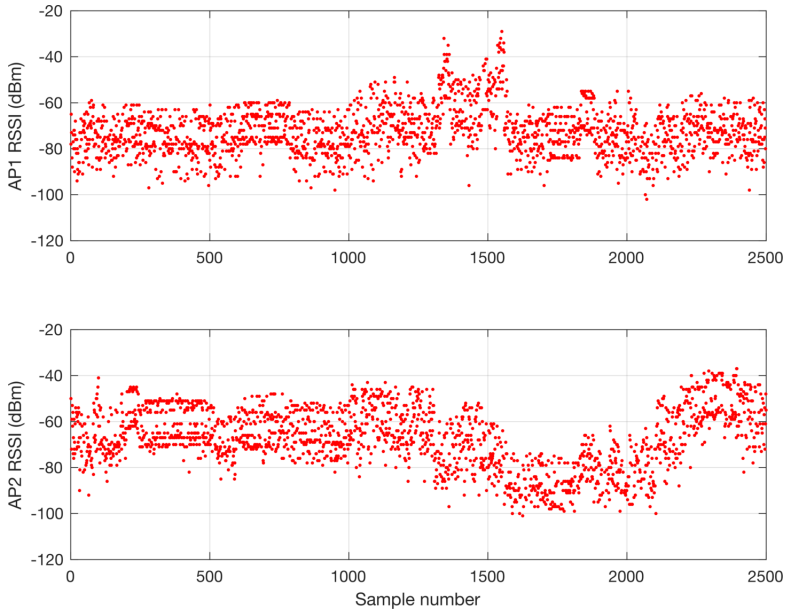

(b)

Figure 2.2: Example of tri-axial Accelerometer (above) and RSS (below) time series data from an indoor localisation 'living' experiment. Courtesy of Byrne et al. [24]

context. Their experiments were carried out in largely noise-saturated environments. In the domain of robotics for indoor localisation Ogiso et al. [153] used a robot-mounted microphone array to attain positioning information of a pre-defined track. The robot would move in an 6m × 6m arena enclosed by four sources of sound, achieving sub-meter performance.

2.4.3 Visible Light Sensors

Visible Light Communication (VLC) is a subset of optical telecommunications concentrating on the visible light spectrum, or 380 to 780 nm wavelengths [172]. It supports faster transmission speeds [89], and offers a relief to congested radio frequency spectrum communication schemes [179]. Its fundamental operation relies on a source of light, such as a Light Emitting Diode (LED), modulated to flicker at a specific frequency, often to obfuscate the flickering. A light sensor is then used at the other end to receive and demodulate the transmission [179].

VLC is often used as part of the Visual Light Positioning (VLP) systems, whereby the modulated LEDs are used to estimate an object's position, relative to lighting beacons [109, 178]. Much like Ultrasound, the schemes used to perform lateral or angular positioning rely on extraction of light signal strength [215] or relative AoA [109].

In their recent work, Rátosi et al. performed a real-time positioning based on LED anchor points [178]. In their work, they localised an object with a fish-eye lens camera extracting the positions and IDs of the LED beacons. They concluded that this approach is viable, even at relatively fast velocities of the object. Wang et al. [215] was able to extract the beam strength of each uniquely-blinking LED through Fast Fourier Transform. Their LIPOS system was able to localise to within 2 meters Euclidean error in 3 dimensions.

Kuo et al. used a smartphone-based system to perform localisation, attempting to simulate the conditions usually found in retail spaces [109]. Their system considered using the lights mounted on the ceiling as beacons and smartphone's front-facing camera as a capture method. Qiu et al. [168] used a kernel-based method to estimate the modulated light intensities. The authors noted, that due to the relative low-cost of the system and re-usability of an already existing lighting infrastructure, it could be used as a practical and efficient localisation implementation in the future.

2.4.4 Radio Frequency Sensors

This is undoubtedly the most examined area of indoor localisation implementations. RF-based sensing and location estimation have been the cutting edge methods of positioning due to their relatively low cost, off-the-shelf sensor availability and solid performance. This, coupled with the recent advances in Internet-of-Things (IoT) and ever-decreasing costs of maintenance have made this type of sensing a go-to for many researchers [11, 15, 24, 68, 100, 101, 136].

Whilst the number of technologies and standards within this group is vast, the basic idea of localisation remains the same. Generally, there exist a number of static anchor nodes, or APs which are able to transmit signals to a sensor traversing an environment of interest. They are comparable with ultrasound and visible light in the way that they are able to utilise similar schemes such as ToA and TDoA. Traditionally, RSS between a transmitter and a receiver was used as a metric to obtain information about the relative distance between the two nodes. This is made possible, as signal strength, assuming perfect propagation medium and lack of multi-path fading, will follow a steady decrease as a function of distance and is more formally described in terms of a path-loss equation [234]:

$$PL(b)[dB] = PL_0(b_0) + 10nlog\frac{b}{b_0} + \mathscr{X}_\sigma \tag{2.1}$$

where b is the measured distance, n is the path loss exponent, $PL_0(b_0)$ is a measured average path loss at a reference distance b_0 and $\mathscr{X}_\sigma$ is a zero-mean Gaussian random variable, with σ denoting the variance of shadowing [234], simulating the fading effect. In this work, the values for this simulation are as follows: b_0 was kept as 1.2m, $PL_0(b_0)$ as -49.4dBm [139], σ as 5 and n as 3 [174]. This model is only an approximation of an indoor environment however, as the signal will vary in different surroundings and even different users [43]. A more realistic example is provided in Fig. 2.2. There, the actual signal is obfuscated in noise, brought on by shadowing effects and fading. Recently, there have been some work done using Channel State Information (CSI) [200, 234]. Using newer standards, such as IEEE 802.11, one can extract the amplitude and phase information from the channel directly, offering better performance [200].

The actual performance of RF localisation is deep-rooted in the technologies which are utilised to achieve it. Wi-Fi [57, 196] has been cited as one of the more popular approaches. Increasingly, the Bluetooth Low Energy (BLE) based sensors have been used, which leverage the low-power consumption with cheap cost and ubiquity [24, 204].

Radio Frequency Identification (RFID) [43] and Ultra Wide-band (UWB) [63] have also been used for location estimation, with UWB achieving sub-metre accuracy.

These schemes often rely on fingerprinting to achieve its performance. This consists of users visiting all fiducial locations in the environment, in order to build up an RF map [24, 237]. Whilst effective, fingerprinting has been recognised as difficult to obtain and maintain [24, 100, 101]. There have also been some work done, with multi-user environments, where it was confirmed that fingerprinting from one user is unlikely to be optimal on a different user [43]. There are however approaches designed to mitigate this difficulty [101].

The work done on RF localisation by Bahl and Padmanabhan [11] is widely regarded as the seminal paper on the subject. There, the authors outlined basic procedure for fingerprinting, where each required sector of the environment was characterised before outlining their algorithm for signal strength localisation. They used a specially fitted wireless adapters. Since then, the literature pertaining to sensor-based RF localisation steadily grew and so did the availability of off-the-shelf- implementations.

Byrne et al. [24] presented a data collection of four different residential houses in Bristol. Each house was parametrised using approximately 1m × 1m states, which permeated the living space. Then, a thorough fingerprinting of each abode took place. The dataset also included living experiments, and was performed using the SPHERE-in-the-box infrastructure [160]. This included Raspberry Pi-based access points and a bespoke SPHERE wearable sensor [55].

Wireless fingerprinting was also tackled by Yiu et al. [237]. They provide a comprehensive overview of fingerprinting methods, noting the online and offline phases of the radio map generation. Offline phase specifies the actual map generation, as in [24], and online phase is the location inference given current sensor output, which in their case was a Google Nexus tablet. They then outline different fingerprinting modalities, such as parametric (using path loss models) and parameter-free (based on Gaussian Processes).

2.4.5 Magnetometer Sensors

Ambient Magnetic Field (AMF) Localisation was inspired by the migration tendencies of certain animals [74]. Many species sense the Earth's magnetic field and use it to navigate [74]. This method uses the extraction of a varying magnetic field inside buildings, in order to build a map of the environment, i.e. fingerprint. These distortions in magnetic field come from ferromagnetic fluctuations caused by the building's metal construction and general topology [74, 232].

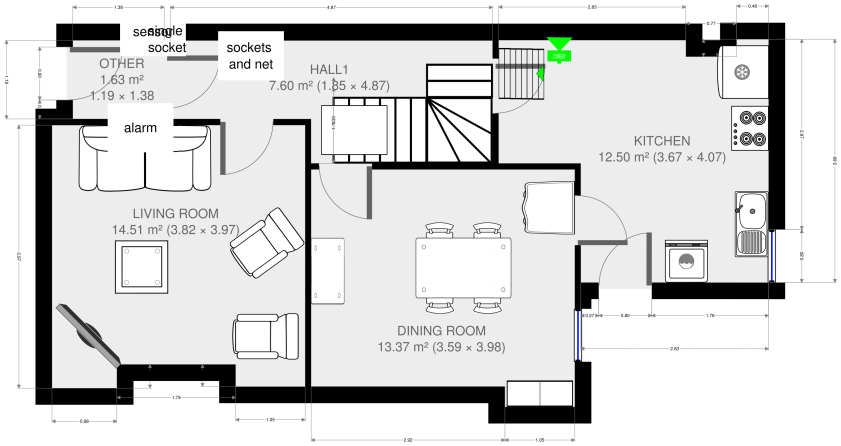

(a)

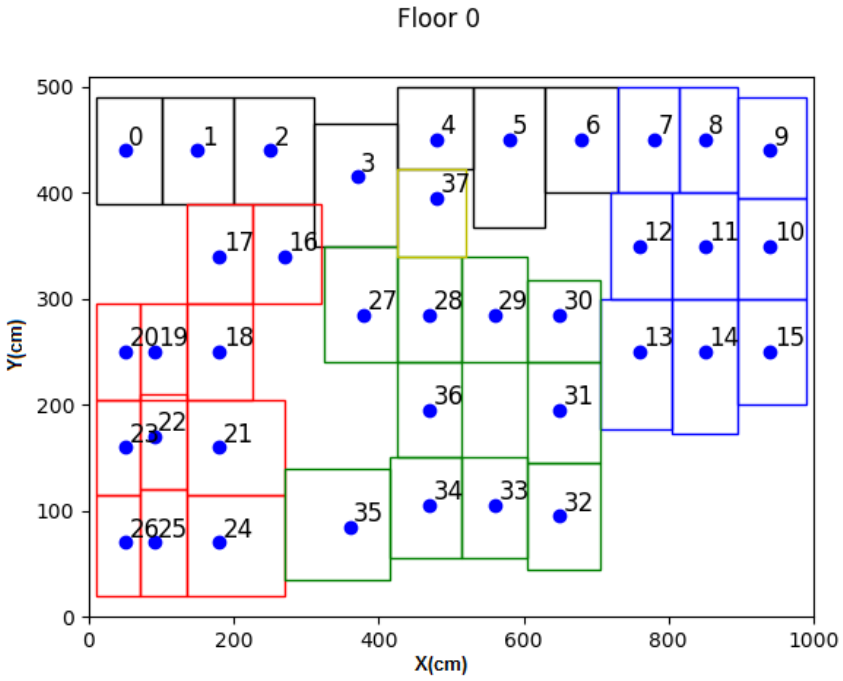

(b)

Figure 2.3: Example of discretised floor plan, for the use with fingerprinting. Figure above shows the corresponding floor plan. Below, each discretised state is 1 meter apart. Different colours of the grids signify different rooms. These approaches have been proven to be notoriously arduous in labour, especially in large industrial and commercial spaces. Image courtesy of Byrne et al. [24]

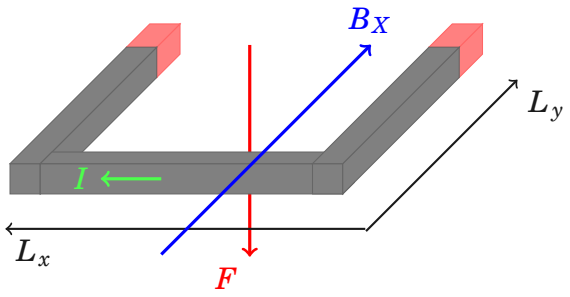

Figure 2.4: Schematic of a basic MEMS implementation of Lorenz Force-based magnetic field sensor in a single dimension. Adapted from Herrera-May et al. [77].

MEMS magnetometers [36, 194] are the most commonly used sensors in service of indoor localisation, due to their relatively low cost and high sensitivity [78]. They are generally used along with accelerometers and gyroscopes as part of PDR implementations [86, 91] where they act as directional sensors. However, they can also be used to estimate the ambient magnetic field in a given location inside a building [74]. They work by estimating the Lorenz force [78], measured as a function of current and magnetic field, given by [117]:

$$F_W = I \times B_X \times W_Z \tag{2.2}$$

where B_X is the magnetic field in T, W_Z is the length of the loop or a wire in m, and I is the current through the wire, in A. This force generates a displacement of a suspended control weight [117], which can be measured through piezo-resistive or capacitive means. The magnetic field induces current in the wire, which in turn forces the loop to move. The red piezo-resistors at the end of the loop in Fig. 2.4 are used to calculate the relative deflection and in turn, the causing magnetic field strength. Comprehensive outline is given in [78] and [117].

Haverinen and Kemppainen [74] stipulated that these anomalies in a magnetic field could be utilised for localisation. A subject wearing a magnetometer on their chest would walk along a corridor, measuring the field. Whilst they first proved its viability in a single dimension, this was later extended to 2 dimensions by Navarro and Benet [149]. However, the latter study was not directly comparable, as it was done using a wheeled robot as opposed to a human subject.

The popular approach of fingerprinting was appropriated to magnetic fields by Chung et al. [36]. In their work, the researchers used an offline map against which the observations were compared. The magnetometer was again worn on the chest, and proved

comparable to other approaches, such as WLAN and RADAR. Similar fingerprinting was done by Subbu et al. [194], who published a smartphone-based localisation technique called LocateMe. The authors exploited the mobile phone's magnetic sensor in order to gather fingerprinting maps of the environment and stipulated that this approach is also able to distinguish corridors with high precision.

2.4.6 Camera-based Sensors

When discussing camera-based localisation, it is important to distinguish between approaches where the localisation is a priority [220], and methods which render location information as a consequence of other inference, such as personalised silhouette detection [72, 204]. Whilst wide-scale indoor localisation with cameras is yet to be attempted, there are plenty of vision based tracking methods which consider smaller spaces [25, 207, 220].

There are many implementations of camera sensors on the market today. Digital cameras are most frequently based on CMOS technology [59] or obtained through charge-coupled devices (CCD) [173]. They are analogue devices, in the way they produce a lattice of pixels excited by the visible light to produce electrical signals, which are subsequently amplified and processed. Owing to its topology, this data is high in resolution and dimensionality [207]. This, in the context of indoor localisation, necessitates a streamlined and latency-free connection to a reference database to compare against a calibration set [207, 220] or a thorough dimensionality reduction study [72] in order to become viable.

Early studies consider localisation through stereo vision. By using a stereo vision sensor, Bahadori et al. [10] presented a method of tracking multiple people in crowded environments, by modelling the background and the people themselves. This work outlined the basic principle of multi-person tracking in an indoor environment and noted issues with tracking identification.

Numerous approaches consider smartphone-based indoor localisation [207, 220]. Werner et al. [220] proposed MoVIPS, a visual positioning system. In their work, the authors used a smartphone to take pictures of the environment and compare them to a training set, with server-side feature extraction based on Speeded Up Robust Features (SURF). Similar approach was attempted by Van Opdenbosch et al. [207], albeit with a larger emphasis on efficient data analysis, with comparisons between lossless and lossy compression.

As the depth-sensitive cameras became more cost effective, the research enquiry shifted to RGB-depth (RGB-D) sensors. Using RGB-D cameras for tracking has been established for some time [191]. In their work, Song et al. provided a large public dataset

of RGB and RGB-D based videos for object tracking. RGB-D cameras are also widely used for SLAM implementations [51, 193]. In these dataset papers, the consecutive depth-perceiving images are compared in order to evaluate location and at the same time produce a map. For example, in [147], Munoz et al. uses cameras in order to real time landmark-based visual SLAM.

2.4.7 LiDARs

Light Detection and Ranging (LiDAR) devices are used as part of popular data association methods in order to obtain the position of the agent. They perform tracking by detecting the immediate vicinity of the agent and comparing it to previous readings [228]. LiDARs used in context of indoor localisation are most commonly found in robotics [79, 99]. There, the LiDARs are used most commonly utilised to perform SLAM [99].

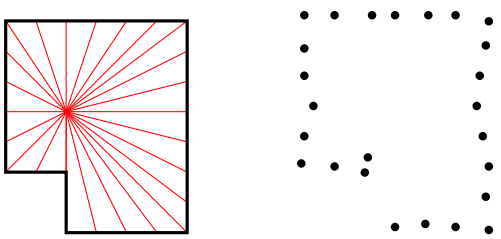

Figure 2.5: Example of a bird's eye view of a room (left) with 2-dimensional laser ranging device. The noisy LiDAR 'returns' are shown on the right.

Whilst theoretically, any part of the light spectrum can be utilised to perform ranging, laser are most popular [80]. The working principle is rather simple, and relies on ToA schemes - a beam of laser is sent out from the sensor and is reflected off the environment. Then, the time it takes to return is calculated from that beam, establishing likely distance between the LiDAR and the environment [39].

The data produced by a LiDAR can be either 2- or 3-dimensional [80]. This data is most commonly referred to as *point clouds*, due to discrete granularity of the environment it produces. These point clouds are later used as descriptors of the indoor environment and most commonly used to perform SLAM [79], usually as part of scan matching techniques [79, 219]. This data is however high dimensional and requires large reserves of computational power to optimise [99]. As shown in Fig. 2.5, point clouds are also susceptible to environment noise and jitter, which additionally creates scan matching issues.

Some early approaches to LiDAR localisation used robots in indoor positioning scenarios [34, 176]. Chmelař et al. used a laser range finder sensor in order to localise a robot in an indoor office environment. They used a compensation method in order to reduce the aggregated error. Rekleitis et al. was one of the first to propose a multi-agent localisation with LiDARs. Whilst the mapping was performed using a sonar, the robot agents were tracking each other using the LiDAR, in order to compensate for odometry errors.

Modern approaches enjoy better LiDARs and more computing power, allowing for faster processing and more resolute mapping [158, 219]. Peng et al. used a novel scan matching technique to achieve robot localisation in an indoor environment. Based on this work, Wang et al. [219], performed a similar study. Note that the robot used in both of the above papers was a ground-based device. Lee et al. [112] has used a LiDAR, along with a Virtual Reality (VR) headset, to obtain high resolution positioning using a drone. This experiment was in part inspired by disaster management and designed for first responders as an aid for finding survivors.

	Accuracy	**Noise Resilience**	**Cost**	**Current Consumption**	**References**
Inertial	1m-10m	Low	Low	$100\mu A$ - $3500\mu A$	[41, 84] [55, 213, 223]
Ultrasound	0.01m-0.1m	Medium	Medium	Varies with application	[148, 167]
RF	1m-10m	Low	Low	Varies with protocol ~ $20\mu A$ per packet	[11, 63, 100] [223]
Camera	0.01m	Mid to high	Mid to high	Usage & processing $\gg$ 1A	[10, 113]
Magnetometer	3m-5m	Mid to high	Low	~ $300\mu A$	[36, 194, 223] [74, 117]
Visible Light	0.2m-5m	Low (LoS)	Medium	~ $5100\mu A$	[82, 168, 215]
LiDAR	0.01m-0.1m	Medium	High	~ $300\mu A$ - $1A$	[79, 80, 189]

Table 2.1: Table of sensor modalities, evaluated using the criteria from Section 2.3

2.4.8 Other modalities

The above list is by no means exhaustive. In the literature, there exist various other implementations of IPS, which utilise less popular modalities. An example of one such implementation include Seo et al. [183], which used an ultrasonic anemometer to compliment the IMU on a mobile robot. Anemometers measure relative velocity of air. In

the above study, the robot was moving through static air, which ensured no erroneous readings.

Some research has also included pyroelectric infrared (PIR) sensors. Luo et al. [126] used a lattice-like sensor, in order to track an agent through the environment, at the same time performing activity recognition. The study motivated the use of PIR sensors, by noting that they are relatively infrastructure-free, and are easy and cheap to deploy. There also exist some data sets, where the PIR sensors are included, such as Twomey et al. [204].

There also exist studies using the piezo-electric effect in order to obtain the location and activity information of the users. The study of 'smart carpets' done by Chaccour et al. [31] does not cite indoor localisation as its main objective. However, this implementation could be used for very coarse location estimation as well. In their work, the authors have considered fall detection using specially adapted carpets with piezo-resistive pressure sensors embedded within them. Similar study was also done by Contigiani et al. [38], which used piezo-electric wire lattice, inside the carpet, as a tracking modality.

2.4.9 Drawbacks and Modality Evaluation

The presented modalities all differ in terms of the data that is being captured, and they way they obtain these readings. All of their topologies offer advantages and disadvantages in the domain of indoor localisation. In this subsection we will discuss the shortcomings of each modality.

Inertial sensors, whilst cheap and relatively energy efficient, often suffer from degrading noise [21, 151]. This noise is usually rectified by the researchers, though meticulous planning and closely controlled experiments [21, 86, 241]. Results 'from-the-wild' indicate that these sensors, are much more effective when used as part of a wider family of activity recognition tasks [24, 43, 44].

Ultrasound and acoustic sensors offer great precision but only at short ranges and in LoS laboratory conditions [153, 167]. Interestingly, most of the studies included in this survey have indicated that aside from these shortcomings, ultrasound is mostly preferred due to its low-cost and ability to reuse already existing sensor infrastructure, such as smartphones [148].

The biggest issue with RF sensing for localisation is the labour associated with training and the unpredictable nature of RF signals in the environment. The topology of this sensor make it great for tailored applications [100, 160], but often fail to generalise to

other environments, and even users [43]. In addition, whilst fingerprinting is a powerful training technique, it is often cited as a drawback in any RF implementation [24, 115].

One of the major drawbacks of camera-based systems is the large computational complexity [207, 226]. Additionally, these sensors suffer performance degrading occlusion and lighting effects [25]. High dimensionality has also been cited as an important consideration [72]. These type of sensors are likely to be omitted in favour of other modalities in IPS settings.

Magnetic field sensing has been proven to be effective, but only in confined spaces, taking advantage of ferromagnetic effects brought on by buildings [232], and under controlled conditions [71, 74]. This type of localisation also suffers from fingerprinting issues [36, 214]. Localisation based on an AMF could still be considered emerging, leaving plenty of opportunity for further work.

Visible light sensors provide a very accurate 3-dimensional positioning results at the cost of big infrastructures and controlled experimental testbeds [178]. Additionally, NLoS conditions are difficult to negotiate with this type of sensors [8, 116]. Modulation of the light beam is an another issue - it requires frequencies large enough as to prevent visible flickering, which has been proved to be detrimental to the user experience [116].

LiDARs are a great intermediary between high dimensional data and reliable efficiency. However, the sizes and cost of these devices are still considerable. They are also prone to environment noise and, since scan matching relies on dead reckoning and will aggregate error over time, requires additional optimisation steps to become viable [79].

These modalities have been tabulated in Table 2.1, and scrutinised against the evaluation criteria provided earlier in this section.

2.5 Sensor Fusion

The above sensors are popular within indoor localisation literature. There exist numerous reasons for using these particular sensors on their own. However, by introducing an additional modality, one can obtain more information about the environment or its dynamics [100, 110]. By not relying solely on a single modality, an IPS can enjoy a number of advantages, ranging from resilience [26], accuracy improvement [33] or energy-awareness [101, 110].

Whilst, theoretically, fusion of any sensors is possible, not every combination is feasible. The most popular combination in the domain of inertial sensing, for example, is the consolidation of accelerometer and gyroscope with magnetometers, in order to

produce robust PDR systems [107]. Nowadays, the relative energy output of these type of inertial sensors is negligible, which makes these sensors a popular choice in low-power applications [43].

RF-centric localisation has also been improved with fusion [26, 76, 198]. The combination of sensors in this context is usually performed for location improvement, as realistically, pure RF can only provide coarse location estimation. Mostly this involves either predicting or compensating the RF prediction with an inertial measurement [76, 100, 187]. Fusion of RF and magnetic field strength for performance improvement has also been explored [141].

In terms of robotic LiDAR SLAM applications, the fusion is also performed using the robot's own IMU and magnetometer, in addition to the LiDAR [108]. VLC positioning has also been complimented by an IMU [248], as has ultrasound [64]. In each case this provides accuracy improvement to the system.

The relative fusion between different sensor modalities are visualised in Fig. 8.1. These sensor fusion combinations are by no means exhaustive. They were picked on the condition of being current examples of fusions between these types of modalities. Likewise in Fig. 8.1, the fusion was visualised only to help expose gaps in the literature pertaining to sensor fusion for indoor localisation. The intention of these is to give the reader a good starting point for their own investigations.

In the following sections we will review the studies which used fusion for a specific purpose.

2.5.1 Objective-specific Fusion Combinations

2.5.1.1 Fusion for Robustness

Fusion for robustness entails combining different sensor modalities in order to make the performance more resilient to outside adversity. Considering indoor localisation as our main motive, this adversity can come in the form of network-wide interruptions [100], dynamicity of the environment [130] or hostile agents [177].

By utilising Particle Filtering (PF), Canedo-Rodriguez et al. [26] was able to fuse a number of different modalities together for a robot-based indoor localisation system. These systems included LiDAR, Wi-Fi signal strength, cameras and magnetic signals from inside a museum. This robustification ensured a steady performance even in the event of dynamic environment, such as body shadowing. Li et al. [119] presented a technique for the fusing of UWB and IMU signals. This was done in the context of robotic

indoor localisation using a Kalman Filtering (KF) . The authors tested the algorithm against Gaussian noise, where their fusion method proved to be a viable safeguard.

Elbakly et al. [49] considered the fusion of a barometric sensor with Wi-Fi signal strength to provide a reliable prediction of floor transitions. It was tested thoroughly across three different environments, using 4 participants, and was proven to provide a robust performance across users. He et al. [76] used a Bayesian Network approach to fuse Wi-Fi and IMU signals. The authors arrived at the conclusion that the IMU was able to robustify the positioning based on a smartphone application.

In the domain of robotics for indoor localisation, Paredes et al. [156] used a hybrid of an ultrasonic and camera-based sensing to achieve 3D positioning for a Unmanned Aerial Vehicle (UAV) . The study concluded that purely ultrasonic localisation result is improved when using a ToA depth information from a camera.

2.5.1.2 Fusion for Accuracy

Accuracy in indoor localisation is most often calculated through the Euclidean error metric, as shown in Eq. 4.2 and [127] and given in meters. Improvement of accuracy is the main ambition of many positioning studies. The fusion in this context would entail pin-point estimation of position based on a number of modalities. Over the years, many fusion attempts have achieved substantial reduction of positioning error, however no consensus among the community regarding the optimal way this fusion has to be attempted.

Similar approach to Canedo-Rodriguez et al. was attempted by Shi et al. [187]. The authors fused LiDAR and Wi-Fi, to robustify the accuracy of the location estimate. They compare a simple PF approach to their own, achieving considerable accuracy boost in a controlled environment. By using a KF, Chen et al. [33] fused Wi-Fi with landmark information on a smartphone sensor. In this study, the landmarks were found through unique locations of signature traces, such as elevators, stairs and steps. The authors were able to reduce the error of a single Wi-Fi based system by approximately 5m.

Zhang et al. [241] considered the fusion of a variety of sensors to achieve improvement on localisation using PDR, where the user was asked to take a challenging route up and down the stairs. Knauth also considered a PDR application [97] using the fusion of inertial, magnetic and RF sensors through a particle filter. It was again proven, that an inertial-based sensor fusion with Wi-Fi is able to outperform simple Wi-Fi-based positioning. Xing et al. [231] used the fusion of inertial, ultrasonic and optical flow sensors, along with ArUco markers in order to improve the positioning of a small drone.

2.5.1.3 Fusion for Energy Efficiency

In order to ensure continued operation of an IPS, the system itself has to be made aware of its energy usage. This is because the use cases of IPS usually necessitate them being operational for prolonged periods of time. Some of the implementations use smartphones as the computational foundation of their systems [97, 148]. Smartphones have been found to be less efficient than tailored implementations [110], which would suggest that there exists an optimal balance between their computational power and efficiency.

Kwak et al. [110] presented a system, based on the fusion of various inertial sensors and magnetic fingerprinting in order to achieve energy efficient IPS. The authors claimed a lifetime of almost a year on a single coin battery, at the same time reporting an error of 1.6m in a controlled office environment. Sung et al. [198] considered a smartphone-based inertial and RF fusion. In this work, the efficiency comes from the novel fusion implementations provided by the authors, and is validated with a thorough study of computational complexity between algorithms.

In our own work [101], we considered the utilisation of various sensor modalities for energy efficiency, using a Reinforcement Learning approach. Here, we were able to fuse BLE RSS with passive infrared and camera sensing to provide performance improvement over time, whilst retaining energy-awareness at all times.

2.5.2 Methods of Fusion

Having established possible reasons for fusion, we now consider the theoretical interpretations of the fusion methods which were previously mentioned. This sub-section covers various generative and discriminative algorithms which make the fusion possible. They are listed in the order of their relative complexity.

2.5.2.1 Bayesian Networks

Bayesian Networks are often used in order to obtain a fusion of sensors [3, 190]. In a broad sense, Bayesian Networks are a subset of directed acyclic Graphical Models. The nodes of the graph represent random variables which are being modelled. In a multi-sensor setting we can assume that the connections between the nodes in the graph represent their conditional dependencies. In other words, given a set of nodes v, the general form of the joint probability distribution between variables is given by [190]:

$$p(x_1,...,x_N) = \prod_{i=1}^{N} p(x_i|Pa(x_i)) \tag{2.3}$$

where $Pa(x_i)$ are the *parents* of the node.

There are many examples of Bayesian Fusion in sensor fusion literature [76, 81, 100]. He et al. [76] considered an HMM approach to fusion of multiple modalities on a mobile device using different graph structures for online and offline processing phases. Our own work, also based on HMM [100] involved scrutinising a number of different data flow models, which fused RSS and accelerometer data for robustness.

Hoang et al. [81] used a Bayesian approach to fuse RSS and steps detection signals for indoor localisation. The fusion proved superior to methods based solely on RSS. Similarly, Han et al. [69] used a novel approach to Viterbi coding to fuse RSS, Magnetic field and IMU traces to obtain an improvement on positioning accuracy.

2.5.2.2 Particle Filters

Particle Filters or Sequential Monte Carlo (SMC) are a subset of Bayesian Estimation methods. The basic algorithm relies on recursive estimation of the posterior probability of the state x_k given some sensor observation z_k at step k. The objective of this algorithm is to estimate a probability density function associated with state x_k, taking into account all sensor observations up to step k, given by $z_{1:k}$ [9]. This is done by first providing the prediction about our belief of $p(x_k|z_{1:k-1})$ and then updating the probability using Bayes' Theorem. More formally [9]:

$$p(x_t|z_{1:t-1}) = \int p(x_t|x_{t-1})p(x_{t-1}|z_{1:t-1})dx_{t-1} \tag{2.4}$$

which is the prediction given by the Chapman-Kolmogorov equation [9]. The update can then be given by:

$$p(x_t|z_{1:t}) = \frac{p(z_t|x_t)p(x_t|z_{1:t-1})}{p(z_t|z_{1:t-1})} \tag{2.5}$$

Simply put, particle filters approximate probability density function of an unknown state as a recursive function of sensor observations which were observed up to some time. This particular approach has found applications in sensor fusion literature ranging from robotics [145], to activity recognition [182].

In the field of indoor localisation, they are most popular among the fusion of inertial sensors, especially when applied to PDR [6, 85, 171]. Hsu et al. [85] considered the fusion of a foot-mounted IMU and GPS signals to rectify noise drift. A similar approach was proposed by Akiyama et al. [6], albeit without the use of a GPS. There, the PF was scrutinised against energy efficiency, in addition to positioning accuracy. Racko et al. [171] also used particle filtering in service of PDR. They did this by predicting steps and heading from an IMU.

2.5.2.3 Kalman Filters

Kalman Filters are intimately related to recursive Bayesian filtering [48]. The popularity of KF was mostly thanks to its formulation, which allows many different sensor modalities to be arbitrarily modelled by the filter [61]. It is also preferred for its ability to obtain the result in real time. The usual KF formulation follows a pattern of state-space modelling, and their subsequent prediction and update [48].

Formally, the Kalman filter equation for state space input and output responses, in continuous time, are given by [48]:

$$\dot{\boldsymbol{x}}(t) = \boldsymbol{F}(t)\boldsymbol{x}(t) + \boldsymbol{B}(t)\boldsymbol{u}(t) + \boldsymbol{v}(t) \tag{2.6}$$

$$\boldsymbol{z}(t) = \boldsymbol{H}(t)\boldsymbol{x}(t) + \boldsymbol{\omega}(t) \tag{2.7}$$

where $\dot{\boldsymbol{x}}$ is the state vector, $\boldsymbol{z}$ is the output vector, $\boldsymbol{u}$ is the control input, $\boldsymbol{v}$ stipulates the response of the process noise and ω is the noise due to measurement. Additionally, $\boldsymbol{F}$ specifies system state matrix, $\boldsymbol{B}$ is the input matrix and $\boldsymbol{H}$ is the matrix specifying the observations. The usual KF approach has two phases, prediction and update, which we will omit in our formalisation and instead refer the reader to [48, 61].

KF can also be used as part of Extended Kalman Filtering (EKF), which is the nominal method used in literature. There exists a body of work dedicated to EKF for indoor localisation [28, 108, 183, 233]. Kumar et al. used a KF to provide a 3D localisation of an indoor UAV, by integrating a LiDAR and an IMU. Here, the authors used KF to fuse the output of two LiDARs together to achieve 3-dimensional localisation.

There is also a dedicated SLAM approach called EKF-SLAM [202]. In their paper, Vivet et al. [212] used a line-based EKF-SLAM for a robot based application. D'Alfonso

et al. [40] also used an EKF-based approach to SLAM for a robotic indoor navigation tasks, supporting their simulated results with subsequent real life experimental work.

By using EKF, Alatise et al. [7] performed fusion of a 6 degrees of freedom (DoF) IMU sensor. They fused accelerometer and gyroscope to obtain the pose of the robot, i.e. the heading and its location. Kaltiokallio et al. [93] compared the relative performance of PF and EKF. The study concluded that for indoor positioning based on RSS, they are largely similar with the exception of the computational overhead, which favours the EKF.

2.5.2.4 Neural Networks

Due to the emergence of Artificial Neural Networks (ANN) in the recent years, a number of researchers have considered the use of a tailored network for sensor fusion. Most of the approaches use Deep Neural Networks (DNN) [111, 123, 218]. While there exists a body of literature dedicated to objective-specific fusion methods using ANN [205, 208, 209, 235], there is an evident lack of standarisation between the positioning methods, and it still remains largely unexplored.

Interestingly, ANN has often been used as a pre-processing step before actual fusion [208, 209, 218]. Whilst not strictly related to indoor positioning application, Vargas-Meléndez et al. [208, 209] used an ANN to estimate the pseudo roll angle of a vehicle, before performing fusion based on a PF. Wang et al. [218] performed indoor localisation, using CSI and deep learning. They were able to extract the location features by weighting them, using an ANN. This was later fused together during an online phase of their algorithm.

Liu et al. [123] proposed using deep learning for scene recognition and fingerprinting tasks. Using a smartphone, they were able to perform scene recognition from pictures using deep learning. Based entirely on the deep learning architecture, Lee et al. [111] performed localisation based on ambient magnetic field. They extracted magnetic features, as well as odometry and fed them to the network to obtain a robot's position.

2.6 Conclusion

In this chapter, we have reviewed the popular sensor modalities which are currently being used for indoor localisation. First, we have detailed each sensor modality and have given a thorough literature overview for each. The modalities were then scrutinised under widely accepted evaluation criteria. Then, we outlined the recent attempts at fusion and the most popular combination of sensors, considering context-specific consolidations. Among

them were Robustness, Accuracy and Energy Efficiency. Finally, we have considered the popular sensor fusion methods, which range from Particle to Kalman Filters. We have also considered the basic modelling and inference methods for the work contained in this thesis.

CHAPTER 3

DATA GATHERING AND DEPLOYMENT TECHNIQUES

This chapter will consider the methods, techniques and approaches for data set collection for residential indoor localisation. The data described in this chapter will be used extensively (but not exclusively) throughout this thesis. Chapter will begin by outlining the related research, with a specific focus on localisation-specific datasets and the sensors used therein. The first half of the chapter will outline the understanding behind indoor localisation using WSNs as applied to residential environments, and provide the reasons why the existing, available datasets fall somewhat short to the main ambition of this thesis.

The remainder of this chapter will concentrate on the author's own data collections. Firstly, we will outline the sensor infrastructure used, as well as methods of ground-truthing of the data. This will be followed by the typical output for sensors used in this study, as well as a rudimentary classification method for indoor localisation. The final section of this chapter will embark on a much more extensive collection spanning numerous houses and participants. This collection can be considered as one of the main contributions of this thesis. We will close by discussing the challenges faced during the collection campaigns, and give novel approaches to mitigate these shortcomings.

3.1 Related Work and Contributions

Collection of data pertaining to indoor localisation, in itself, is not a novel task. There exist various studies which are concerned with indoor data gathering involving various robotic [56] and human tasks [135, 197, 203, 204]. Fallon et al. [56] produced a comprehensive dataset containing RGB-D, LiDAR and proprioceptive sensing, in the service of indoor mobile robotic training. Torres-Sospedra et al. [203] created a database of fingerprints for WLAN applications using handheld smartphone devices, across multiple buildings. Sun et al. [197] used LiDARs and Cameras to obtain a thorough dataset for camera-based localisation.

The above datasets, however, are not all suited for the testing of models for residential applications. This either due to the fact that their intended application did not consider human participants [56] or the target environment does not resemble residential abodes [203]. Acquiring and modelling data from real residential environments using real human residents is, understandably, difficult. However, there exist some dataset which have tackled this problem. Twomey et al. [204] produced a SPHERE Challenge dataset, comprising of various environmental and on-body sensors in a residential environment. This dataset included as many as 20 participants performing scripted activities. McConville et al. [135] performed similar residential study, using novel method of sensor calibration for activity and localisation estimation.

The above methods are most closely related to the work undertaken in this chapter. We aim to alleviate some of the challenges and issues which presented themselves during the collection and subsequent analysis of the above datasets, by reusing the same house as Twomey et al. [204] and same infrastructure as McConville et al. [135] and Pope et al. [160]. We show that the residential environment can be modelled with granular resolution and that the proposed structure prediction algorithms are viable. The contributions of this chapter include:

1. We present the infrastructure which is used to perform data collection, as published in [135, 160].

2. Then, we show the raw data which is to be expected from this sensor infrastructure, by outlining a brief infrastructure testing study.

3. Later, we outline a new dataset, as published in [24].

4. Finally, we illustrate the viability of this dataset and provide the theory behind modelling of the above data for the subsequent analysis in this thesis.

3.2 Indoor Localisation with RF Sensors

3.2.1 On Residential Environment in Indoor Localisation

Residential localisation is just one of possible application areas pertaining to an IPS. As it was mentioned in chapter 2, there exist various other environments where obtaining a viable positioning result is important [83, 94, 131, 216]. Indeed, with such a broad application area, the space for algorithmic design tailored to a specific function is correspondingly large. As an emerging field of study, the area of residential localisation has enjoyed a steady increase in published literature, with methods ranging from simple path loss models [20] to fine-grained probabilistic algorithms [100]. Continuing with this trend, we aim to show how residential localisation can be utilised in the context of healthcare, and how its utilisation can benefit those in society, which require the most assistance.

The main beneficiaries of a residential indoor localisation system vary, from the dwellers themselves, to clinicians who would be analysing their progress. Assuming a non-intrusive nature of a given IPS, the system itself can fit seamlessly around the lives of its users, possibly used in a longitudinal setting. Having access to this information, the users can in turn adjust other aspects of the house to fit their needs, for example automated location-centric heating providing energy savings over time. As it was mentioned in the introductory example, clinicians are able to monitor their patients relatively non-intrusively, showing them a real picture of their patients in their home environment.

At first glance residential localisation might appear a simple problem, when compared to, for example, localisation in industrial halls and hospitals. However, even though smaller on average, residential environment rarely enjoys concessions attributed to these examples. The main difference is the granularity of the possible space, which the algorithm has to negotiate in order to become viable. Taking hospitals as an instance, the main objective of its localisation system is to keep track of patients which might for example, be confused and lost in the building. In this case, the granularity of room, or even floor level would suffice. This is not the case in a residential setting, where the user can be performing different tasks in different areas of the same room. The resolution of available locations would need to be correspondingly small, as to account for the large space of typical household activities.

However, while the residential aspect of localisation brings numerous advantages, it also suffers from various challenges which have either not been addressed yet in the

literature. One of the central issues surrounding these methods is their continuing invasiveness. Thus far, there exist very few implementations which address this particular theme. The other issues with residential IPS include the need for it to become generally applicable. Houses, even when built on similar plans, cannot be assumed to sustain localisation models in the same way, that is, expecting the models to perform at the same level of performance. Current applications require arduous fingerprinting, the method and challenges for which were outlined in chapter 2. This method however, cannot be realistically generalised to other abodes, if only due to the furniture in different house almost guaranteed to differ in shape, material and placement. The adaptability of an IPS remains a crucial, yet relatively unexplored, section of the literature.

Residential localisation also suffers from signal occlusion and shadowing effects. Whilst this is also true for other application areas, such as hospitals, the sources of shadowing in residential localisation are mostly the users themselves. This, coupled with the fact that they traverse much smaller spaces, makes the environment much more dynamic and, accordingly, less predictable. Finally, there exist numerous examples of adversaries which, under some conditions, are able to not only obtain the tracking information of a house dweller, but also would be able to identify them outright. Attacks can also come through spoofing attacks and injection of noisy and erroneous data. This can be very detrimental to the recovery efforts of a patient if targeted by such an attacker.

3.2.2 Wireless Sensors in Networks for Residential Dwellings

The current state-of-the-art solution for indoor localisation is concentrated around WSNs. These networks offer an infrastructure solution, which can provide a relatively seamless integration into a user's life. Their non-intrusive nature has been studied before in residential settings [160, 225, 226], and have been proven to perform well in this context. The recent influx of literature pertaining to pervasive network for monitoring of health can be attributed to decreased cost of sensors, as well as their ubiquitous availability, as addressed in chapter 2.

Localisation in WSNs follow the method outlined in chapter 2. The popular way of utilising RSS ranges from deterministic [20] to probabilistic [100], in that the locations can be estimated with respect to some confidence metric or can be established by calculating the position exactly, relative to path loss models [20]. Both avenues offer their unique advantages and disadvantages.

Ordinarily, residential location based purely on probabilistic models is difficult to estimate exactly. This is because no one general model exists, and each model would have

to be tailored to each unique house. Exemption to these, are models designed specifically with generalisation in mind. Path loss models, especially ones considering in-depth propagation, can offer a much more fine grained localisation result. However, parameters and coefficients will not be transferable between houses. That is, radio propagation characteristics are as unique as the house they describe. This makes deterministic localisation difficult to generalise. In the context of residential localisation, the method would have to be easy to implement and easy to train, due to the uniqueness of each individual house, as well as due to speed and efficiency of infrastructure deployments.

In this thesis, we will use the SPHERE-in-the-box infrastructure developed as part of the EurValve project [160]. This particular infrastructure leverages ease of use, availability of the hardware and quality of data. It is based on a widely available hardware, as well as bespoke sensors produced as part of the SPHERE project [55]. The main aim of this infrastructure was to make it simple enough for non-technical users to deploy and use effectively, whilst at the same time collecting fine-grained sensor data about the user.

This thesis' main contribution to the method outlined in this particular section is the validation and testing of the deployment kit. This kit has been provided as part of the study, in order to test the viability of this infrastructure. It was tested throughout a weekend in 2017. The second contribution is the subsequent pre-processing and analysis of the collected data, including the classification, as seen in Figs. 3.2 and 3.3.

The user carries a wearable sensor on their body at all times. This particular wearable sensor [55] was designed to be worn on the wrist, in order to remain as unobtrusive as possible. The wearable uses a ADXL362 accelerometer sensor processed by a CC2650-based system-on-chip Cortex M3 processor. The accelerometer samples the acceleration of the user's wrist at the rate of 25Hz in 3-dimensional space [55]. The infrastructure also includes a number of AP nodes, which act as signal anchors and main processing plants of the infrastructure. In this implementation, a number of Raspberry Pis (3 Model B) have been used. These particular models include a PCB chipset BCM43438 antenna. The node utilises BLE protocols to transmit data between the wearable and the AP at the rate of 5Hz [24, 160]. The entirety of the system is then connected, via Wi-Fi, to a TP-Link modem, which enables the analyst to access individual Raspberry Pis and extract encrypted data and information.

From this implementation, two unique sensor modalities are monitored. Firstly, the acceleration of the user's wrist as the user performs every day activities. The output of this sensor has be used to perform activity recognition [160] and used as a complimentary modality in location inference [100]. Acceleration can also be an indicator of the relative

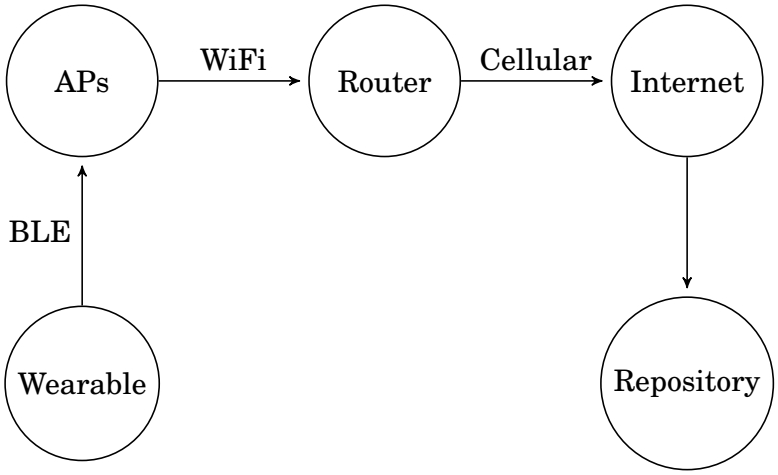

Figure 3.1: Block diagram showing the links in the SPHERE-in-a-box system. Courtesy of Pope et al. [160].

level of activity in the house, and serve as a measure of calibration quality during training [136]. Secondly, the wearable send the data directly to each available AP via BLE. As mentioned previously in this thesis, the calculation of received signal strength from a wearable is a good indication of relative distance between the transmitter and the receiver. As the user traverses the environment, the signal strength from APs located further away, or occluded by obstacles, will be small or non-existent (so called dropped packets). Interestingly, the measure of packet drop, as a function of all packets sent in a given time interval, is also a good indicator of location [100].

Figures 3.2 and 3.3 show an example of raw RSS and accelerometer data. This data was collected by the author, over two days, using the aforementioned SPHERE-in-a-Box infrastructure. They are provided to acclimatise the reader with the raw readings which the infrastructure produces. In Fig. 3.2, the Received Signal Strength Indicator (RSSI) measure shows the radio strength in dB from 3 unique APs placed in prescribed locations in the author's house, that is Living Room, Bedroom and the Kitchen. This figure also shows the output of the location classifier, which works by estimating the location based on the highest signal strength at a given time.

This basic classifier assumes direct mapping from sensors to locations and as such can only provide a very coarse estimation of location. This is possible due to path loss characteristics [20], where signal strength will be largest in LoS conditions. This can usually provide acceptable performance [20, 100] at so called 'room-level'. Figure 3.3 shows the magnitude of the acceleration, and the output of a binary activity classifier as seen across the same time scale as Figure 3.3. The k-NN classifier was trained on

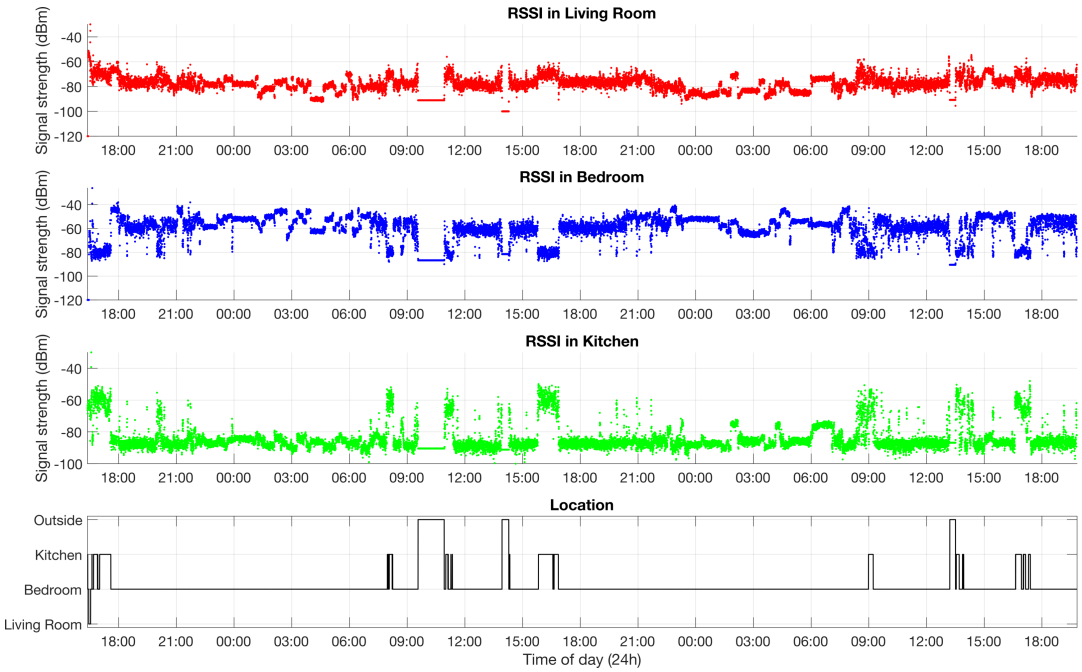

Figure 3.2: Example of RSS Indicator data, with a basic room-level location classifier, as collected by the author over a weekend in Feb. 2017. Courtesy of Pope et al. [160].

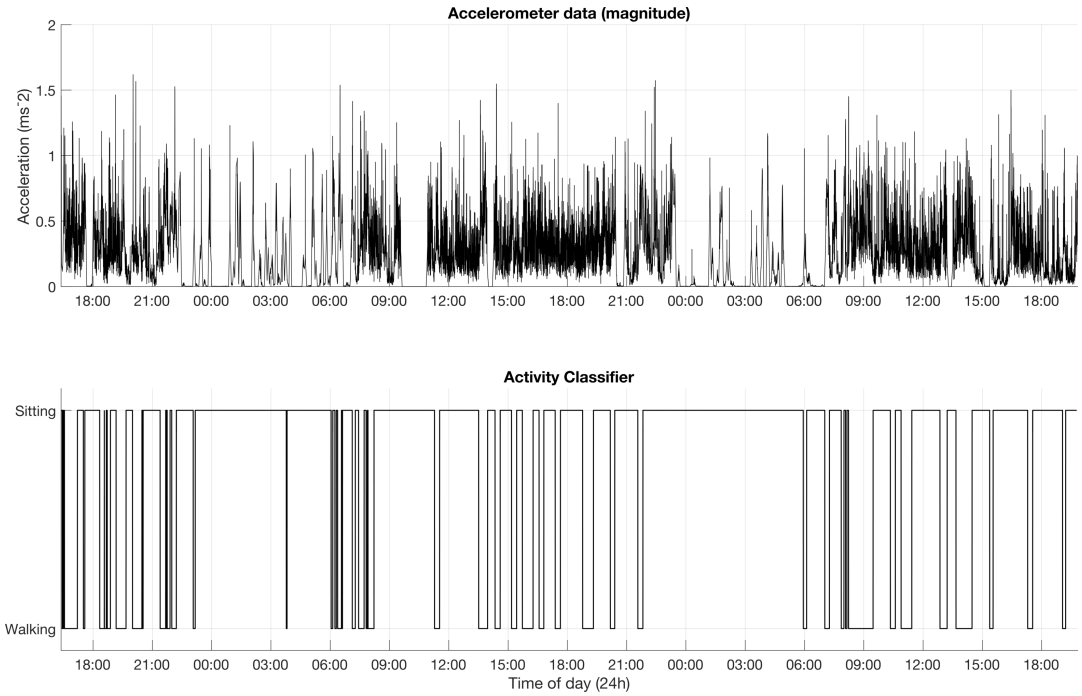

Figure 3.3: Example of accelerometer magnitude data, with a basic activity classifier, as collected by the author over a weekend in Feb. 2017. Courtesy of Pope et al. [160].

the author's own data which included 10 minutes of walking and 10 minutes of sitting, effectively providing a binary classification between movement activity and no activity.

From the classified activities and locations, the patterns governing a normal day are quite evident. The kit was installed at 17.00pm on a Friday, signifying the beginning of collection on the graph. Immediately after installation, dinner was being cooked. This is shown on Fig. 3.2 by classifying the location as kitchen, and increased accelerometer activity on Fig. 3.3. These types of patterns are actually evident throughout the entirety of the experiment. Note, that there are visible spurs of kitchen location with an increased wrist activity, during breakfast, lunchtime and dinner time. Additionally, the activity classifier was able to show how well or poorly the author has slept, by correctly identifying that the user has an increased activity at 3am on a Saturday morning (which was confirmed by dairies kept the author throughout the experiment). The grey labels show the time when the author left the house.

The previous figures show, that even the most rudimentary classification can show valuable information about the user. It also served to motivate WSN in the context of residential IPS. Clinicians with access to such data could have a small, approximate, picture of their patient's lives. This in turn would enable them to provide valuable feedback regarding their recovery, as well as be able to tailor the treatments using their unique data.

The purpose of this analysis was to show how this data can be presented and what conclusions can be drawn from it. This analysis is not exhaustive, and served only to illustrate the capabilities of this infrastructure. In order to obtain a much larger picture of a patient's well-being, the localisation should be more resolute. By having a system with a larger resolution, it is theoretically possible to uncover a much larger space of behaviours, as the rooms themselves can be split into smaller segments where patient's dwell and perform different activities. Additionally, the activity classifier was only able to show a binary output. By obtaining a larger space of user-specific data pertaining to activities, it would also be possible to uncover a wider range of possible actions taken by the participants.

3.3 High Resolution Residential RSS Measurements with Activity Labels

In this section, we outline data collected between April 2017 and January 2018, which included high resolution labels, as well as activity information for a range of different

users. This collection utilised the same infrastructure, described in 3.2.2. This collection was performed across 4 different residential abodes in the Bristol area [24]. This dataset will henceforth be referred to as High Resolution Localisation (HRL) [1] dataset. There are a number of aims which this novel dataset will address:

- Show the impact of high resolution labels for residential indoor localisation.
- Demonstrate the difficulty with generalising IPS across different residential environments.
- To provide high resolution activity data, and show its usefulness in the context of localisation.

3.3.1 Methodology and Scale of the Collection

To start, we will discuss the issues with collection of high resolution localisation data from residential houses. Then, we will outline the procedure followed to solve this challenge. After briefly describing the types of data collected, as well as the labels contained therein, we will proceed to showcase and analyse this dataset, as to prove its viability and highlight specific issues found when performing this type of collection, using the described infrastructure, across various residential environments.

When considered as a localisation test bed, the 2-dimensional floor plan of a residential house can be thought as continuous, in that there exist infinitely many descriptions of locations in that plan. Estimating location in such a space would not be tractable, in that, given an infinite space, its description is also infinite. In order to approximate this space, we perform discretisation of the floor plan into specific states, as a representation of a small section of the living area. The floor plan of all 4 houses was therefore discretised into 1m $\times$ 1m states. Here, it is important to note, that the sizes of the states are also not exact. The topology of the house plan often disallowed perfectly sized states, and so they have been rendered to the best of the authors' knowledge and experience.

The house is outfitted with the same aforementioned wireless infrastructure. The states are then labelled with a specially adapted fiducial markers, with their label clearly encoded. These fiducial markers are all directed toward the same relative direction in the house, as to preserve the direction of movement, when traversing the house. The participants are then asked to wear the wearable sensor, like before, however in addition,

[1] Available at: `https://figshare.com/articles/Residential_Wearable_RSSI_and_Accelerometer_Measurements_with_Detailed_Annotations/6051794/1`

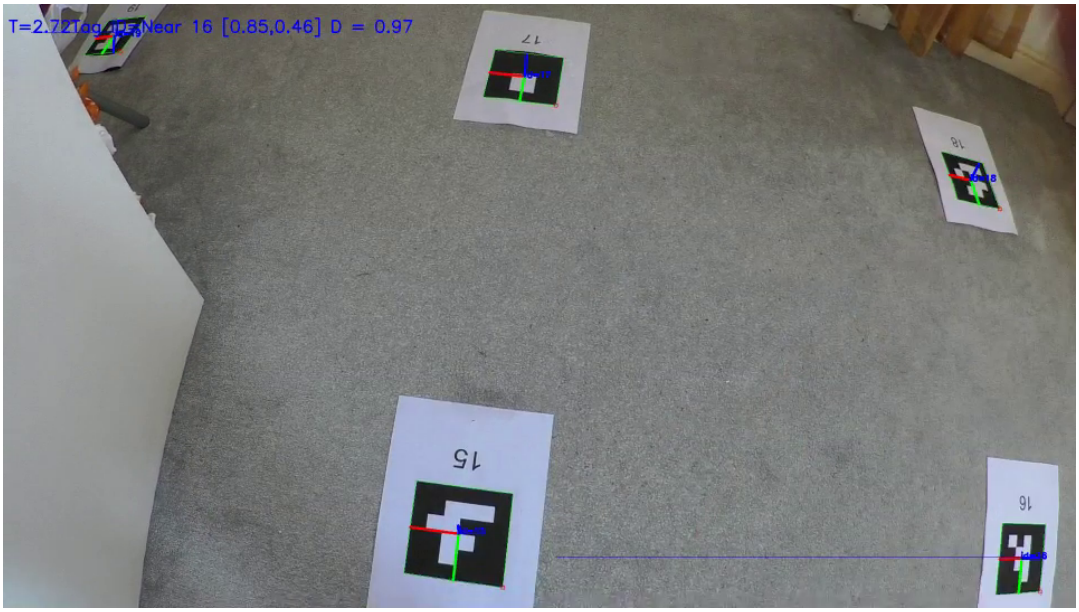

Figure 3.4: Example of a camera still from the data collection. The fiducial tags are visible, all pointing to the same direction. This picture was taken after the processing, and the estimated location coordinates and orientation are visible in the upper left corner.

they also have to wear a Panasonic HX-A500E-K camera on their abdomen area, as to ensure clear visibility of the floor.

The experiments begin when the user flashes the clock in front of the the camera, synchronised with an Network Time Protocol (NTP) server, to ensure proper coordination between infrastructure timestamps and the camera footage. This is assured through ELAN Software [1]. The same is then done at the end of each experiment. The user is then free to roam, performing experiments inside the parametrised area. After the experiment, the relative location and orientation of the user at specific times can be extracted by estimating the distance of the camera to various tags within the Field of View (FOV). Note here, that the tags are all coordinated, relative to 'Tag 0'. Figure 3.4 shows the example screen capture from the processed footage from House 1.

The users perform various experiments in the houses. The variability of experiments ensures that the collection in each house is as thorough as possible. We will now discuss their viability. First and foremost, the houses were carefully fingerprinted. Fingerprinting is the mechanism of acquiring the description of the state space, by visiting all prescribed locations. Each house was provided with two different fingerprints:

1. Slow Fingerprint, where the user spent 80 seconds in each state, turning towards

each cardinal orientation. This type of fingerprint took 16 minutes on average.

2. Fast Fingerprint, where the user would 'fly-through' each state, spending only a few seconds in each location. This would take 7 minutes on average.

In addition to these fingerprints, the users also performed 'living' experiments. These types of studies originated from the need to provide a viable picture of a living participant in their house. The basic principle was that the users would perform every day activities, such as cooking or watching TV, but whilst monitored by our infrastructure. Additionally, these types of experiments would associate accelerometer signatures (and consequently activities) with specific locations in the house.

Living activities varied from house to house, as to best provide a range of possible 'candid' scenarios of everyday life. Some specific activities during these experiments would include, for example, watching television, or making a cup of tea. Some data has also been collected for house-specific activities. This could have been because this house included a special room (such as a study or living room/kitchen combo), or included a specific piece of furniture.

The fiducial tags would also serve as labels for activities during living experiments. These activities would be labelled by unique integers as to ensure no ambiguity between activities and states. Each user would again 'flash' the fiducial tag in front of the camera to signify the beginning of the activity and 'flash' again to signify its conclusion. These labels would later be used to timestamp specific accelerometer traces, corresponding to high-level activities like 'Living Room Activity', 'Bedroom Activity' and 'Bathroom Activity'.

The dataset includes 4 unique houses. Each of the house would also include new participants. There are varying amounts of living experiments across the houses, as this was not standardised. The collection of fingerprints and activity labels was however necessitated from all of the participants. This ensured, that at the very least the dataset consisted of viable training data, for both location and activity recognition, in each house. The floor plans, presented as the quantised 'tile' structure outlining the positions of the states, rooms and APs, are given in Figs. 3.5, 3.7, 3.8 and 3.9. Note that these floor plans also include the location density derived from the camera post-processing step. Additionally, the description of all experiments performed in these four houses, including their duration, users and brief descriptions can be found in Tables 3.2, 3.3, 3.4 and 3.5. The high level description is given in Table 3.1.

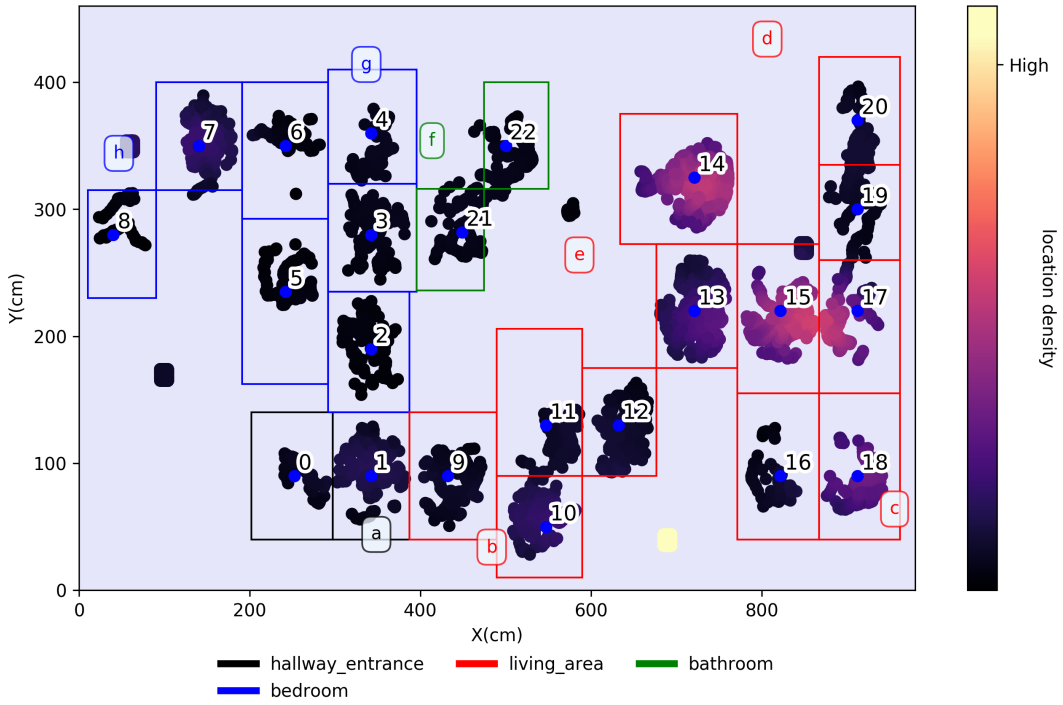

Figure 3.5: Example of the discretised state space of House 1, with extracted locations. The colours intensity signify the frequency of occurrence in these locations. Courtesy of Byrne et al. [24]

Figure 3.6: The author performing 'Living Room Activity'.

3.3.1.1 Cross-validation and Data Stratification

This chapter introduces the reader to the scope of the available data. This data included experiments, which were specifically designed for the training phase of the algorithm, as well as more candid living observations. The relatively varied spectrum of these experiments allowed for the choice of the training and testing data to be equally varied.

Fingerprinting experiments have been used to train the data where applicable. While these experiments would describe the entirety of the state space in detail, they would, for example, fall short when describing the acceleration of the user as they traverse the environment and perform various tasks. This is with the exception of the fingerprint_activity, which exists for this particular reason, and which could be used in conjunction to fingerprint_location in order to train the algorithm.

Living experiments would also be used to train the model if required. However, since living experiments were much less structured than fingerprinting, they covered a larger (and more realistic) space of state transitions, as opposed to fingerprinting. Therefore, the use of living experiments for training would be warranted in cases where the model is being tested for robustness.

Additionally, the model could be trained on a cross-validation scheme. In order to obtain a viable picture of the environment, the training strata could include a subset of the living experiments, which prescribe the realistic training scenario, as well as fingerprint data, which populates the state space model with data in every state.

The strategy of cross-validation and subsequent stratification of the data would be dictated mostly by the problem which they are set to solve. As such, the training and testing splits will be described in the forthcoming chapters.

3.3.2 Collected Data

The timestamped and labelled accelerometer and RSS data was then associated with the locations extracted from the video. Each state would therefore be described in terms of this data. By acquiring data in such a high resolution, the dataset ensures that the granularity of each descriptor is high. For the fingerprinting experiments, for every existing state in the environment, there are at least 80 seconds of RSS signals. However, in terms of free 'living' experimentation, the users would not visit certain states for the duration of the experiment. This was done to closely simulate the possible consequences of daily life, as there exist spaces where the participants are less likely to visit.

The RSS data itself has to be modelled in terms of arriving signals. When projected

House	**Type**	**APs**	**Floors**	**Rooms**	**Duration** (minutes)
1	Apartment 1 Bed	8	1	4	89
2	Terraced 2 Bed	11	2	11	171
3	Terraced 3 Bed	11	2	9	319
4	Terraced 2 Bed	11	2	10	250

Table 3.1: Outline of the houses used in the data collection study. Courtesy of Byrne et al. [24]

Experiment	**Duration**(minutes)	**Type**	**User**
fingerprint	32.6	Four orientations of floor tags	a
walking_rapid	3.0	walking hastily	a
walking_natural	3.4	walking naturally	a
living_1	8.5	living	b
living_2	9.2	living	a
living_3	26.5	living	a
living_4	5.4	living	a

Table 3.2: Outline of the experiments in House 1. Courtesy of Byrne et al. [24]

Experiment	**Duration**(minutes)	**Type**	**User**
fingerprint_floor	107.0	Four orientations of floor tags	b
fingerprint_activity	5.2	Activity training	a
fingerprint_rapid	5.6	Rapid training of floor tags	a
walking_rapid	3.0	walking hastily	a
walking_natural	3.0	walking naturally	a
living_1	14.4	living	b
living_2	7.4	living	b
living_3	14.2	living	a
living_4	11.2	living	a

Table 3.3: Outline of the experiments in House 2. Courtesy of Byrne et al. [24]

into histograms, the data follows, approximately, a Gaussian distribution. This is best visualised by plotting the distributions of each AP in each room. Note, that the resolution of these labels was increased, to help visualise how the data differs in different areas of the house. The corresponding house plan is available in Fig. 3.5.

Regarding accelerometer data, the actual modelling would follow extraction of feature traces with respect to required model. For example, real time tracking application would favour extraction of acceleration and velocity from the data, whereas offline modelling would consider various activity traces as performed in various locations.

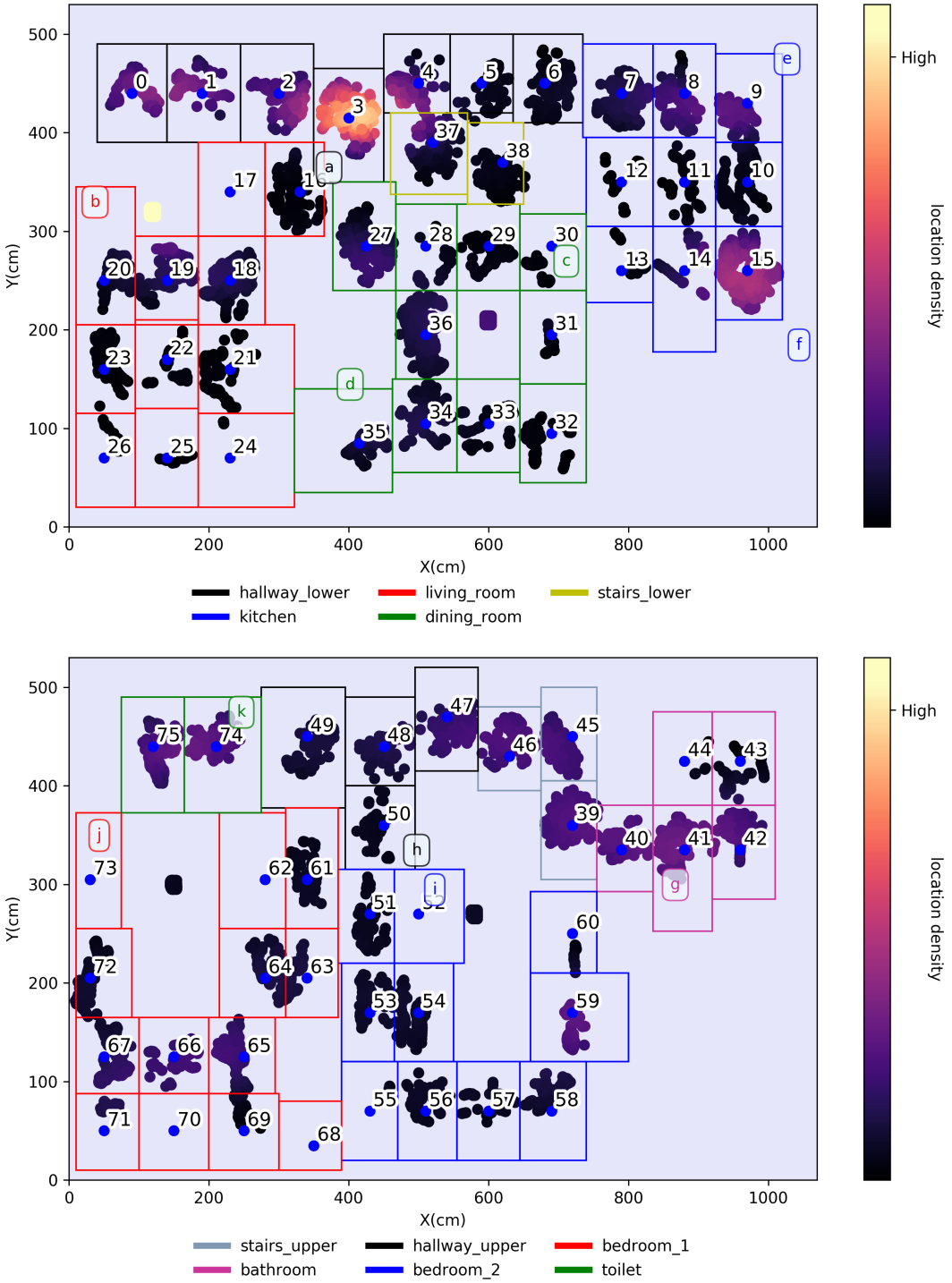

Figure 3.7: Example of the discretised state space of House 2, with extracted locations. The colours intensity signify the frequency of occurrence in these locations. Courtesy of Byrne et al. [24]

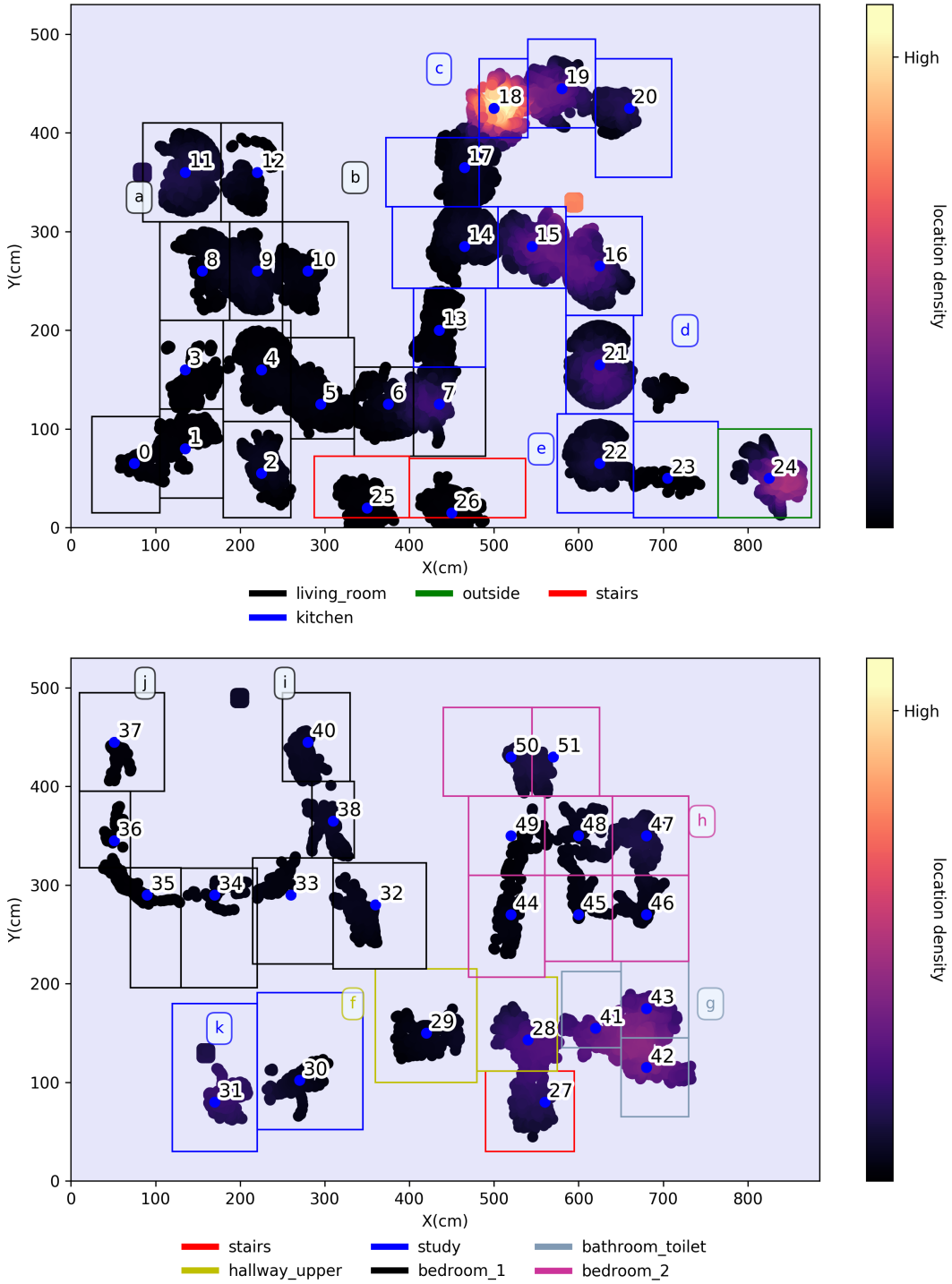

Figure 3.8: Example of the discretised state space of House 3, with extracted locations. The colours intensity signify the frequency of occurrence in these locations. Courtesy of Byrne et al. [24]

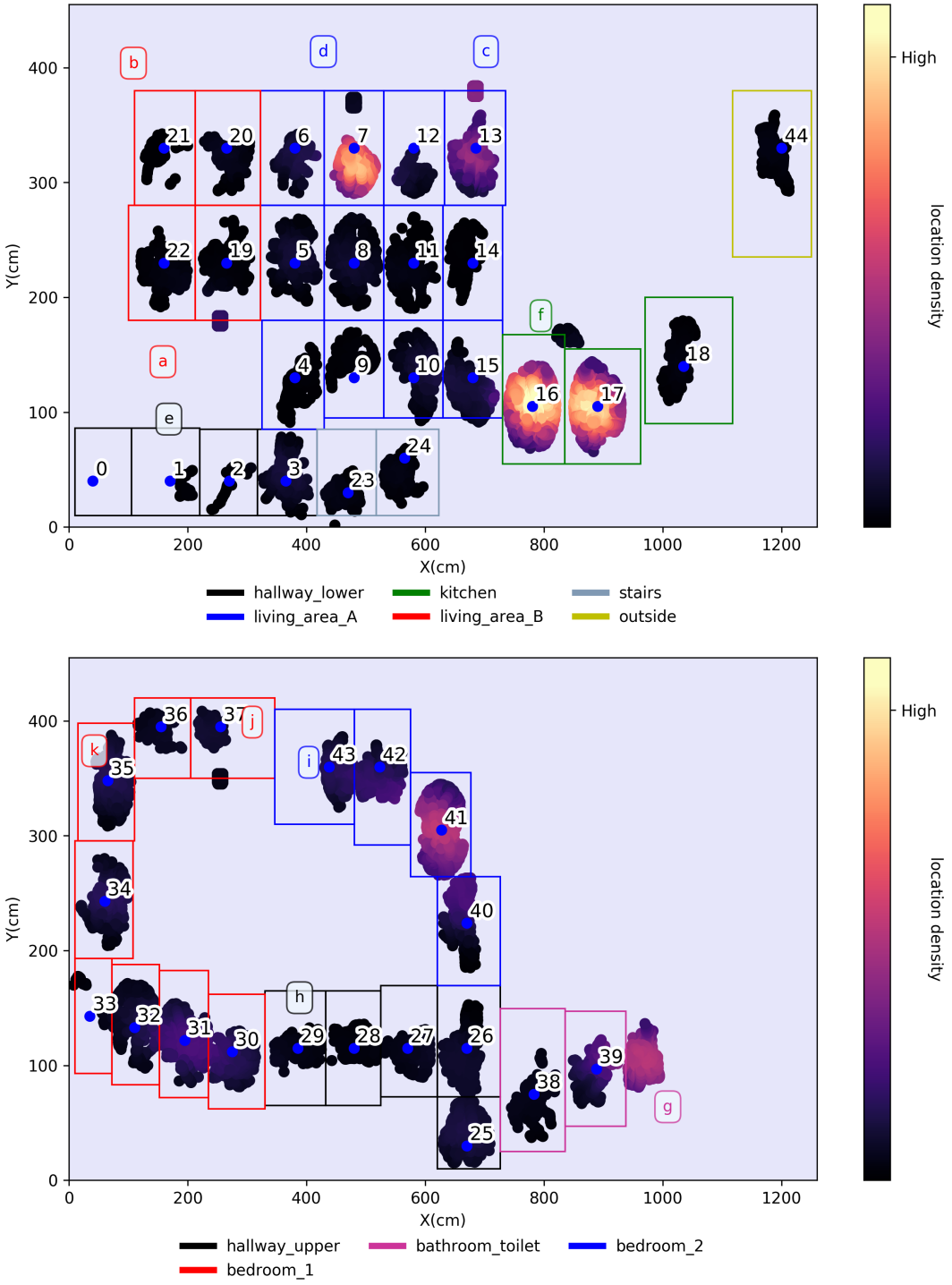

Figure 3.9: Example of the discretised state space of House 4, with extracted locations. The colours intensity signify the frequency of occurrence in these locations. Courtesy of Byrne et al. [24]

Experiment	**Duration**(minutes)	**Type**	**User**
fingerprint_floor	71.4	Four orientations of floor tags	c
fingerprint_activity	4.6	Activity training	c
fingerprint_rapid	6.0	Rapid training of floor tags	c
living_1	30.7	living	c
living_2	5.4	living	c
living_3	22.1	living	c
living_4	8.0	living	c
living_5	9.7	living	c
living_6	60.0	living	c
living_7	30.8	living	c
living_8	8.4	living	c
living_9	8.6	living	c
living_10	53.3	living	c

Table 3.4: Outline of the experiments in House 3. Courtesy of Byrne et al. [24]

Experiment	**Duration**(minutes)	**Type**	**User**
fingerprint_floor	62.9	Four orientations of floor tags	b
fingerprint_activity	4.8	Activity training	b
fingerprint_rapid	4.0	Rapid training of floor tags	b
living_1	29.8	living	b
living_2	58.7	living	b
living_3	16.9	living	b
living_4	30.0	living	b
living_5	43.0	living	b

Table 3.5: Outline of the experiments in House 4. Courtesy of Byrne et al. [24]

The actual modelling of this topology will follow later in this thesis. Here we will only demonstrate how well this data can differ between various locations in a residence. Here, we consider the variance of accelerometer magnitude. We will initially examine the data as prescribed to a 'walking/standing' activity, before considering the more granular activities themselves.

Note here, that the traces seen in the above Figures are generated from high level labels of 'walking/standing'. As such, there exist many underlying activities which compound into said labels. This describes why these traces are not wildly different. Regardless, the extracted variance clearly shows that walking generates more varied signal traces than standing. Additionally, it is evident that the traces behave differently

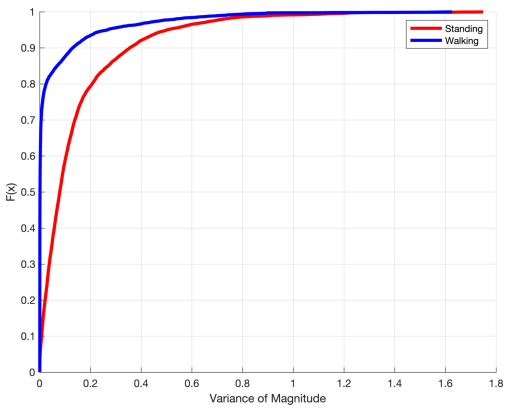

Figure 3.10: House 1

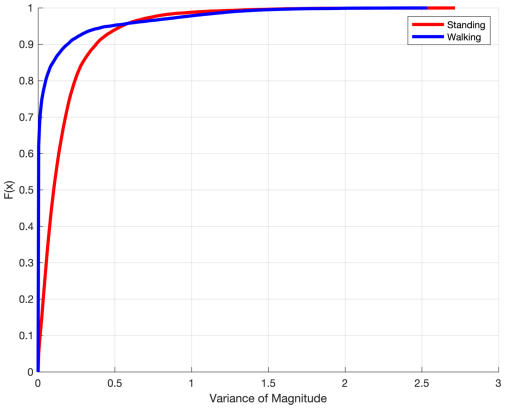

Figure 3.11: House 2

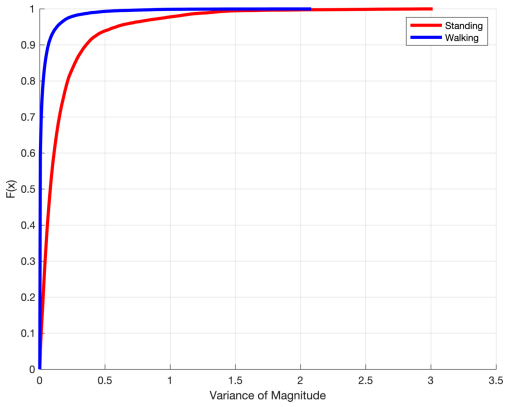

Figure 3.12: House 3

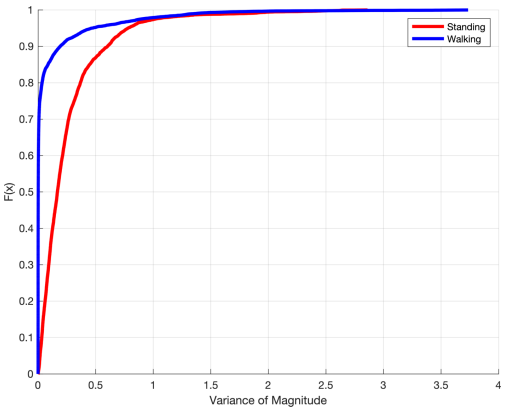

Figure 3.13: House 4

across different houses. For example, House 3 in 3.12 provides a less 'vigorous' stationary action than other houses.

The low-level activity labels provide a more in-depth insight into the differing accelerometer signals in each house. Consider Figs. 3.14, 3.15, 3.16, 3.17. The plots again represent the extracted variance of the accelerometer magnitude for various labelled tasks. The graphs have been colour coded in order to show similarities and differences between similar tasks across all of the houses. It is evident, that where available, the 'Sink Activity' in the bathroom provides most varied signals. This is largely due to the actions performed in that location, i.e. brushing teeth. A more vigorous teeth brushing provides large acceleration in all three dimensions. 'Kitchen Activity', also where available, follows closely after that. Clearly, describing kitchen through washing-up traces shows largely varied signals across various residences.

The above Figs. 3.10, 3.11, 3.12, 3.13 and 3.14, 3.15, 3.16, 3.17 are calculated using the

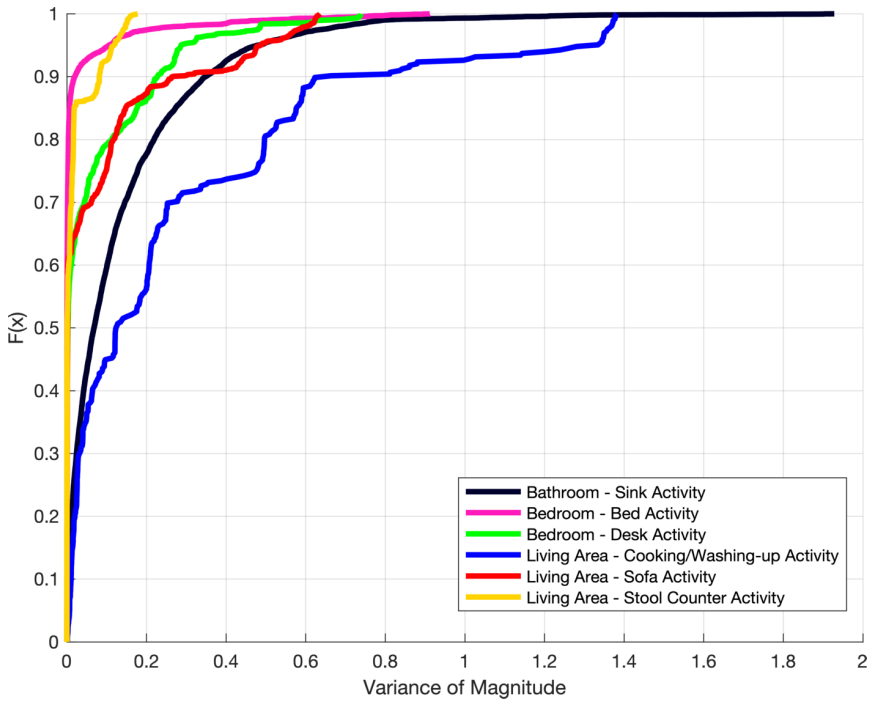

Figure 3.14: House 1

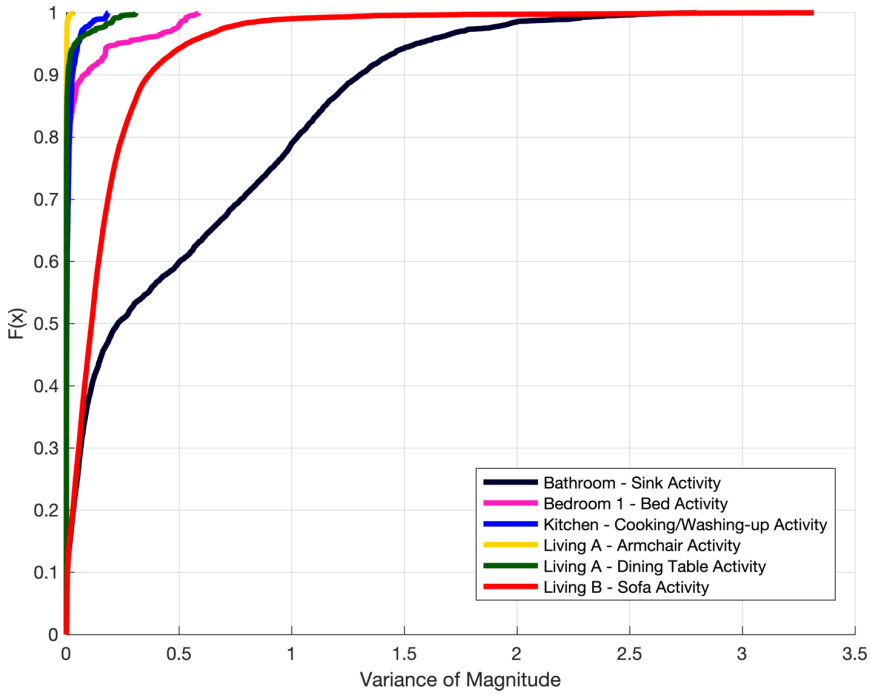

Figure 3.15: House 2

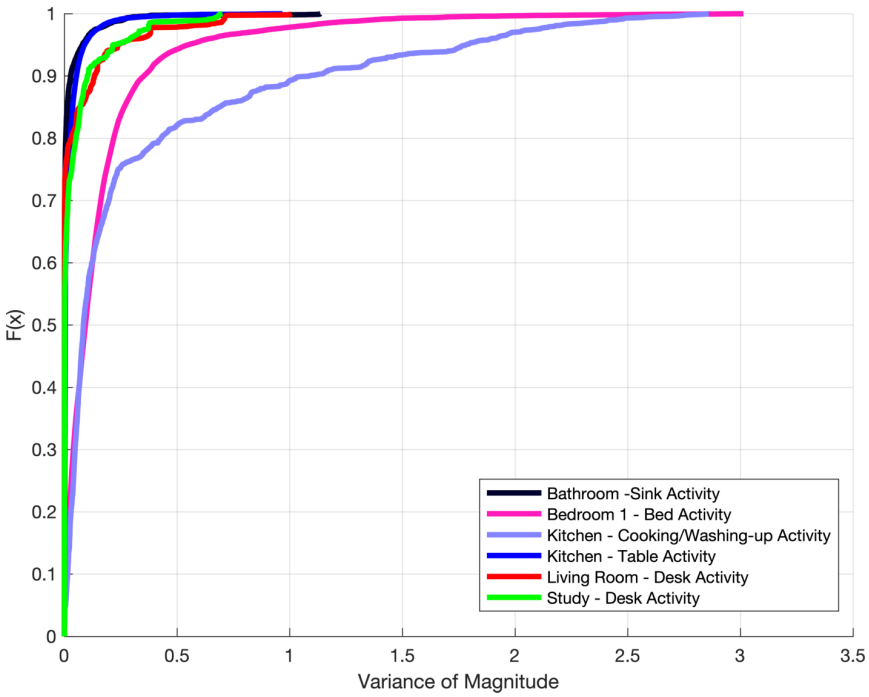

Figure 3.16: House 3

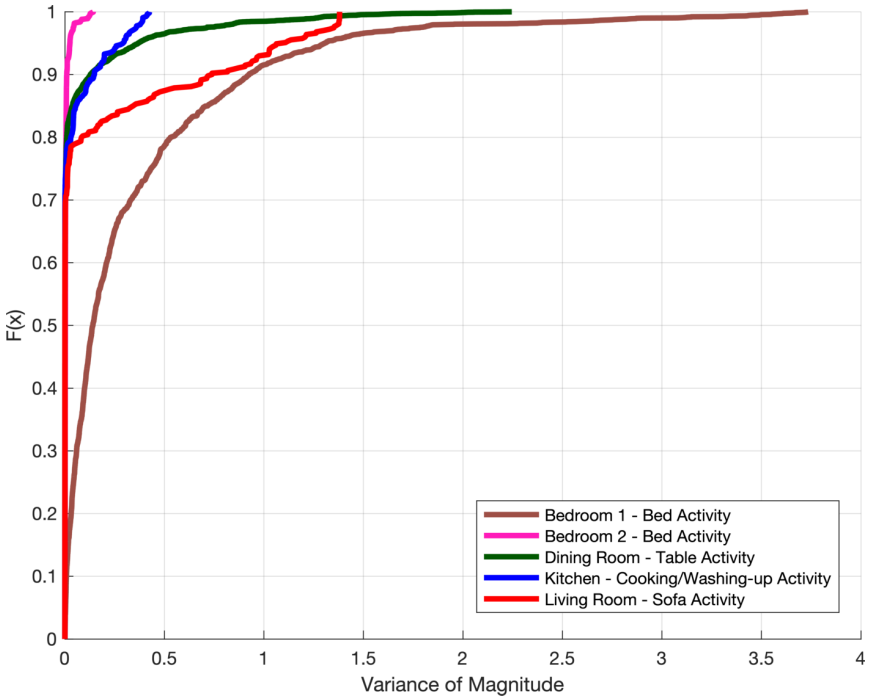

Figure 3.17: House 4

calculation of empirical cumulative distribution function of the variance of the magnitude of the accelerometer signal. The window of calculation was set at 6.4s. Formally, if $||\mathbf{x}||$ is the magnitude of x, y and z, then the variance is given by:

$$Var(||\mathbf{x}||) = E[(||\mathbf{x}|| - \mu)^2] \tag{3.1}$$

We conclude this section by noting that whilst wrist-worn accelerometer data might not be optimal in terms of 'dead-reckon' navigation, it can paint the picture of various activities which are being performed in the house. Considering the likely location of these activities, one can use this data to further robustify the location estimate. Additionally, any dynamic model of localisation can use this data in order to establish likely transition mechanics for a given house, and a given user.

Presented data serves to illustrate the type of sensor signal trace to be expected as part of a high resolution localisation. We have outlined the RSS data and provided a viable model which can be used in order to approximate the generating source. We backed up this model by showing the distributions of RSS in various places in the house, and its relationship to APs. We also described how to deal with missing data, in the context of dropped packets, and stipulated that simply by knowing the total expected number of packets, we can calculate the drop rate for specific locations in the house. Additionally, we presented the accelerometer trace data, and demonstrated how its dynamics across houses. Firstly, we showed that there exists a difference in what accelerometer traces we can expect from different houses, suggesting that the topology of the house has a direct impact on the amount of activity. Then, we outlined more granular activities, and established that even across different residential houses some activities are comparable.

3.4 Conclusions and Challenges

This chapter outlined current trends in indoor localisation test beds, provided reasons due to which this thesis required a collection of novel data, presented a method for the collection of indoor localisation data using a pervasive monitoring infrastructure and showed methods of modelling of the sensor output of said infrastructure. Whilst considered state-of-the-art, this type of methodology of collection still presents numerous obstacles, which will be outlined shortly. These challenges should not, however, decry the potential of this method for residential deployments. The following observations were

made after the data was collected, and should serve as motivation for further chapters in this thesis, where they were addressed.

Firstly, in order to correctly measure out the states, APs and the rooms themselves, a very precise manual measurement needed to be performed. This often involved measuring the x, y coordinates of each state, relative to 'Tag 0'. Even though this collection was performed in 2-dimensional space, some of the houses were multi-level. This necessitated the encoding of an additional dimension in our measurements. There is also a possibility of noise associated with manual measuring, which in turn would skew the location error, as this depends entirely on accurate spatial coordinates of corresponding ground-truth states.

Despite the fact, that the camera is objectively accurate in establishing the location based on fiducial tags, the high-dimensional output from the camera can cause the processing times to be long and the required compute to be large. As such, the training of such system could not be considered for real-time deployments simply due to the relatively long, off-line computing time needed to process the locations. Additionally, the house plans which were collected from these residences were made entirely off-line, based on the prior measurements of the states and available plans. This can increase the possible measurement error further.

Finally, we consider the problem with per-user training scheme. Due to the relative arbitrarity of RF signals in a constrained environment, the model which is trained on a specific user is unlikely to perform well on other users. This is because every human body would exhibit different propagation characteristics. This would translate to different signal strengths for different people in the same areas of the house. This implementation stipulates that the primary user of this system would perform the training themselves. In terms of localisation for healthcare, this would necessitate patients to perform the arduous ground-truthing themselves. Furthermore, the model would only realistically show the picture of the signal propagation on the day of its training. However, signals drift, along with propagation characteristics of their medium. This additionally suggests that a system of this kind would require some kind of 'lifelong' training scheme to mitigate these effects.

CHAPTER 4

METRICS AND METHODS

In the previous chapters, the thesis covered a literature review of the subject matter, as well as a comprehensive overview of the data collection and system deployment methods. Here, we outline the metrics and methods which will be employed here. The forthcoming chapters all share the underlying inference approaches and evaluation metrics. These metrics are used in order to evaluate the indoor localisation methods and approaches and require a rigorous mathematical formalisation. The aim is to include the most important concepts in a single, easy to parse chapter. It will serve, as a general overview of the most prominent approaches used in this text.

First, the chapter will give a mathematical introduction to the metrics used as part of the evaluation of the results in the forthcoming chapters. However, since these chapters set to solve different challenges, not all of the metrics of evaluation can be considered as applicable and therefore not all of the metrics are used for every chapter. The reasons for the use of the metrics and their suitability for the problem of indoor localisation will be discussed in this section. The preceding chapter has outlined the environments in which the experiments used in this thesis were carried out. Small subset of this characterisation will be used in this chapter as an overarching application example. It will be used to introduce the notion of Bayesian Networks and provide their subsequent extension into Hidden Markov Models. Typical inference methods used in the forthcoming methodical chapters will be addressed. We will conclude by formalising the typical training methods of Hidden Markov Models.

4.1 Metrics

There exist a variety of metrics which serve to quantify the performance of an indoor localisation model. The most common of these metrics take into account the spatial discrepancy between a label and its corresponding ground truth [127]. However, while effective in measuring the performance of the localisation algorithm, this method might not be useful when evaluating the performance of the underlying machine learning model [100]. In this section, we aim to outline the metrics which were used to scrutinise the performance of the indoor localisation and machine learning models alike. We also formalise novel metrics which we believe to be advantageous in upcoming experimental scenarios.

First, let us outline the formal mathematical notion of a 'state' in this work. From chapter 3 we define a 'state' as an enumerated $1m \times 1m$ section of the floor plan. We will denote each ground truth state l, which contains a tuple of information about its coordinate location. In this work, the location is calculated predominantly in 2 dimensions (unless specified otherwise), such that $l = \{x, y\}$. The vector representing ground truth states will be denoted as $\boldsymbol{L}$ and we will assume that predicted location is given by $\hat{\boldsymbol{L}}$, with each individual state as $\hat{l}$. Note that the states can be quantised as numerical labels, and that the correspondence between their spatial position and given enumeration is an arbitrary choice.

4.1.1 Accuracy

Accuracy is one of the most popular performance metrics for machine learning models. The stipulation here is that the model performance is assessed, subject only to enumerated labels. It follows the basic idea behind the calculation of model accuracy, namely:

$$\text{Accuracy} = \frac{\text{Number of correctly predicted locations}}{\text{Total number of predicted locations}} \times 100 \tag{4.1}$$

Whilst useful for the calculation of relative model performance, this metric should not be used exclusively when considering an indoor localisation model. This is because this metric is invariant to the discrepancy between the locations of predicted and ground truth locations; in other words, it provides no penalty for performance, even if the relative distance between two examined states is large.

4.1.2 Distance Error

Distance error, or euclidean error, is a popular metric for evaluation of indoor localisation models [127]. This metric incorporates the coordinate system into its metric calculation, such that the relative discrepancy is calculated as a function of distance in d-dimensional space. If the location in d dimensions is given by $\boldsymbol{L} \in \mathbb{R}^d$, and its prediction $\hat{\boldsymbol{L}} \in \mathbb{R}^d$, then:

$$\text{Distance Error} = \sqrt{\sum_{i=1}^{d} (l_i - \hat{l}_i)^2} \tag{4.2}$$

At any time t, the euclidean distance between two examined states is calculated, using their x and y. This distance is then averaged across all time, and the absolute value of this distance is used to provide performance evaluation.

4.1.3 Path Error

Path Error's genesis is a consequence of the environments used as part of this thesis. The basic stipulation of path error is to improve upon the distance error's 'obstacle blindness' in order to account for environmental obstruction and interference.

The basis of this metric lies in Dijkstra's Algorithm [45], which aims to find the shortest path between two points in a connected graph. Formally, the path error is calculated as a sum over the shortest route between the prediction and ground truth. More succinctly, if $\boldsymbol{L}^*$ (with $|\boldsymbol{L}^*|$ as its length) is the sequence vector of states, which specify the shortest route link between state l and its prediction $\hat{l}$, then assuming $l \in \boldsymbol{L}^*$, and $\hat{l} \in \boldsymbol{L}^*$:

$$\text{Path Error} = \sum_{h=2}^{|\boldsymbol{L}^*|} \sqrt{\sum_{i=1}^{d} (l^*_{i,h} - l^*_{i,h-1})^2} \tag{4.3}$$

The difference between path and distance errors, is that the former introduces further penalisation if two states are not in direct contact. This penalty aims to contain the error within the boundaries of the parametrised state space, as opposed to assuming that the space between any given two states is free of obstacles. This is illustrated using the example in Fig. 4.1.

4.1.4 Suitability of Metrics

The above metrics aim to evaluate the performance and accuracy of indoor localisation models. However, their usefulness is not always justified. Adopting one or more of those metrics is subject to the challenge that the evaluated algorithm is posed to solve.

Accuracy, for example, can be misleading when compared directly to distance error. Due to the stringent nature of accuracy, it may come to pass, that the model yields a high percentage error, yet is able to maintain a viable distance discrepancy. This can happen if the model predicts states close to the ground truth, but not ground truth itself. The distance error can therefore be maintained at low value, whilst accuracy might be low.

Alternatively, consider how the error is calculated using the above formulations of distance and path. Distance error disregards the obstacles, opting instead to calculate the error using a uninterrupted 'straight line'. The path error first calculates the shortest path between the two states, and then sums the distances of each 'hop'. In this work, this error was utilised to scrutinise whether the models are able to perform well in residential environments with large number of rooms and multiple floors.

As an additional example, consider how distance error can be misleading when considering states, which share similar x and y coordinates, but lie on different floors of the same house. While distance is simply the height of the room, the actual traversal between the two states would yield a much larger error. In this case, the path error would actually be the true indication of a problem, as opposed to distance.

The choice of metrics in the following chapters will be dictated by the problem formulation, as well as the appropriateness of each metric related to the problem. If any single above metric is deficient, their combination will serve as a viable set of evaluation mechanisms, properly scrutinising the performance of the algorithm.

4.2 Example of Sensor Model

In this section we introduce an example of a sensor model which will serve as a foundation for further explanation of the methodology. In the interest of brevity, we will only consider House 1 as the experiment environment. The modelling, methods and metrics however can be generalised for the use with each of the remaining three houses. The objective of this example, is to project the general methodology used in this thesis into the problem at hand. By explaining how the indoor localisation problem can be formalised using these methods, we aim to clarify how the remaining methodical chapters have been designed, and what kind of methods and algorithms were used to evaluate them. This example

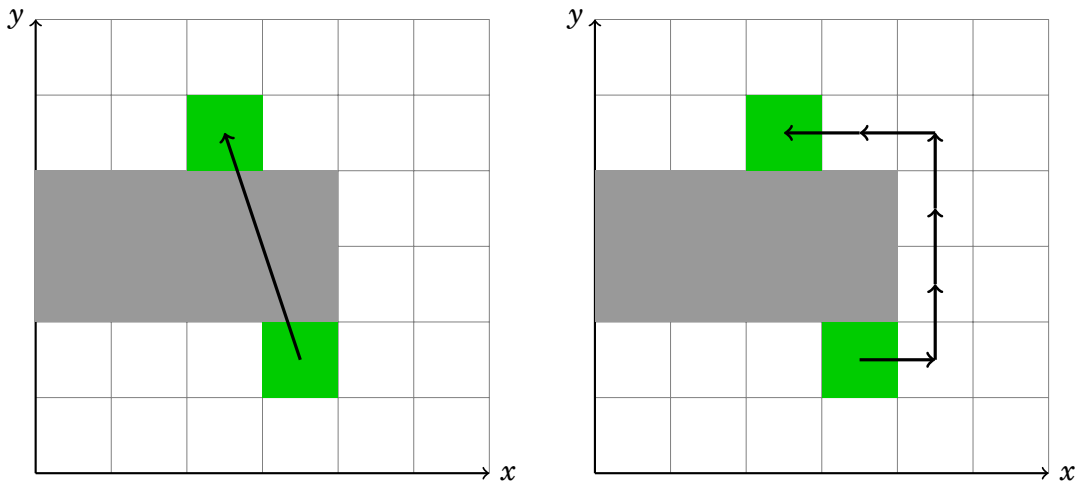

Figure 4.1: Simple grid world example showing the differences between Distance (left) and Path (right) error metrics. The states, whose discrepancy is being calculated are shown in green. Gray block specifies an arbitrary, impassable obstacle. Arrows show how the error is calculated.

will also serve as a platform for outlining the use of the nomenclature associated with the problems contained in this thesis.

The ideas relating to the resolution of the states should also be mentioned. In this thesis, we consider the use of two, distinct levels of granularity, in order to evaluate the performance of models. These levels include 'room-level' and 'tile-level'. They can be visualised in Fig. 4.2. The visible tiles are additionally separated into distinct sets, which constitute physical rooms inside the house, as seen by different colouring of the tiles in the figure. The average of the euclidean coordinates of the tiles in a given room subset specify the x, y centre of the 'room-level' state. The 'tile-level' state is accordingly the use of the more granular, individual tile states, and their euclidean coordinates.

Recall from chapter 3, that the given residential environments are tessellated into (approximately) 1m × 1m states. This is given by Fig. 4.2, where the result of tessellation of one of the houses, is provided. Note, that the number of these states varies from house to house and each state is given by l, enumerated such that $1 \leq l \leq L$, where $L = |\boldsymbol{L}|$ is the total number of states. Note also, that each house contains a finite number of APs. Each AP is given by k, their indices given by $1 \leq k \leq |G|$, where $|G|$ is the total number of APs.

As seen in Figs. 4.3 and 4.4, the description of each state, in terms of its signal trace distribution, differs. We can describe these signals more formally, by assuming that they have been generated by a Gaussian distribution:

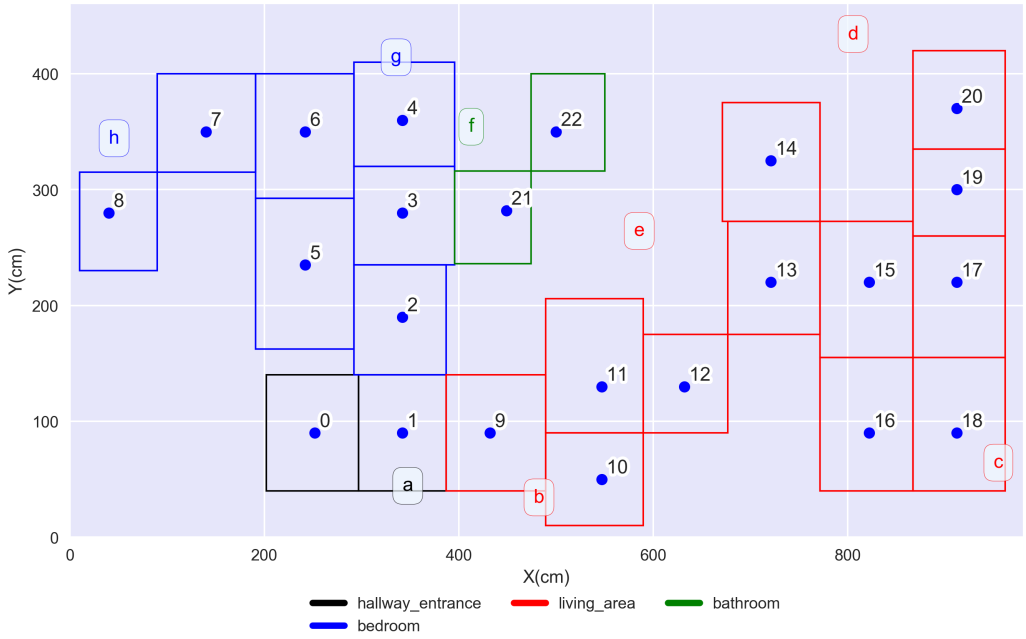

Figure 4.2: Discretised state space of a residential abode. Each of the enumerated states represent an approximately $1m^2$ square in physical floor plan space of the house.

$$p(RSS_t|l,k) \sim \mathcal{N}(\mu_{lk},\sigma^2_{lk}) \tag{4.4}$$

With the signals described, we aim to clarify an additional problem of packet drop. This problem was outlined in detail in Section 3.2.2. Inherent to wireless networking, packet drop can occur due to, for example, extending out of range of the transmitter or environment signal fading. Interestingly however, packet drop can also be used to describe specific location in the house. Consider the probability of observation given the location and AP, $p(RSS_t|l,k)$. For freely arriving symbols the above formulation holds. However, if the observation contains no information i.e. dropped packet, we can calculate the probability using a Bernoulli distribution:

$$p(RSS_t|l,k)\begin{cases} Bin(1,1-\frac{r_{lk}}{q_{lk}}) & \text{if } RSS_t = \text{-120dBm} \\ \mathcal{N}(\mu_{lk},\sigma^2_{lk}) & \text{if } RSS_t \sim= \text{-120dBm} \end{cases} \tag{4.5}$$

where r specifies number of packets with 'information' (as opposed to number of symbols specifying dropped packets, which in the dataset is set as -120dBm) and q is the total number of packets, arriving from specific location l from specific AP k.

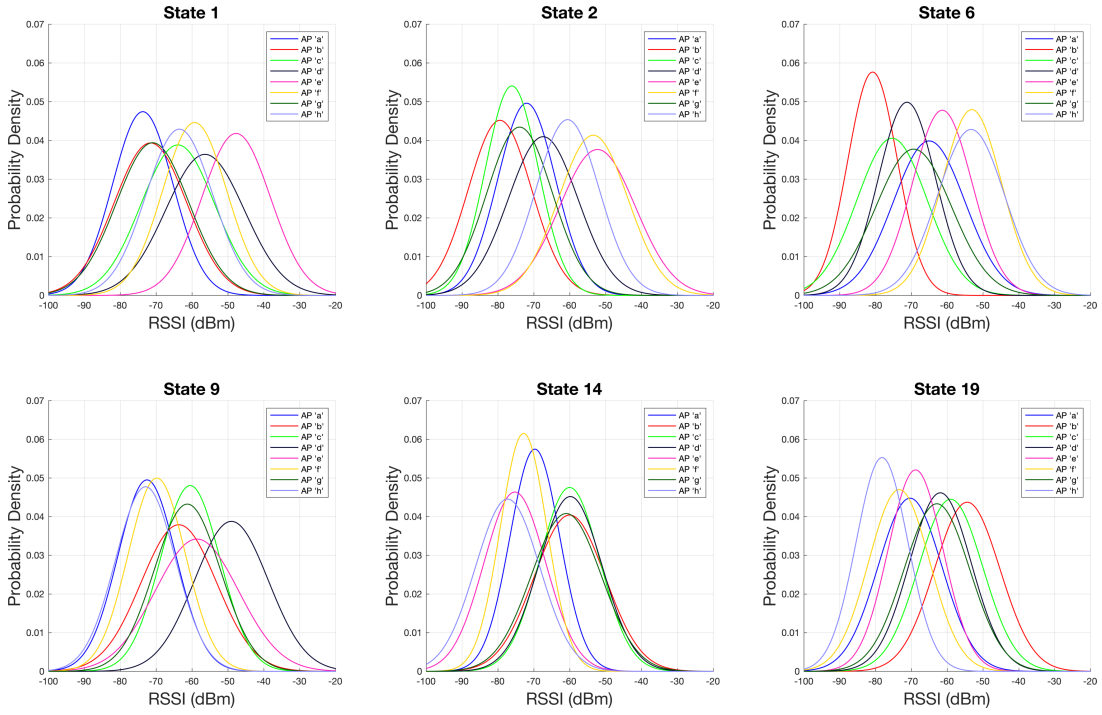

Figure 4.3: Example of the distribution of signal from all 8 APs in a few discerning states. The difference between RSSI signal traces can be used to establish location.

4.2.1 Supervised Learning through Label Frequency Counting

The parameters of the models in this thesis were predominantly trained on the available training data. The estimation of parameters from data uses the provided training set only, in order to infer the values of parameters, upon which the models are later evaluated. Supervised learning approaches allow the user to provide a good approximation of the underlying model, based on the available data. However, one of the shortcomings of this method is the amount of data required to build up a viable model of the environment and prevent under- or over-fitting.

The most basic approach, employed in this thesis, is the counting of available state transitions/state emissions as a way of parameter approximation. This relies on the frequency of either state transitions, or symbol emissions conditioned on particular states [23]. Emission probability of observations given states was calculated by aggregating the vector of all of symbols arriving at a certain prescribed state, as described by ground truth labels. The mean, standard deviation and packet loss rate would then be extracted from this vector (Note that the 'hats' above the mean and standard deviation represent that the respective parameters are merely approximations of underlying distributions):

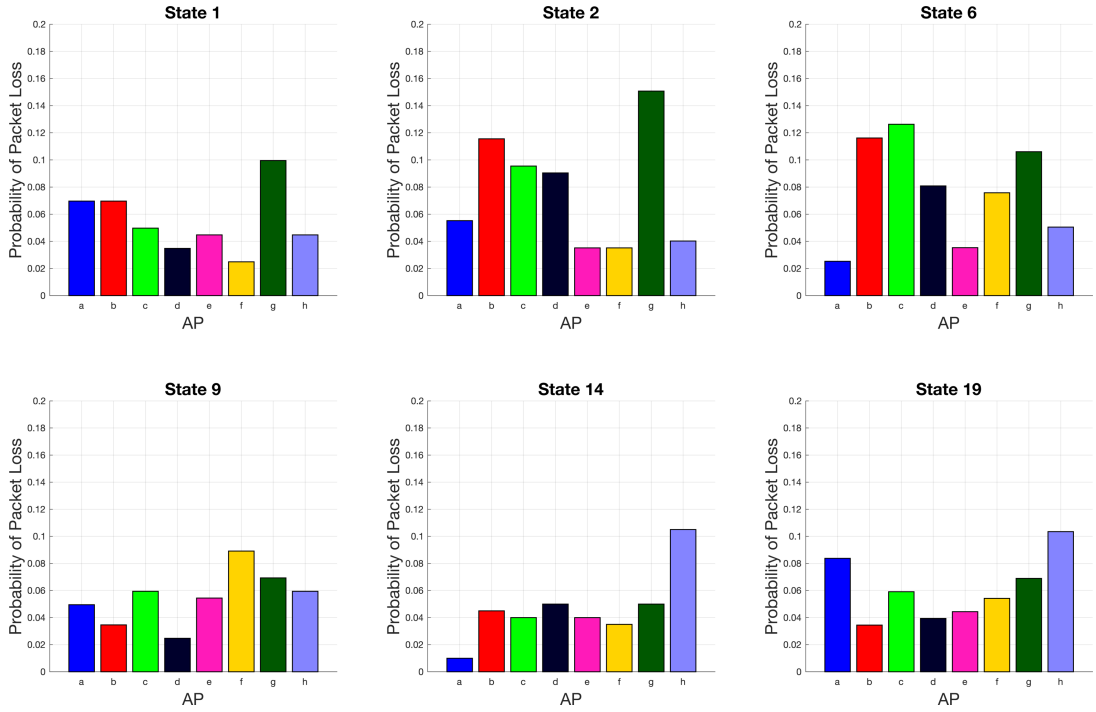

Figure 4.4: Example of the packet loss rate of signal from all 8 APs in a few discerning states.

$$\hat{\mu}_{lk} = \frac{\Sigma_{q_{lk}} RSS}{q_{lk}} \tag{4.6}$$

$$\hat{\sigma}_{lk} = \sqrt{\frac{\Sigma_{q_{lk}} RSS - \hat{\mu}_{lk}}{q_{lk} - 1}} \tag{4.7}$$

where $q_{lk} = |RSS|$, the total number of RSS observations in a given vector, in location l from AP k. These calculations take place iff $\forall$ RSS ~= -120dBm. The estimation of dropped packets is trivial, and its calculation involves symbols which $\forall$ RSS = -120dBm:

$$r_{lk} = \frac{\Sigma_{q_{lk}} \mathbf{1}_{-120}(RSS)}{q_{lk}} \tag{4.8}$$

where $\mathbf{1}_{-120}(RSS_t)$ is an indicator function.

The use of fingerprinting data for training would indeed yield a good description of sensor traces in the corresponding states, but would not be a faithful description of the transition potential between states. Consider, that in order to build up a viable transition matrix, a lot more 'free-living' data would be required, as to capture these movements

between states. The synthetic movements produced by fingerprinting would therefore not be used, and the transitions would be engineered separately using the adjacency matrices between states.

4.3 Methods

This section will outline the methods which are employed in the remainder of this thesis. Note here, that the notation of the formalisation of the established algorithms was kept standardised to the literature as to maintain readability.

The algorithms which are presented in this chapter, and form the basis for the algorithms developed in the later part of this thesis have are not in real time. This effectively means, that the algorithms and methods contained therein are validated on data which has been previously collected off-line.

4.3.1 Bayesian Networks and Graphical Models

Bayesian Networks have been mentioned in Sec. 2.5.2 as a method of fusion of sensor modalities. BNs are a way of modelling conditionality between variables in a Directed Acyclic Graph (DAG). The basic idea involves modelling the variables as nodes in a directed graph. If a generic Bayesian node is given by n, then the general form of joint probability of all variables is:

$$p(n_1,...,n_N) = \prod_{i=1}^{N} p(n_i|Pa(n_i)) \tag{4.9}$$

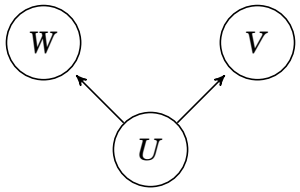

Figure 4.5: Example of a graphical model with three variables. In this example, the conditionality of variables stems from their 'parent' node, or U.

Consider the example in Fig. 4.5. The variables U, V and W are given as nodes in a connected graph. From Eq. 4.9 we can derive the joint probability between them as such [14]:

$$p(U,V,W) = p(U)p(W|U)p(V|U) \tag{4.10}$$

That is, the prior probability of variable A, multiplied by the conditional probability of the remaining variables, given the parent node. In order to infer information about any of the variables, the model can be marginalised over the 'nuisance' variables. Consider, that we want to condition the model on variable C. The marginalisation would then be:

$$P(W|U,V) = \frac{p(U,V,W)}{\Sigma_W p(U,V,W)} = \frac{p(U)p(W|U)p(V|U)}{\Sigma_W p(U)p(W|U)p(V|U)} \tag{4.11}$$

In this work, the BNs are used as a mechanism for fusion of different sensor modalities. These sensor modalities include RSSI, Accelerometer and Video, amongst others. They serve as a modelling tool, in order to find the causal correspondences between a variety of sensors. This particular approach is well resourced in the literature [3, 190] and provides a solid basis for the formulation of the problems contained herein.

4.3.2 Hidden Markov Models

Hidden Markov Models (HMM) are a popular example of dynamic Bayesian Networks, which are used to evaluate temporal processes. The models play an important role in this thesis, as all of the forthcoming chapters utilise this method as a validation step for the proposed approaches.

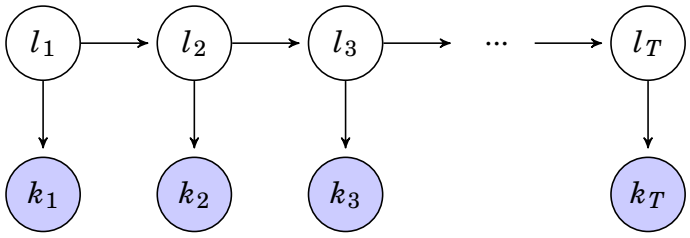

Figure 4.6: Example of a Hidden Markov Model. The observable emissions are shaded blue, the hidden states are white. The basic idea behind HMMs is to evaluate the joint probability $p(l_{1:T}, k_{1:T})$, given the knowledge of a prior distribution, symbol emissions and state transitions.

HMMs can be encapsulated using a tuple of parameters:

$$\lambda = \{A, B, \pi\} \tag{4.12}$$

where the parameters are described as follows:

$$\pi = p(l_0), \quad A = p(l_t|l_{t-1}), \quad B = p(k_t|l_t) \tag{4.13}$$

The equation below formalises the evaluation of joint probability between the aforementioned symbols:

$$p(l_{1:T}, k_{1:T}) = p(l_0) \prod_{i=1}^{t} p(k_t|l_t) p(l_t|l_{t-1}) \tag{4.14}$$

The equation 4.14 above describes the overall process of evaluating joint probability between state l and emission k as a function of prior probability $p(l_0)$, emissions (i.e. likelihood) $p(k_t|l_t)$ and transition dynamics $p(l_t|l_{t-1})$. For further reading, we refer to [169].

In our application example, the use of states and hidden observation symbols can be outlined in terms of physical states in a residential abode, as well as the discretised RSSI readings, observed at certain times. The evaluation of the joint probability would then mean, that the indoor localisation would be performed with respect to the initial starting conditions, as well as the inference of the subsequent location state sequence, given RSSI observations.

4.3.3 Inference and Learning

Assume, that given the observation sequence $RSS = RSS_1, RSS_2, ...$, the model was asked to obtain the probability of said sequence given the model parameters λ, $p(RSS|\lambda)$. As proven by Rabiner in [169], the computation of said probability becomes intractable for problems with large enough state spaces [169]. One solution to $p(RSS|\lambda)$ is an approximation algorithm called the Forward-Backward. On the basis of the Forward-Backward, we also outline the use of Baum-Welch algorithm, an Expectation Maximisation (EM) algorithm used to iteratively learn the model parameters from the observed data.

4.3.3.1 Forward-Backward Algorithm

The Forward-Backward approximates the posterior marginal probability of $p(RSS|\lambda)$. The algorithm calculates the probability of a *forward* as well as a *backward* pass for temporally governed processes. In this thesis, the Forward-Backward algorithm is used to

predict the log-likelihood of the most likely states which would emit a certain observation at time t, i.e. the distribution over all states at time t.

Consider the possible sequences between states in a given state space. The combinations between states can be written as a sequence of states in time:

$$\Xi = \xi_1, \xi_2, ..., \xi_T \tag{4.15}$$

More formally, assume that the Forward and Backward variables are given respectively by [169]:

$$\alpha_T(i) = p(RSS_1 RSS_2 ... RSS_T, \xi_T = l_i | \lambda) \tag{4.16}$$

$$\beta_t(i) = p(RSS_{t+1} RSS_{t+2} ... RSS_T | \xi_t = l_i, \lambda) \tag{4.17}$$

The approximate solution to the Forward-Backward algorithm allows for the estimation of $p(RSS|\lambda)$ with much less computation than exact inference. The Forward part of the algorithm is therefore initialised by:

$$\alpha_1(l) = \pi_l B_1(RSS_1), \quad 1 \leq l \leq L \tag{4.18}$$

The following probability is then induced through:

$$\alpha_{t+1}(j) = \Big[\sum_{l=1}^{N} \alpha_t(l) A_{lj} \Big] B_j(RSS_{t+1}) \tag{4.19}$$

with $1 \leq j \leq L$ and $1 \leq t \leq T-1$.

Similarly, the Backward pass performs a similar induction, albeit in the reverse order of the provided sequence, i.e. $t = T-1, T-2, ..., 1$. For its initialisation, the final state of the sequence is given as certain, $\beta_T(j) = 1$. The induction is, then:

$$\beta_1(l) = \sum_{l=1}^{N} A_{lj} B_j(RSS_{t+1}) \beta_{t+1}(j) \tag{4.20}$$

where, again, $1 \leq j \leq L$.

4.3.3.2 Baum-Welch Algorithm

The Baum-Welch algorithm is a widely utilised parameter learning method for HMMs [201]. The algorithm utilises a lot of the previously outlined implementations from Section 4.3.3.1. The aim is to re-estimate parameter values given a sequence of observations.

Initialisation of parameters plays an important role in correct convergence of this algorithm. The most popular way of initialising the parameters is either random or pseudo-random [169]. Alternatively, the parameters can be estimated with respect to the method in Section 4.2.1 and later iteratively converged using the observations.

The method follows from Equation 4.12 and Section 4.3.3.1, we can initialise the parameters as required, and later iteratively improve them, by increasing the log-likelihood of the result. The algorithm is capable of re-estimating the parameters of the model (including the distributions of the signal) in each state.

After calculating the likelihood of the observation sequence using the Forward-Backward procedure, the re-estimation is subject to an iterative Expectation Maximisation. Using α and β from section 4.3.3.1, we can re-estimate the prior, transition and emission probabilities. Note, that for continuous emissions, we re-estimate the parameters of the Gaussian distribution, μ and σ [201].

Beginning with the prior probability, the re-estimation follows the simple normalisation over all states:

$$\hat{\pi}_l = \frac{\alpha_1(l)\beta_1(l)}{\sum_{j=1}^{N} \alpha_1(j)\beta_1(j)} \tag{4.21}$$

The algorithm would re-estimate the parameters of a normal distribution, given the set of available observations. The re-estimations make use of a temporary variable γ_t given by:

$$\gamma_t(l,k) = \frac{\alpha_t(l)\beta_t(l)}{\sum_{j=1}^{N} \alpha_t(j)\beta_t(j)} \frac{\mathcal{N}(RSS_t|\mu_{lk},\sigma_{lk}^2)}{\sum_{m=1}^{G} \mathcal{N}(RSS_t|\mu_{lm},\sigma_{lm}^2)} \tag{4.22}$$

The parameters (μ and σ) would then be re-calculated:

$$\hat{\mu}_{lk} = \frac{\sum_{t=1}^{T} \gamma_t(l,k) RSS_t}{\sum_{t=1}^{T} \gamma_t(l,k)} \tag{4.23}$$

$$\hat{\sigma}_{lk} = \frac{\sum_{t=1}^{T} \gamma_t(l,k)(RSS_t - \hat{\mu}_{lk})(RSS_t - \hat{\mu}_{lk})^T}{\sum_{t=1}^{T} \gamma_t(l,k)} \tag{4.24}$$

The exit state of the algorithm tests for convergence of the parameters. This is usually done through a step-increase condition of log likelihood. Effectively if $|\hat{\lambda} - \lambda| = \theta$, where θ is the threshold, the algorithm is stopped. Otherwise $\lambda = \hat{\lambda}$, and iterated again.

4.4 Conclusion

This chapter has outlined the use of methods and metrics, best suited for the task of indoor localisation. The use of above-mentioned metrics show how indoor localisation models can be evaluated both, in terms of their model performance, as well as the discrepancies between states in physical navigation space. The chapter introduced the notion of Distance error, as well as Path error, which was designed to mitigate some of the shortcomings stemming from Distance's rigid state disparity calculation.

Thanks to the highly structured environment the use of well established structure prediction methods, such as HMMs, as well as their approximation algorithms was proven and was shown to be warranted. The models can provide a viable base for a variety of different algorithms, as proven in later chapters.

CHAPTER 5

Efficient Fingerprinting using SLAM-derived Map and Poses

As it was mentioned in the previous chapter, one of the main shortcomings of RSS based indoor localisation is the need for arduous radio-frequency fingerprinting of the surroundings. In order to mitigate most of the presented challenges, we present 'H4LO' (Helmet for Localisation Optimisation) [103] , a low-cost system designed to cut down on the labour by utilising an off-the-shelf Light Detection and Ranging device. This system performs Simultaneous Localisation and Mapping, providing the user with an accurate pose estimation and map of the environment. The high-resolution location estimation can then be used to train a localisation scheme where RSS data is acquired from a wearable device. We examine the usefulness of this method by relating it to the camera-based fingerprinting methods from previous chapter by testing both ground-truthing approaches using a novel dataset. We find that the new algorithm is comparable in performance, whilst removing the need for time-consuming labour associated with with registering the participant location.

The utilisation of this system, in tandem with the SPHERE-in-the-box architecture, allows the user to perform extremely quick fingerprints, by cutting down on the logistical overhead associated with transferring and processing highly dimensional video data. Instead, LiDAR data, which produces data of lower resolution is used. It extracts the locations at the fraction of required labour of the previous method, whilst at the same time providing a map of the environment.

5.1 Related Work and Contributions

The aim of the proposed system is to improve upon the method used to gather HRL from chapter 3, by utilising a LiDAR device to obtain the users position and pose directly related to RSS signatures during fingerprint training. However, the literature relating laser range finders and RSS fingerprinting is sparse and not entirely comparable. We evaluate the need and motivation behind this system in this section.

As it was stated in the previous chapter, the procedure for RSS fingerprinting is notoriously arduous to perform, having to acquire an accurate spatial location of the user position. A floor plan is often required to derive a list of training locations which are subsequently annotated in space. Then, depending on the use case, a tailored method is devised to accurately denote when the participant visits these predefined locations [24, 136].

Another major shortcoming of this technique is that it suffers from performance deterioration over time and requires periodical re-training [115]. This can happen due to various environmental dynamics [130], or through deliberate hostile action [177]. It is therefore in the best interest of the system for the fingerprinting method to be as simple as possible, in order to be easily performed when required.

The literature relating laser range finders and RSS fingerprinting is sparse [114, 144, 162] and not entirely comparable. The presented literature indeed collects the RSS fingerprints and LiDAR data, but through the use of trolleys and rigs, specifically designed to be traversed through the environment by a technician or on its own. In our implementation, we use a human user which collects their own unique fingerprints in a residential environment.

The use of human participants performing the fingerprinting can be motivated by considering the uniqueness of each person's walking gait and radio propagation characteristics. It was shown that the performance of the algorithms differ, depending upon the training which was received from the participants [136]. This is especially true in the case of residential indoor localisation, where the environment is small but saturated with various obstacles, as outlined in chapter 3. It is therefore likely, that trolley-based fingerprinting methods are unable to capture each user's unique propagation characteristics.

Some applications of LiDARs use human handlers [125, 180]. These implementations assume that the LiDAR device is not used as part of a robot's perception sensor, but rather as a mapping tool [125, 180]. We aim to exercise a similar operation of the LiDAR

in this chapter, by attaching the device on the participants themselves. However, our implementation uses the entirety of SLAM pipeline, as in order to be effective, the fingerprinting method requires reliable ground-truth locations and corresponding map to be available.

There exist implementations which utilise SLAM for sensor signal-based localisation through Gaussian Process (GP) regression [57]. For example, WiFi-SLAM appropriates the SLAM pipeline of localisation and mapping in a setting of RSS modelling, as opposed to spatial features. Work by Liang et al. used various ambient background sensor traces to perform PDR which was subsequently optimised through SLAM techniques.

As is evident, there exist a need for reliable, automated indoor localisation ground-truthing platform. This platform would be worn by the users themselves as they perform RSS fingerprinting of the environment. Furthermore, it has to be robust enough as to capture each user's unique gait and propagation characteristics, and at the same time flexible enough to be able to deal with various environmental obstacles which the users can encounter, such as stairs and doorways.

The 'H4LO' system therefore combines the need for cheap and accurate RSS fingerprinting with proven reliability of 2D SLAM. In this chapter we present the hardware used, recent experimental findings, and show the viability of this method as compared to previous work. The main contributions of this chapter therefore are:

- We outline the proposed hardware for 'on-the-cheap' LiDAR scan acquisition, utilising popular 'off-the-shelf' devices.
- Then, we present the exhaustive 'free-living' and fingerprinting experiments gathered to prove its viability, using different users and different scenarios.
- We introduce a novel dataset, which associates corresponding RSS symbols to location and point cloud data.
- Lastly, we compare the performance of this method to the HRL data from previous chapter, where floor tags were used to provide location labels.

In Section 5.2 we outline all of the methods which are utilised by our system. Section 5.3 will detail the pipeline of the system, from the hardware setup to map generation and localisation. In Section 5.4 we reflect on the experiments performed and present the results, comparing our approach to fingerprinting method used in previous work. We conclude and provide points for future work in Section 5.5.

5.2 Map Generation and Pose Estimation

The map, along with the approximate location is provided by 2-dimensional SLAM. The algorithm used in this chapter utilises the MATLAB Robotics Toolbox, based on [79]. Here, we will outline the basic interpretation.

SLAM in two dimensions is formalised by considering the LiDAR returns as scan point clouds $\boldsymbol{C} = \{\boldsymbol{c}_t\}_{t=1,\ldots,T} \in IR^2$. Each scan is recorded as a set of polar coordinates in a corresponding location, given by $\boldsymbol{R} = \{\boldsymbol{r}_t\}_{t=1,\ldots,T}$, such that each $\boldsymbol{r}_t$ specifies a pose estimate in SE2:

$$r_t = \{x, y, \theta\} \tag{5.1}$$

The locations are constrained within the boundaries of a map M. SLAM aims to extract $p(\boldsymbol{r}_t, M|\boldsymbol{C}_{0:t-1})$, or the location $\boldsymbol{r}_t$ and the map M simultaneously by matching consecutive scans $\boldsymbol{C}_{0:t-1}$ together. The procedure of scan matching attempts to find a rigid transformation of the scan at $t-1$ into the frame of scan at t, given by [18, 79, 99]:

$$\boldsymbol{C}_t(\xi) = \begin{bmatrix} w_x \\ w_y \end{bmatrix} + \begin{bmatrix} \cos\phi & -\sin\phi \\ \sin\phi & \cos\phi \end{bmatrix} \begin{bmatrix} x \\ y \end{bmatrix} \tag{5.2}$$

where $\xi = (w_x, w_y, \phi)$ is the transformation vector. In terms of a global map, this transformation aims to minimise the non-linear least squares error between the current map and the transformation of the most recent scan [79]:

$$\arg\min_{\xi} \sum_{t=1}^{T} (1 - M(\boldsymbol{C}_t(\xi))^2 \tag{5.3}$$

The mapping of our environment is done through an occupancy grid. Occupancy mapping is a technique of probabilistic modelling of the environment. Basic interpretation of this method entails calculating the posterior distribution over the map, given available sensor measurements and prior estimated locations. More formally [202]:

$$p(\boldsymbol{M}|\boldsymbol{C}_{0:t-1}, \boldsymbol{l}_{0:t-1}) \tag{5.4}$$

The environment can be parametrised into grid squares, which themselves carry information about the immediate surroundings of the sensors. This information is encoded in the form of integer probability of cell occupancy, where '0' specifies that the

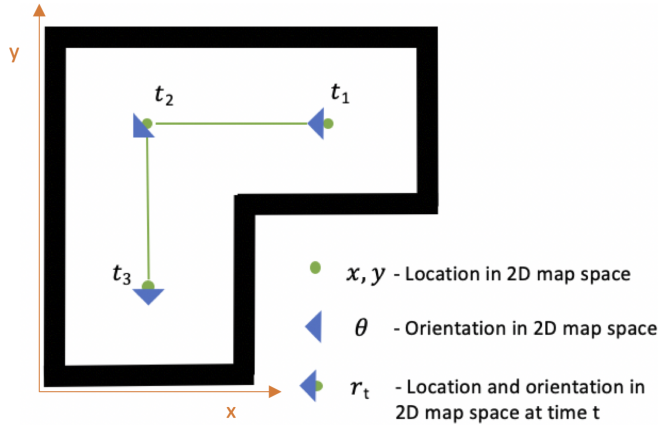

Figure 5.1: Bird's eye view of an arbitrary map, which specifies 3 distinct locations in time. The green point shows the location, the blue arrow is the orientation, and together they constitute r_t.

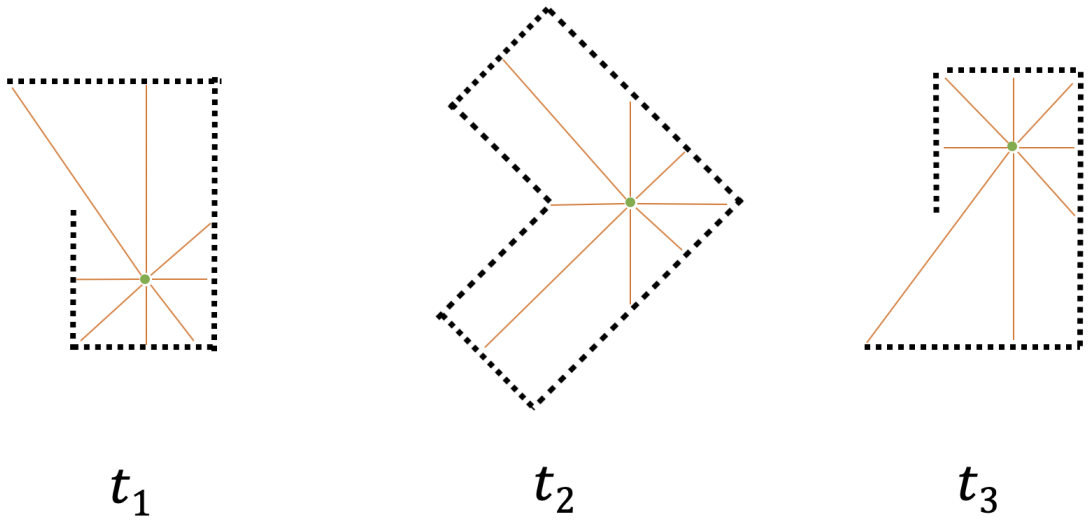

Figure 5.2: Corresponding point clouds C from the map example in Fig. 5.1. They all differ, in that they have been gathered in point cloud reference frame.

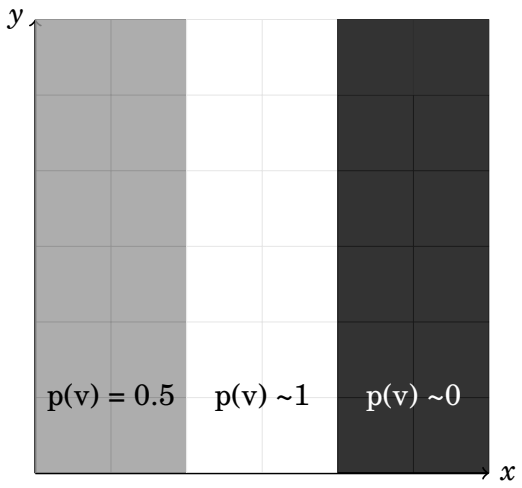

Figure 5.3: Simple grid world example showing the color gradients between occupied and unoccupied spaces. This is an illustration of a log-odds model of occupancy grid mapping employed in this chapter.

grid is an empty space, and '1' suggests that the grid is an obstacle. In terms of a LiDAR, this can mean that at some t the beam of laser has returned a certain distance from the sensor to the obstacle. This distance can then not only be used to establish the position of the obstacle, but also show the available 'free space'. This is specified by taking the log-odds probability of occupancy:

$$v = \log \frac{p(\boldsymbol{M}|\boldsymbol{C}_{0:t-1}, \boldsymbol{r}_{0:t-1})}{1 - p(\boldsymbol{M}|\boldsymbol{C}_{0:t-1}, \boldsymbol{r}_{0:t-1})} \tag{5.5}$$

The use of log-odd probabilities prevents the instabilities associated with probabilities near 0 and 1 [202]. The actual map can be separated into grids, each containing probability of being occupied. The color gradient shifts from black (unoccupied space) to white (occupied space).

Due to the unpredictability in data collection and the environment, the scans, even if collected at the same location, might not be precisely the same. A method relying purely on scan matching will therefore accumulate error and make the location and the map drift over time. To rectify this, the accumulated error is minimised when visiting previously unveiled locations, as in GraphSLAM [66] and Google's Cartographer [79]. This aims to minimise the squared error between the expected and relative measurements of a scan and an underlying sub-map [79].

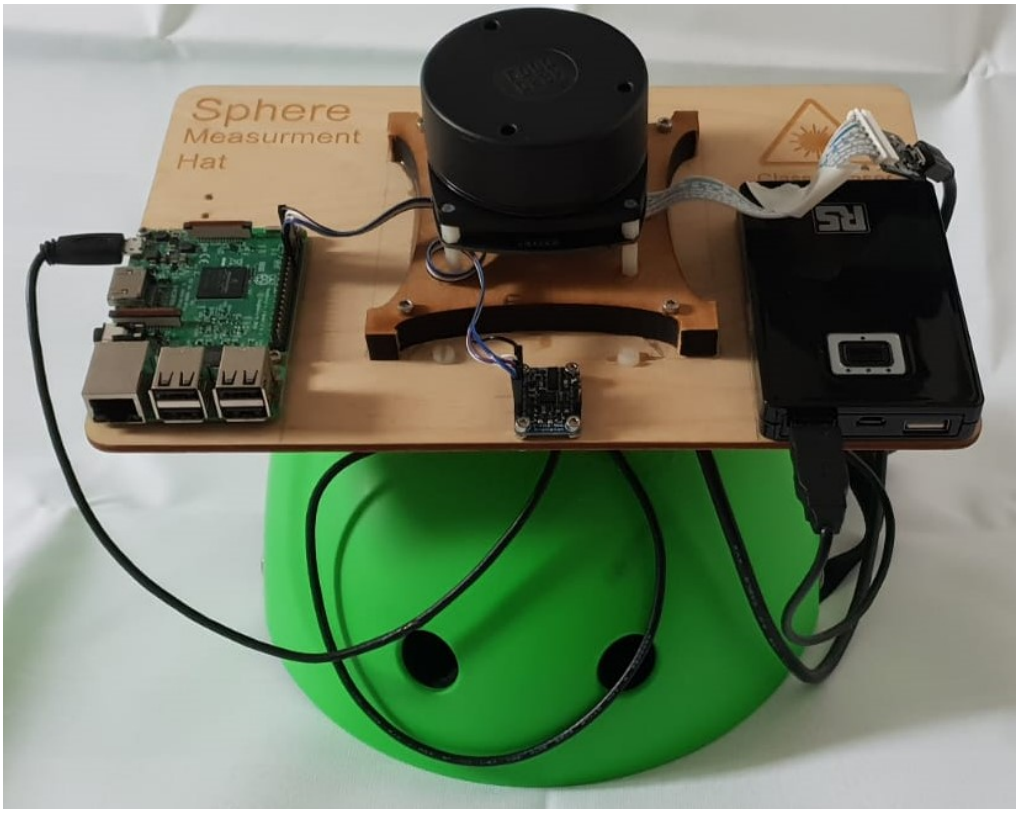

Figure 5.4: The ‘H4LO’

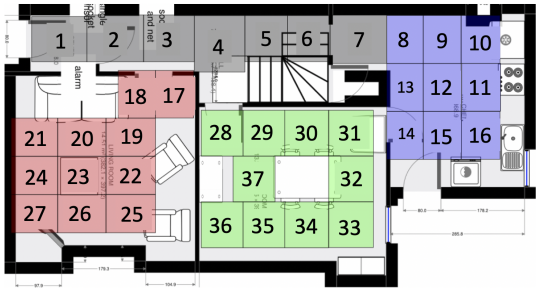

Figure 5.5: Downstairs Ground-truth.

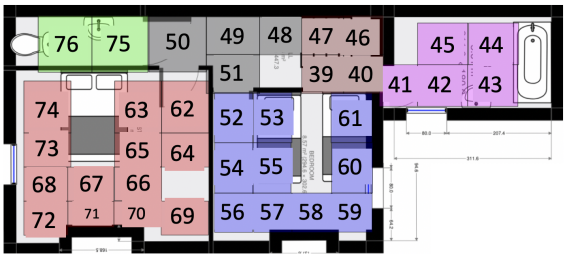

Figure 5.6: Upstairs Ground-truth.

5.3 The ‘H4LO’ System

5.3.1 RSS and Ground-truth Acquisition

The system makes use of the SPHERE-in-the-box infrastructure, described in [161] and in chapter 3. Note, that this infrastructure, on its own, does not provide labels.

The ground-truth labelling method which we will use as a reference baseline in this

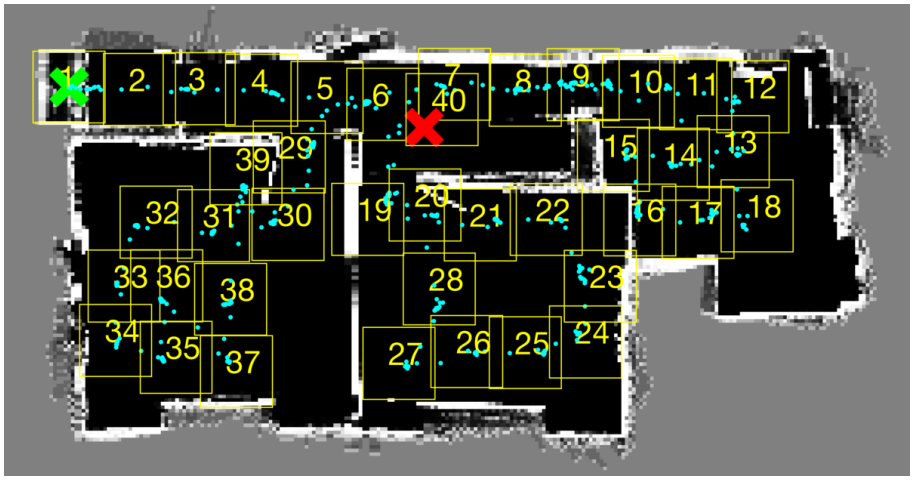

Figure 5.7: Downstairs area map recovered from User 1.

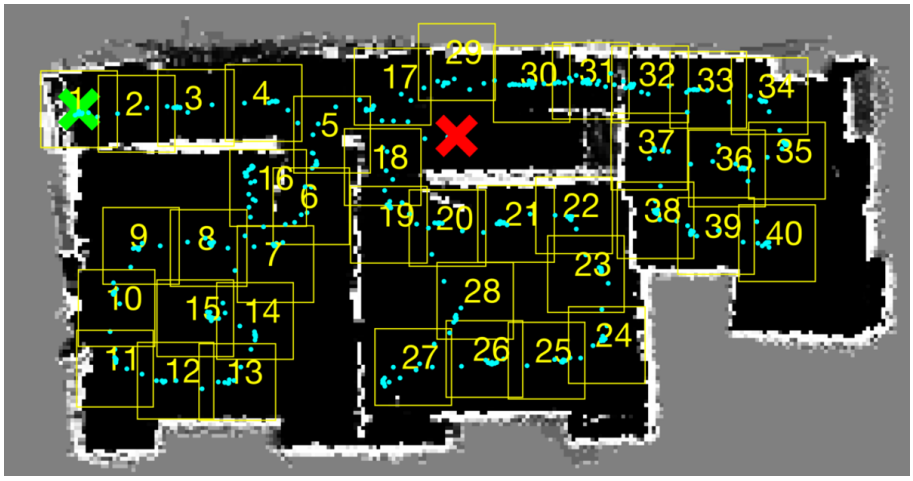

Figure 5.8: Downstairs area map recovered from User 2.

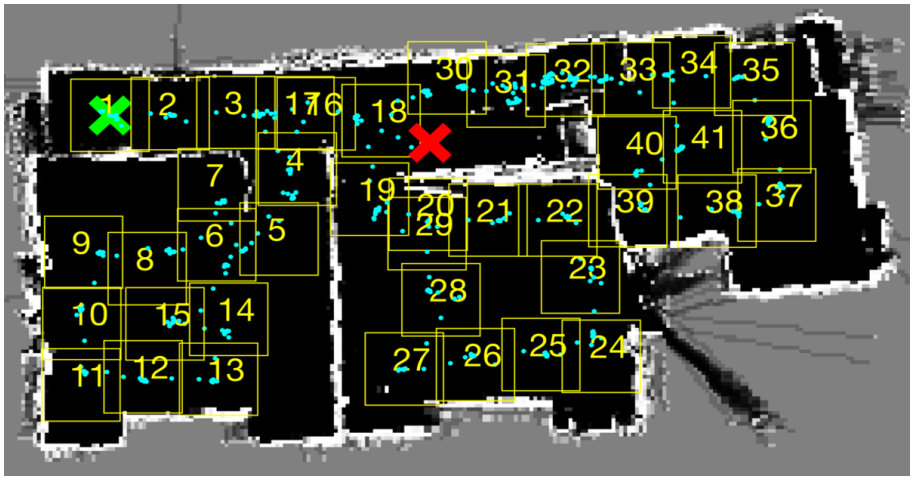

Figure 5.9: Downstairs area map recovered from User 3.

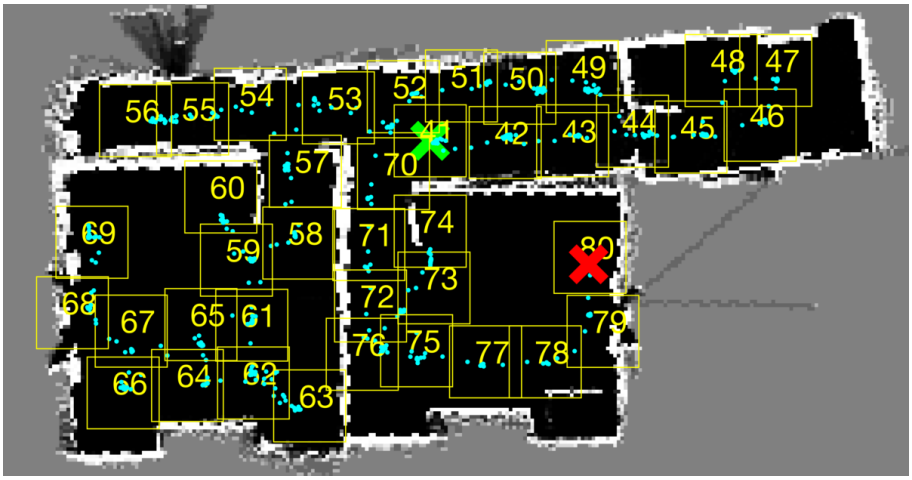

Figure 5.10: Upstairs area map recovered from User 1.

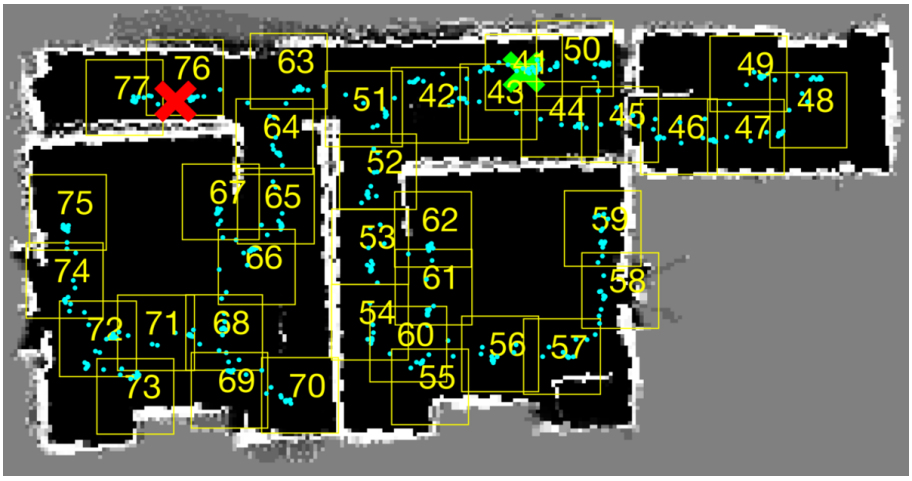

Figure 5.11: Upstairs area map recovered from User 2.

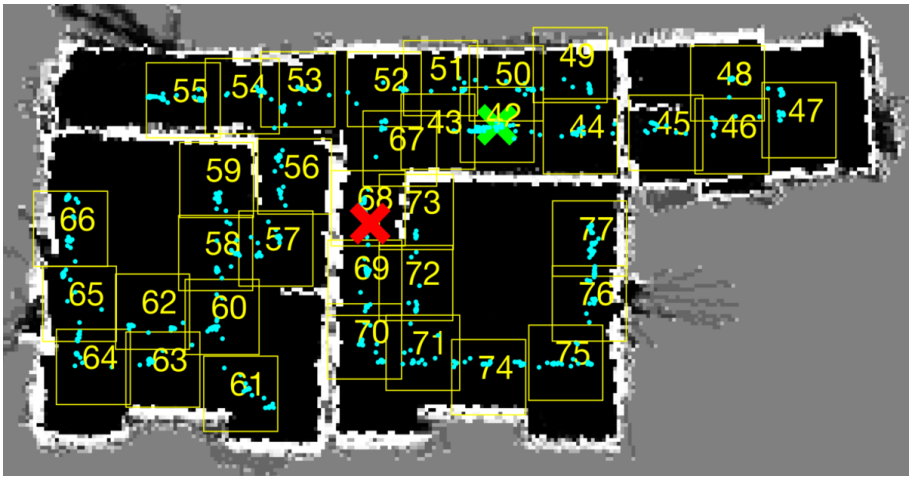

Figure 5.12: Upstairs area map recovered from User 3.

study is exactly the same as the method from previous work, detailed in chapter 3. This method is based on a abdomen-mounted camera, and relies on floor-mounted fiducial tags, specifying empirically created state space. The synchronisation between the labels and the RSS is done through the extraction of floor tag labels [62] from the camera video. Whilst accurate, this method requires manual distribution of the floor tags, measuring of the tag position and lengthy processing of the camera data.

'H4LO' relies on the LiDAR scan collection from head-worn helmet, shown in Fig. 5.4. During data collection, the user performs fingerprinting much like before, by walking around the environment and collecting the RSS measurements. In our system however, the helmet also provides the corresponding LiDAR point clouds, representing different areas in the environment. This ensures that the data from both RSS and LiDAR collected is user-centric and unique across all participants.

The helmet comprises of a bike helmet, a power bank, Raspberry Pi 3 and RoboPeak RP1 LiDAR device mounted on top of plywood. The LiDAR collected scans at 10Hz, within a 6m range [186]. A 9-DOF BNO055 IMU [19] is present in the resulting data set but was not used in this study. Timestamps are acquired through NTP from the SPHERE-in-the-box infrastructure [161] to match with the RSS data. This entire system was designed with cost in mind and comprises a total of £200 worth of hardware at the time of writing.

As described in Section 5.2, the sequential nature of the scans make it straightforward to recover the map and the pose simultaneously. After obtaining both, the system recovers the RSS signals corresponding to the locations in the environment. By segmenting the map into states using spatial constraints, the system assigns the data to each state and learns the dynamics governing each state using an adjacency matrix, which is later used to acquire the state transitions.

5.4 Experiments and Dataset

In order to compare the two methods fairly, the environment was parametrised into states at exactly the same positions as in HRL data, in chapter 3, shown in Figs. 5.5 and 5.6. This dataset only included residence described as House 4 from the previous work.

There were 3 unique users performing fingerprinting using the 'H4LO' and the camera based approach at the same time. Each user traversed the same environment at a different rate, taking different routes. They performed two types of fingerprinting - one longer (16 minutes on average), staying at each state for a few seconds, and also a

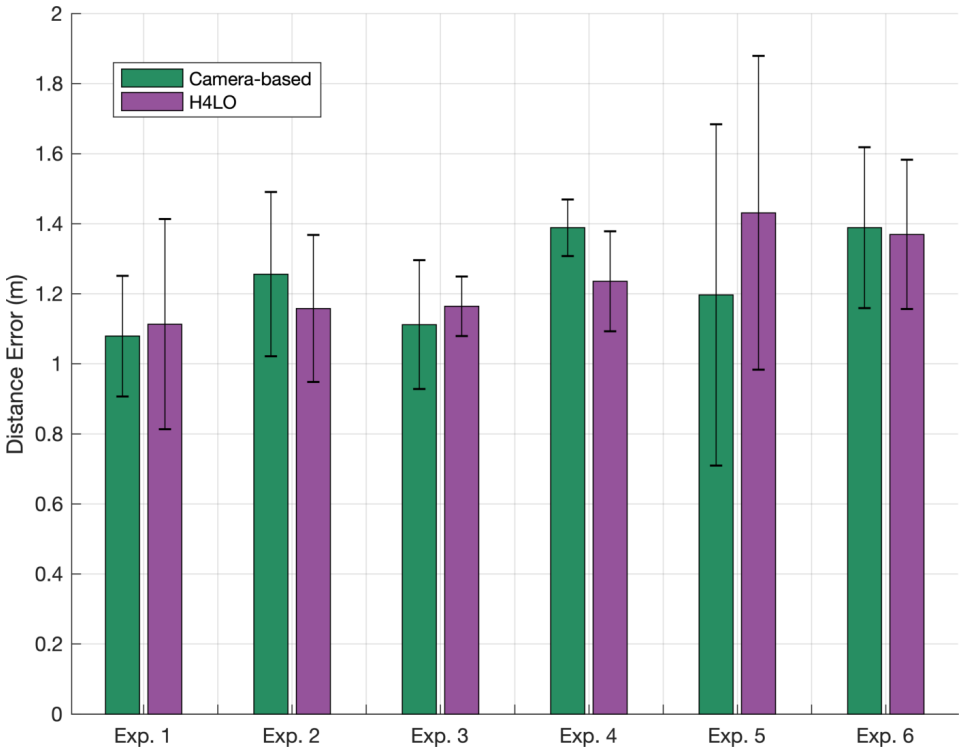

Figure 5.13: Results of the fingerprint experiments.

quicker 'fly-through' fingerprint (7 minutes on average).

In addition to the fingerprinting experiments, two of the users also performed 'free-living' experiments, performing everyday routines. These 'free-living' experiments did not utilise the 'H4LO' system and instead relied solely on the infrastructure described in chapter 3. These candid experiments can be further separated into 'single free-living', where only one user took part and 'dual free-living' where both users participated at the same time.

The resulting dataset comprises of the data from the wearable and the 'H4LO' [1]. The wearable data includes the wrist-worn acceleration and RSS, both sampled at 25Hz. The 'H4LO' primarily provides data from the LiDAR device, with the scans arriving at an average rate of 10Hz. Additionally, the IMU attached to the 'H4LO' provides data for roll, pitch, accelerometer and gyroscope, sampled at 100Hz, and heading and magnetometer sampled at 50Hz.

The map was then stored locally on the Raspberry Pi. The pre-processing was minimal, in that the scans were only downsampled, as to help reduce the computational cost of the SLAM algorithm. After the pre-processing, the point clouds were fed to the

[1]Available at: https://github.com/mkoz71/h4lo_fingerprint_automation_system

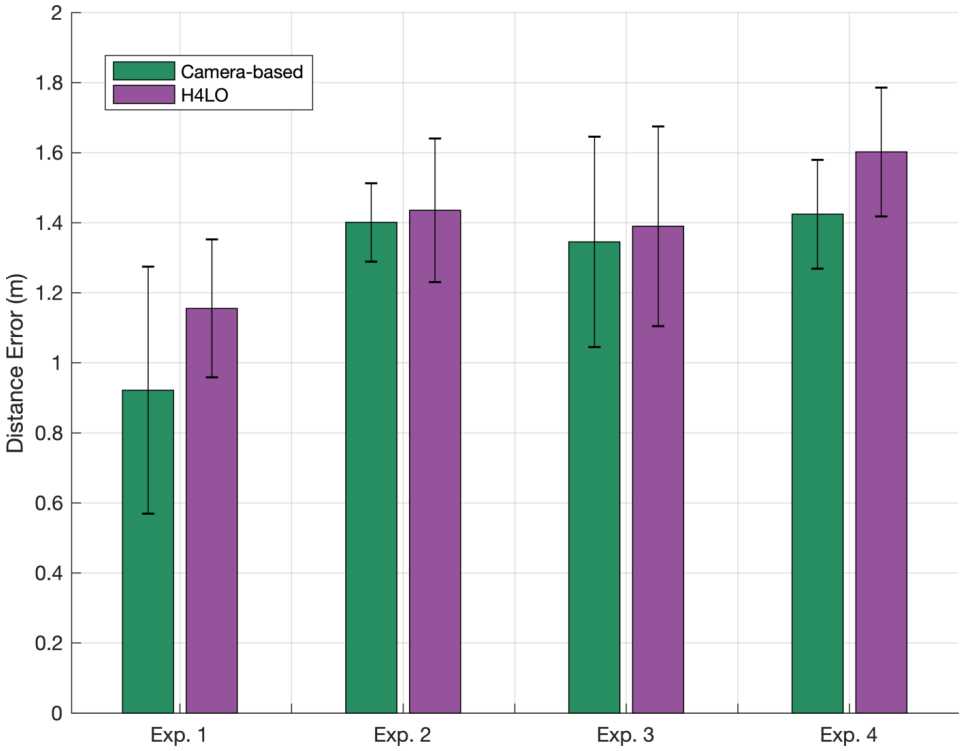

Figure 5.14: Results of the single living experiments.

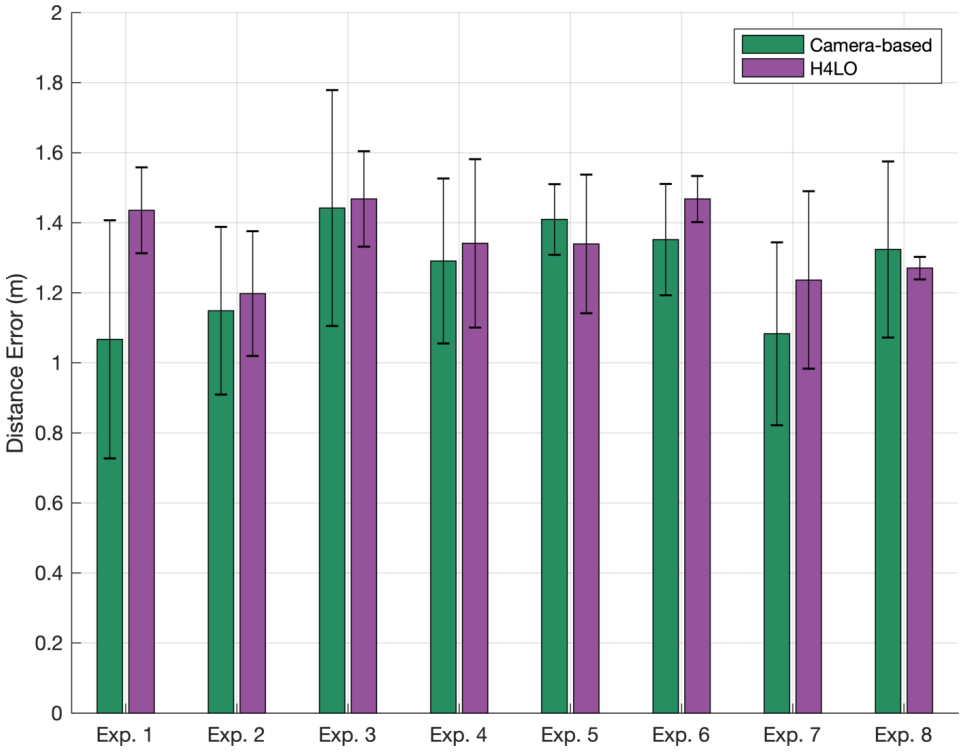

Figure 5.15: Results of the dual living experiments.

MATLAB Robotics Toolbox for SLAM, where their locations and map were extracted. After extraction, the maps were rotated, as to face the same way, and the locations were used to parametrise the floor space into states. The algorithm used to parametrise can be found below:

Input: $\{\boldsymbol{R}\}$ = Extracted poses, $\{\boldsymbol{L}\}$ = Location state vector, $\{b_l\}$ = Buffer distance of specific state l, $\{RSS\}$ = Sensor readings
while *t available* **do**
  if $\boldsymbol{L} == \emptyset$ **then**
    $l \leftarrow \{r_{t,x}, r_{t,y}\}$ // Input x and y from extracted poses at t.
    $l \leftarrow RSS_t$ // Assign sensor readings and store in the new state.
    $\boldsymbol{L} \leftarrow l$ // Create new location state in global state vector and store.
  else
    for *all available states in* $\boldsymbol{L}$ **do**
      if r_t *within* b_l **then**
        $l \leftarrow RSS_t$
      else
        $l \leftarrow \{r_{t,x}, r_{t,y}\}$
        $l \leftarrow RSS_t$
        $\boldsymbol{L} \leftarrow l$
      end
      for *all available states in* $\boldsymbol{L}$ **do**
        $l \leftarrow$ assign possible adjecent states from $\boldsymbol{L}$
      end
    end
  end
end

Algorithm 1: State creation algorithm

The algorithm begins by establishing the initial state at the pose extracted at $t = 1$. The location of this pose will serve as the center point of the state, which is then assigned 'hard' boundary, visible as yellow squares in Figs. 5.7, 5.8, 5.9 and 5.10, 5.11, 5.12 and also 'soft' boundary, so called buffer, which acts as a decision border of whether or not to create a new state. If passed, new state is created. If not, the sensor readings are assigned to that state. At any time $t > 1$, the algorithm iteratively searches whether the given poses fall into an already assigned state. If so, the sensor readings are updated, as is the adjecency between states. If not, a new state is created.

The results of the SLAM run for a single user are shown in Figs. 5.7, 5.8, 5.8 and 5.10, 5.11, 5.12. The green and red '×' specify the beginning and end of the SLAM run. The states are given as yellow squares, and are enumerated as such. The cyan dots signify the locations extracted from the LiDAR scans. To make the comparison between the methods fair, when running SLAM, the data was manually segmented into downstairs

and upstairs areas.

Type	User	Experiment	Train	Test
Fingerprint	b	1	'fingerprint_1'	'fingerprint_1'
	b	2	'fingerprint_2'	'fingerprint_2'
	a	3	'fingerprint_1'	'fingerprint_1'
	a	4	'fingerprint_2'	'fingerprint_2'
	d	5	'fingerprint_1'	'fingerprint_1'
	d	6	'fingerprint_2'	'fingerprint_2'
Single	a	1	'fingerprint_1'	'living_1_single'
	a	2	'fingerprint_1'	'living_2_single'
	a	3	'fingerprint_1'	'living_3_single'
	b	4	'fingerprint_1'	'living_1_single'
Dual	a	1	'fingerprint_1'	'living_1_dual'
	a	2	'fingerprint_1'	'living_2_dual'
	a	3	'fingerprint_1'	'living_3_dual'
	a	4	'fingerprint_1'	'living_4_dual'
	b	5	'fingerprint_1'	'living_1_dual'
	b	6	'fingerprint_1'	'living_2_dual'
	b	7	'fingerprint_1'	'living_3_dual'
	b	8	'fingerprint_1'	'living_4_dual'

Each model was trained on the same fingerprint in two ways - one on the camera labels and the other using the 'H4LO'. Then, both of the models were tested against specific subsets of all the experiments. The results from these tests are separated into the fingerprinting, single and dual living results, seen in Figs. 5.13, 5.14, 5.15 respectively. They are averaged across all participating users. Note, that there were only four dual living experiments - results for both participants result in 8 test sets.

As described before, the metric used to test the performance of this system is the Euclidean error, found in Eq. 4.2 in chapter 3. As is evident from the graphs, 'H4LO' has a comparable performance to the method used to gather HRL in chapter 3, in some instances even outperforming the baseline. It is important to note here, that the expected results were not supposed to outperform the fingerprinting method outlined in chapter 3. These results, even if not entirely superior to the HRL, come at a fraction of the labour.

A possible reason for the results could also lie in the way the labels from both of the ground-truthing approaches are gathered and quantised. Camera-based approach has

an inherent advantage, in that it is considered as the ground truth when gathering the data, considering only a single x, y position on the floor plan. The error for H4LO was calculated from the available extracted poses on the map $\mathbf{R}$. Extending the Euclidean distance error from Eq. 4.2:

$$\text{Distance Error} = \sqrt{\sum_{i=1}^{d} (l_i - r_i)^2} \tag{5.6}$$

That is, the error is calculated between the quantised camera-based labels and much more resolute poses, extracted from the SLAM process. Inherently, this will yield more error, as the poses are spread across a larger area of the map, and thus would generate more uneven and unfair, discrepancy between the prediction and label.

5.5 Conclusions and Challenges

This chapter has shown, that the efficient 'H4LO' system can be used to generate a fingerprint training dataset with comparable results to the time-consuming camera approach [24]. Through the utilisation of head-worn robotic rig, the 'H4LO' system performs mapping and localisation simultaneously. This solves a number of challenges which were set out in Section 5.1, specifically regarding the arduousness of the fingerprinting method. In addition to providing automation to the entire process, the system also ensures a very reliable location estimation. Whilst the labelling system in chapter 3 did provide similar localisation performance, it relied heavily on the fiducial tags and their annotated coordinates within a house plan, both of which must be known *a-priori*. 'H4LO' removes the need for floor plans, tags, human coordinate measurements and costly processing of high dimensional camera data.

Since 2-dimensional SLAM is often sensitive to well-controlled topology and dynamics (e.g. the extraction plane is assumed to be at a constant height), the relative freedom of data capture in our setting is unusual and could be considered to be detrimental to the quality of the model's outputs. This includes each user's unique traits such as body build, gait, walking speed and having to negotiate various environmental challenges like stairs and door thresholds. Despite this, our system is capable of collecting good quality data which can be subsequently processed by existing state-of-the-art SLAM implementations.

The relative space of application of this system presents a number of interesting challenges. This includes typical human characteristics. Each user in this study was

of differing height, weight and overall build. Combining this with unique, individual attributes of each participant's gait, creates substantial ambiguity between users, making this system difficult to generalise across various users. Yet, even in these challenging circumstances, data from each participant produced accurate maps, even with particular human traits and habits (e.g. stooping under door thresholds).

This system also performs well when exposed to different routes taken by the users through the environment. Recall from Section 5.2 and [79], that the algorithm relies on the creation of local sub maps of the environment when minimising the aggregated error. The rate at which this error aggregates is highly dependent upon the local spatial features of the environment, or simply put, the routes taken by the user. All unique users took different routes, which involved visiting specific rooms in specific order. We have shown, that the hardware is robust enough to collect data from various users, from challenging residential environments, traversing at different trajectories, and is able to provide a viable result when applied to state-of-the-art algorithms.

CHAPTER 6

Robustification and Resilience of Residential Localisation Systems

This chapter presents two studies, where the localisation performance is scrutinised under a number of adverse conditions. As was stated in chapter 1, WSNs are susceptible to various environment changes, noise and outside attacks [87, 177]. Range-based radio signals will be highly dependent on shadowing effects [88] and the user's current position indoors [11]. Understandably, with increased amount of noise in the system, the accurate inference of position becomes correspondingly more challenging [100].

In this chapter, we address these concerns by introducing two separate studies of efficiency and resilience. Firstly, we tackle the robustification of the location estimation through the use of additional information sources. The amalgamation of several passive sensors can be used to provide an accurate location. This location often bears unique signatures of activity, especially when considering residential environments. However, it is only the basic human instincts, such as periodicity and routine, that make this possible. The fact that behaviours and actions recur naturally is an important assumption in this section. Secondly, using novel adaptive techniques, we introduce a new framework, which continuously performs weak training in an energy-aware system. The method is cheap in terms of work-hours, calibration and energy usage. It achieves this by utilising other sensors available in the environment.

6.1 Contributions

The initial study proposes a method, whereby semantic information about the location is learned from an additional source. This method deals with the question of robust indoor localisation prediction by extracting additional activity information available from a wrist worn acceleration sensor. A number of different fusion models are considered, before choosing and validating the model which provides highest improvement in accuracy and robustness over the baseline example. The performance of the methods is examined on different unique datasets, which closely resemble residential living scenarios [100].

Later, we approach the challenge of energy awareness and efficiency in WSNs. Our implementation is evaluated on a simulated localisation environment and validated on a widely available pervasive health dataset which facilitates realistic residential localisation using RSS. We show that our method is cheaper to implement and requires less effort, whilst at the same time providing a performance enhancement and energy savings over time [101].

The majority of the hypotheses in this chapter are validated through the use of a pervasive health dataset which was collected within the SPHERE project [204]. The house which was used to perform this data collection is equivalent to House 4 in chapter 3 dataset, as well as the house of the H4LO dataset in Chapter 5. The experiments performed as part of this dataset aim to resemble 'natural' residential behaviours as closely as possible, by including numerous participants performing scripted and non-scripted actions in a test bed environment. It includes data from bespoke sensors which are popular within the pervasive health community. These include RGB-D cameras, environmental sensors (ES), PIR and wearable accelerometer and RSS data. ES often act as APs for the wearable RSS.

This dataset was deemed appropriate for use in this thesis, as in addition to using the same rigorous, real-life environment as the other datasets, the context of indoor localisation was approached in a similar way [204]. Whereas SPHERE Challenge dataset lacks the resolution of HRL, it includes a variety of environmental and on-body sensors not covered by HRL. Additionaly, the number of participants in the SPHERE Challenge dataset is larger than HRL.

The contributions of this chapter include:

1. Novel data flow models, linking passive acceleration information to RSS using unique data.

2. A study on how an additional source of information is not only beneficial to location inference, but can also safeguard against noise and loss of data.

3. Finding the limits of these models, in the context of pervasive activity monitoring, and providing reasons as to why they exist.

4. Novel, energy-aware adaptive localisation algorithm: We create a simulated environment, closely resembling a real-life localisation system and exhaustively test our method in various simulated experiments.

5. Validation on true pervasive health dataset: We show that the algorithm is easy to generalise to different environments, and can be adapted to various localisation models. We do this using data of differing levels of calibration.

6. Effects of action selection: We compare the effects of different action selection mechanisms in terms of energy-efficiency, and discuss which method is best suited for this purpose. We perform this test on both the simulated and real-life experiments.

6.2 Data Fusion for Robust Indoor Localisation in Digital Health

This section presents a range-based probabilistic method of localisation and the fusion of passive acceleration sensors. In chapter 2, we outlined the most popular fusion methods for indoor localisation, showing that inertial sensors are very likely to be complimented by an another modality of sensor, such as a BLE radio. In order to enrich the data in this study, a wrist-worn accelerometer is used as an additional source of information about the activity.

Processing the accelerometer data involves feature extraction and classification of predefined tasks. The process of activity recognition using sensors has been noted as difficult due to the human tendency to interleave concurrent tasks [67]. Also, considering the activities themselves, the emphasis in various research avenues is to establish how coarse the labels should be for optimal estimation performance. The position of the accelerometer on the participant is also a subject of debate [13]. Wrist-mounted accelerometer activity recognition is usually inferior to prediction from sensors mounted on different parts of the body [132]. Regardless, the wrist remains the least intrusive and most socially acceptable place to wear a sensor, especially in the context of monitoring well-being [55].

6.2.1 Method

The probabilistic models presented in this section will initially be analysed on SPHERE Challenge Dataset [204]. The 4 APs available in the house were moved from their nominal positions in-between experiments. This meant, that learning a model on two affected experiments could produce different signatures of the RSS in the same locations. In addition to this, an AP would occasionally be out of commission for a period of time and would not be sending information about the signal strength. This dataset, however, is a good platform to perform studies relating to real-life pervasive monitoring based on WSNs. This is due to the fact that it will faithfully reproduce the possible shortcomings often encountered whilst rolling out this kind of localisation system.

Out of the 20 activities labelled in the dataset, there are only a handful which could help with localisation. A number of specific labels would be grouped together into a single class. The reason for their groupings stems from the sparsity of RF coverage in the test bed house. As the vast majority of the scripted experiments took place downstairs, the SPHERE dataset study included only one AP upstairs. The rooms with poor coverage included two bedrooms, a toilet and a corridor area. By distinguishing the activities performed in the bedrooms, such as 'sit-to-lie' and 'lie-to-sit' transitions, it was easier to predict the upstairs locations more accurately. This was because these particular movements are more often performed in these rooms and could be used to aid the RSS-only prediction of location.

The labels from SPHERE Challenge dataset were banded into 5 separate groups. These are tabulated in Table 6.1. Group 1 helped with ambulation information. Group 2 was used to aid the localisation upstairs, as the tasks in that group were found to be most prevalent there. Group 3 aided with the staircase determination, in order to make the floor transitions more accurate. Group 4 only includes sitting, which was performed in a variety of rooms, much like squatting in Group 5.

The SPHERE Challenge Dataset lacked the granularity required to examine performance of localisation algorithms thoroughly. This was because only room-level labels were available. This necessitated the generation of a more diluted dataset, which could later be used for testing the robustness of the methods.

6.2.1.1 Feature Extraction

There are a number of studies concerned with time series feature extraction, and accelerometer in particular. Common features include mean, mode and median, zero

Table 6.1: Optimal label groups for activity recognition in SPHERE Challenge data

Group 1	Group 2	Group 3	Group 4	Group 5
Jump	Bending	Ascend	Sitting	Squatting
Walk-with-load	Kneeling	Descend		
Walk	Lying	Stand-to-bend		
	Standing	Kneel-to-stand		
	Lie-to-sit			
	Sit-to-lie			
	Sit-to-stand			
	Stand-to-kneel			
	Stand-to-sit			
	Straighten			
	Turn			

crossing rate and first five values of Short Time Fourier Transform [164, 175].

In order to extract the features from SPHERE Challenge data, a window of 6.4s as per Zhang et al. [240] was used. The windowing method was an overlapping rolling window, producing $K - N$ extraction samples, where K is the number of aggregated time bins. It segmented the data, sampled at 20Hz, into vectors of length $N = 128$, from which simple features were extracted based on direction-invariant magnitude. Each feature was then recorded and a number of different classifiers were used. Those classifiers were chosen on the basis of the state-of-the-art within the community [164, 175]. They include k-Nearest Neighbours (k-NN), Decision Trees, Linear Discriminant Analysis (LDA), Quadratic Discriminant Analysis (QDA) and HMM.

Not all of the features have the same relative impact over the classification accuracy. Minimum-Redundancy Maximum-Relevance (mRMR) [159] was used to choose the most effective subset of features based on the mutual information. The most dominant features were also the simplest – full list is shown in Table 6.2.

For HRL data however, temporal aggregation was required. Temporal aggregation is the accumulation and averaging of data points into respective temporal bins of specific duration, effectively down-sampling the data. HRL was sampled at 5Hz, outputting 5 separate unique values at each sample. Data was then aggregated into 0.2s time bins. It was found that a window of 1.2s performed best for feature extraction. This yielded $N = 6$ data points in each window. The better performance was likely due to the quality of data available.

Table 6.2:
Ranking of accelerometer features.

Feature
1. Variance
2. Mean/Median/Mode
3. Sum
4. RMS
5. Standard Deviation
6. Range
7. Kurtosis
8. Skewness
9. Max/Min
10. Area
11. 25% Percentile

6.2.1.2 Models

The notation in this section is as follows: L denotes location, RSS is the observation of the RSS, Y is the inferred activity and Acc are the observations of the accelerometer features.

The model from Fig. 6.1 is be used as a Baseline. It only uses RSS as its location observation. At a given time t, the trained model will compare the current observation of the RSS against all the location states. This method is widely accepted in literature [81, 150]. The stipulation in this model is that the distinctiveness of the signal in each room/tile is enough to localise a user in a residential environment. This model does not account for the user's activity information, nor does it make any contextual assumptions about the layout of the localisation environment.

Fig. 6.2 shows a first improvement on the Baseline. In addition to the previous RSS observations, it assumes that the location is also determined by the current activity of the user. This model came out of the belief that, for example, it would be more likely to assume the user is in the kitchen because they are cooking, instead of inferring the opposite. In order to infer the activity however, the feature observations are required.

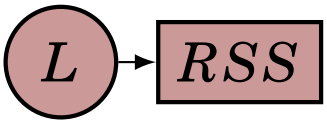

Figure 6.1: Baseline

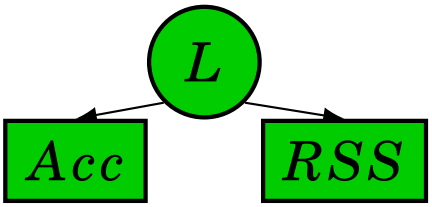

Figure 6.2: Model 1

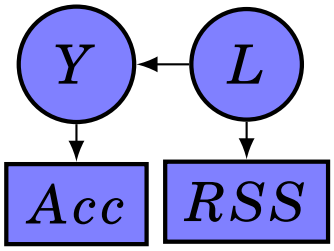

Figure 6.3: Model 2

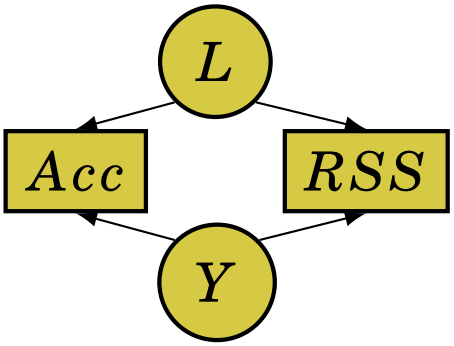

Figure 6.4: Model 3

The second model in Fig. 6.3 ignores the activity information. It instead relies on the fact that the user's raw accelerometer features are enough to distinguish specific location in the house. This model is the simplest of all three and only considers observations to infer a single level network. This model is likely to be the most robust out of the three, mainly due to lesser complexity.

The final model in Fig. 6.4 does not directly link activities to locations, but the two nodes are nonetheless jointly dependent through observations. It is stipulated that the extra activity information might have some influence on how the location is inferred.

The estimation of the Bayesian posterior using HMM and graphical models follows the method given in chapter 4. Equation 2.3 specifies, that the calculation of the probability of a hypothesis, given evidence is the product of the probability of a variable, given its parents. In dynamic systems, inference can be approximated using the Forward-Backward algorithm. This is also known as belief propagation.

The modelling of accelerometer signatures in this section follows a Gaussian distribution. Due to the granularity of the dataset, the relative range of accelerometer traces in various locations in the house can be aggregated to represent a probability density function over some variable, in this case the magnitude of the accelerometer. This is

described as:

$$p(Acc|\hat{\boldsymbol{L}}_j) \sim \mathcal{N}(Acc|\mu_j,\sigma_j) \tag{6.1}$$

where $1 \leq j \leq T$ are the location states.

6.2.2 Evaluation

The SPHERE Challenge Dataset was used to analyse how the models would perform on low-resolution but well labelled data. The dataset was separated into 10 identical experiments performed by different users. In order to test the model, 10-fold cross validation was used across all experiments. Two experiments - 6 and 7 - were underperforming. After removing those from the fold, the performance of the remaining bins increased.

The relative performance of the algorithm was found to increase if those experiments were removed from the fold. There are a number of reasons why this might happen. For example, due to the large number of annotators involved during the labelling process [204], the labels of the locations might have been erroneous. The performance of the sensing systems could have also been at fault, as these experiments took place over a number of days, with a number of sensor outages evident in the data [204]. Finally, the positions of the AP nodes may have been disturbed, as the experiments took place in a busy experimental test bed abode, with various experiments taking place concurrently. Due to those reasons, they have been omitted from subsequent analysis.

The metrics of evaluation of these models have been previously outlined in chapter 4. Here, we use all three metrics: Accuracy, Distance error and Path error, to evaluate the performance.

Every enhancement model improved the nominal result, suggesting that the inclusion of accelerometer data is advantageous. The small deviations between the models were, in addition to their architectures, likely caused by their complexity. Model 3 is the most complex of the remaining two. Fig. 6.5 shows that it performed similarly to Model 2, never deviating for more than 5%. Those two models share similarities in the way they infer the location, but the prediction coming from a less complex Model 2 is more accurate. Model 1 did not follow any other method. It was more accurate when predicting the path error than Model 2. However, it required more elaborate pre-processing and inference methods, as it would be inferred on two levels. The increased number of inference steps

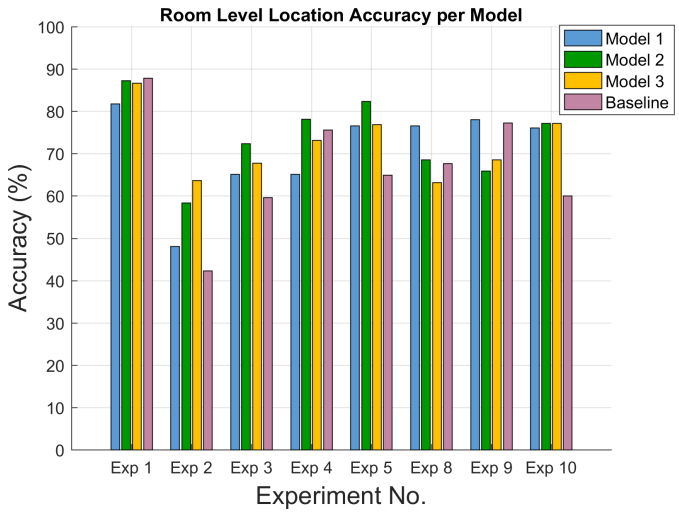

Figure 6.5: Accuracy of each model. Experiments 6 and 7 were omitted due to under performance.

are more likely to harbour inaccuracies and false positive activity predictions. This in turn translates into inaccurate location result. Table 6.3 shows the overall average result of the SPHERE Challenge data analysis.

Model 2 was therefore chosen as the optimal network, by leveraging the result obtained to the complexity of the system. It was used to validate the hypothesis set out on the previous dataset. The data consisted of three separate 'free-living' experiments. Those experiments included 'everyday' behaviours and tasks which are likely to be found in any Digital Health data collection study. As with the SPHERE Challenge data, cross-validation was used train and test the model. It is important to point out that the chosen method did not require any activity labels. The results can be seen in Table 6.4.

This chapter will test the robustness of different models by presenting two exper-

	Room-level Accuracy (%)	**Distance (m)**	**Path (m)**
Baseline	70.4	1.28	2.11
Model 1	74.2	1.05	1.47
Model 2	75.9	1.01	1.51
Model 3	73.3	1.09	1.61

Table 6.3: Results of testing the models on SPHERE Challenge data.

	Room-level Accuracy (%)	**Tile-level Accuracy (%)**	**Distance (m)**	**Path (m)**
Baseline	100	14.66	1.65	1.96
Model	100	15.88	1.54	1.95

Table 6.4: Results of Model 2 with HRL.

iments on the HRL data. Firstly, packet drop rate, (as explained in chapter 4), will be iteratively increased. This is to see how the baseline and the enhanced model will perform when faced with missing data. Secondly, the APs will be gradually removed. This will mean that there will be fewer sources of information. The experiment will check how the enhanced model will perform when faced with less data in a smaller indoor environment.

When using the HRL data, the resolution was reduced to 1m × 1m. This meant that the actual distance error could remain similar, whilst the tile-level accuracy metric would fail to provide a viable result. The finer resolution increased the overall temporal error. Consider Table 6.4, where the room-level accuracy is now perfect, but tile-level reduces to 15.88% in the best case. Due to that fact, only the path error and the distance error were considered during the robustness study.

6.2.3 Validation & Discussion

Our RSS-based system achieves comparable performance to the state-of-the-art RSS implementations in the Microsoft Localisation Competition [127]. The average distance error achieved by our method in Table 6.4 (1.59m) is similar to the error achieved by Chen et al. [32, 127] (1.37m) using analogous infrastructure. However, our experimental scenario and the testing environment differs from the competition setup and as such the two cannot be directly compared.

Although the improvement over the Baseline is slight, one of the goals is to study the robustness of the Model against different types of perturbations. Firstly, the packet loss rate between the APs and the wearable, which is naturally present with a value of 22.75%, was increased. Fig. 6.6 shows the path error of the Baseline and Model to increasing packet loss rates. Similarly, Fig. 6.7 illustrates the distance error. Both of graphs show the average performance of $n = 57$ random injections of noise into the system together with the standard deviation. The Model's path finds a minimum at

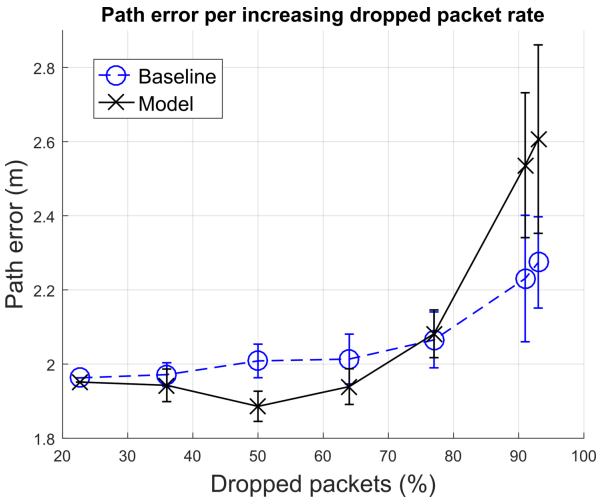

Figure 6.6: Path error per increasing packet drop rate.

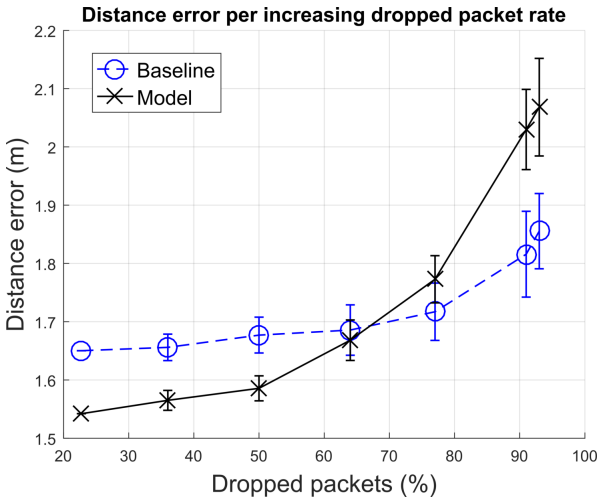

Figure 6.7: Distance error per increasing packet drop rate.

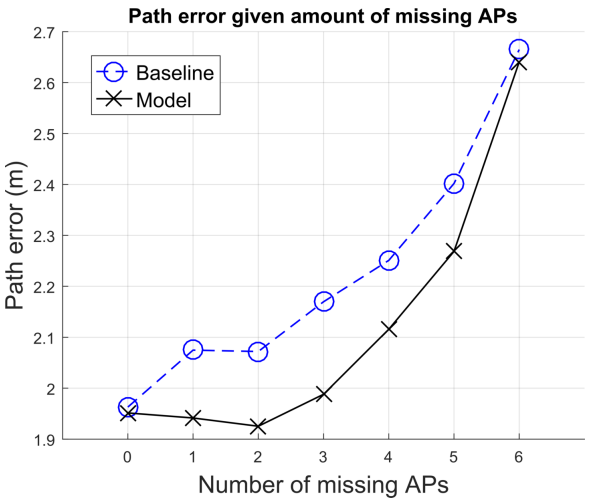

Figure 6.8: Path error given increasingly fewer Access Points.

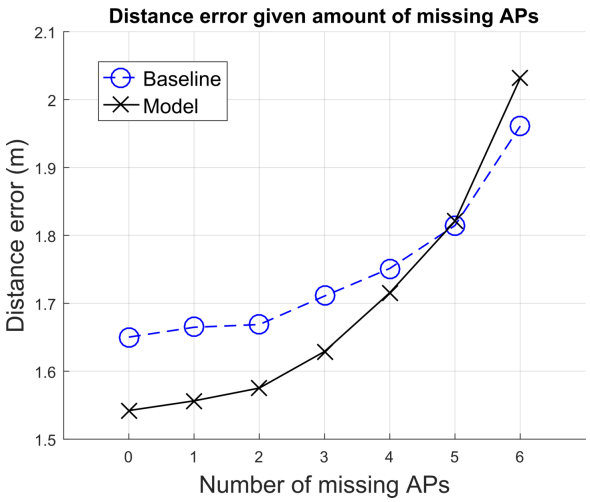

Figure 6.9: Distance error given increasingly fewer Access Points.

50% of dropped packets. It is at that point that the result shows an improvement of 10cm over the Baseline. This happens as the accelerometer values, originating in the wearable, are invariant to range, whereas RSS are not. The former will appear the same or similar at each AP, whereas the latter will vary with each AP. This makes accelerometer information complementary and thus more immune to added noise. After 50% of noise however, the Baseline begins to outperform the Model. It appears that, again, the complexity plays an important role in the prediction. Since the Model requires the accurate estimation of more parameters than the Baseline, it is prone to overfit the data. This can also be confirmed by the standard deviation of the error at high packet drop percentage. Model's error fluctuates more broadly than the error for the Baseline. Additionally, the distance error confirms this, but to a lesser extent as it presents a much smoother increase. This is due to less rigorous distance measurement – any deviation from the label will be scaled linearly, as opposed to being a function of the layout of the environment.

Secondly, an experiment was devised to understand how the Model performs when APs are removed to simulate a scenario with reduced numbers of APs. This study involved taking the RSS distributions for each AP and ranking them according to their pairwise overlap, computed as the Weizman's measure (also known as the overlap coefficient). The APs were then removed one by one according to this criteria in order to reduce the total number of APs removing as little information as possible. Figures 6.8 and 6.9 show the performance for the Baseline and Model for both path and distance metrics. Similarly to the previous experiment, the behaviour is consistent with the hypothesis that the Model, given relatively noiseless data, will outperform the Baseline, even when faced with fewer sources of information.

6.3 Energy Efficiency in Reinforcement Learning for Wireless Sensor Networks

Aided by RL techniques, we propose a new method, designed to alleviate the need for rigorous training and dependence on energy-consuming sensors. We do this by performing weak training across the entirety of the sensor network's lifespan. Additionally, by utilising more power-hungry sensors sporadically, we can achieve continuous improvement of performance while at the same time reducing the need to use them. We aim to provide a reliable and cheap indoor localisation solution capable of adapting to a persistent environment. This adaptability is required because, as it was mentioned in

previous chapters of this thesis, RSS-based localisation is notoriously arduous to deploy and unforgiving in a dynamic environment [115]. The dynamics in this context can be understood as constantly changing RF signatures due to human or non-human factors.

6.3.1 Related work

The problem in this section was inspired by the work done in [163]. Here, the authors attempt to classify activities of the user by on-body sensors and video cameras. They also consider the energy consumption of the camera, utilising a Markov Decision Process (MDP) to decide whether to use weak, but efficient accelerometer and gyroscope, or strong but inefficient video cameras.

Let us consider the above study in terms of indoor localisation. The idea of energy-efficient localisation has been proposed before [4, 244]. These methods calculate the energy efficiency directly - either by adapting the transmission power to the environment, or by inherently using low-power devices. In this chapter we consider energy-efficiency in terms of number of sensors. We aim to reduce the usage of different sensors, with only a broad idea of their power consumption. This makes our method easy to generalise and adapt to already existing sensor networks.

The available pervasive health monitoring sensors, such as PIR or ES [52] differ in their usability and the quality of their readings. They also differ in how much energy it takes to operate them and process their results [50]. Low-power wearable sensors [55] are also popular within the community, providing not only the on-board acceleration observations, but also acting as a RF anchor for an agent traversing the environment.

There is a clear need for an adaptive method of continuous weak learning. We can alleviate the concerns of energy efficiency by making the system aware of its consumption, even in the broadest of terms. Further, this model could be adapted to more complicated energy studies. We can also remove the need for user-specific training by re-estimating the model at certain intervals. The system would be thus indifferent to specific user training, relying instead on weak re-estimation over time to tailor the model to specific users.

6.3.2 Method

6.3.2.1 Markov Decision Processes and SARSA

MDPs are tuples of $\{S, A, P, R\}$, where S is the state-space, A is the action space, P is the transition kernel, R the immediate reward function. Additionally, we recognise two

parameters, γ and α – the discount factor and learning rate respectively. For any MDP, there exists an optimal policy $\pi^* : S \rightarrow A$. The desired outcome of the MDP is to estimate this policy. We utilise the SARSA algorithm defined as follows [199]:

$$Q(s_t, a_t) \leftarrow Q(s_t, a_t) + \alpha[r(s_t, a_t) + \gamma Q(s_{t+1}, a_{t+1}) - Q(s_t, a_t)] \tag{6.2}$$

where Q is the state-action value matrix, which is updated at each iteration, α is the learning rate, γ is the discount factor, and $r \in R$ is the immediate reward at state s_t and action a_t. We assume that the dynamics P are equally likely for each state, given each action.

We will now formalise our problem in terms of the above. The reinforcement state space is given by $S = \{S1, S2\}$. These two states specify whether at time t we use 'enhanced' or 'low-power' sensing. We specify $S1$ to signify the 'enhanced' sensing, which provides reliable labels at the cost of high-energy usage. This state also allows for the system to perform the re-estimation of the parameters, using the labels which were recently observed by these sensors. 'Low-power' sensors will be covered by $S2$. Accordingly, each state will be able to perform one of two actions $A = \{A1, A2\}$, which in turn lead the system to their respective states.

The reward function was designed to be simple and intuitive. It penalises the system if it remains in $S1$ and rewards if in $S2$. More formally:

$$r(s_t, a_t) = \begin{cases} -1 & \text{if } s_t = S1 \quad \text{and} \quad a_t = A1 \\ +1 & \text{if } s_t = S2 \quad \text{and} \quad a_t = A2 \\ 0 & \text{else} \end{cases}$$

Additionally, at each time step the system is rewarded if the performance error is reduced or remains the same, and penalised if it increases. This forces the system to continuously seek performance improvement, even if in S2. The error in these iterations is only calculated during $S1$ from the currently observed labels - in $S2$ the system retains the value from $t-1$. We denote this boost as ψ and error as e:

$$\psi_t = \begin{cases} -1 & \text{if } e(t) \geq e(t-1) \\ +1 & \text{if } e(t) < e(t-1) \end{cases}$$

This reward boost can be trivially added in (6.2) as follows:

$$Q(s_t,a_t) \leftarrow Q(s_t,a_t) + \alpha[\psi_t + r(s_t,a_t) + \gamma Q(s_{t+1},a_{t+1}) - Q(s_t,a_t)] \tag{6.3}$$

The MDP environment is shown in Fig. 6.10. The states are given by circles, the actions are the squares. The numbers next to the arrows specify the reward for each transition. It is crucial to mention that the state space, parametrised by the MDP in Fig. 6.10 differs from the inference state-space, which uses a Hidden Markov Model. The inference space serves to represent physical surroundings, as in Fig. 2.3, whereas the MDP state-space is an abstract representation of a system state machine.

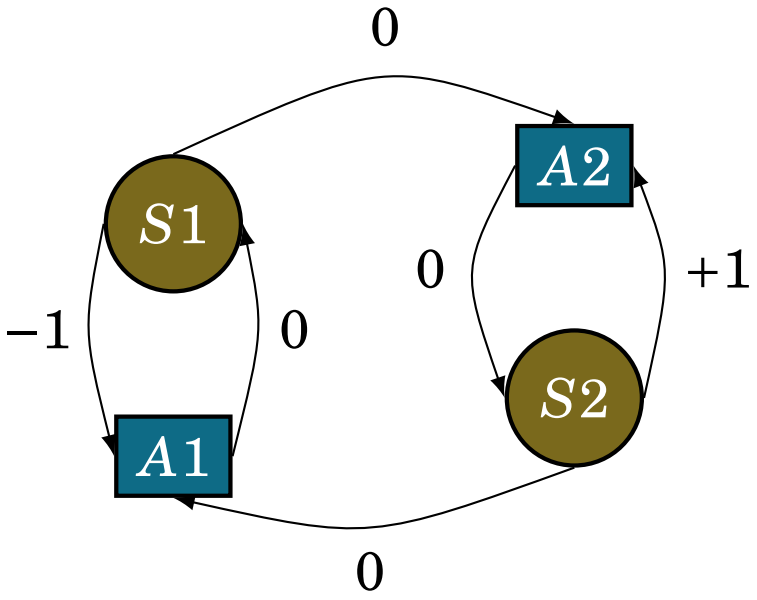

Figure 6.10: Diagram of the MDP state space.

6.3.2.2 Action Selection

Selecting the appropriate action for each iteration is not trivial. There exist methods ranging from completely random, pseudo-random and greedy. Greedy selection makes use of the expected future rewards, and exploits them with no regard to any other alternative trajectories, even if the chosen one is sub-optimal. In our approach, the trade-off between exploration and exploitation should be leveraged, such that we converge quickly as to preserve energy, but also retain a degree of exploration, to continue looking for an optimal trajectory and ensure constant training. To do this, we use the ϵ-greedy algorithm.

The difference between Greedy and ϵ-Greedy lies in the parameter ϵ. Where Greedy chooses the next action as $Q(s_t, a_t) = max_a Q(s_t, a)$, ϵ-Greedy selects an alternative action with probability ϵ, ensuring that we explore the trajectories more thoroughly in the search of the optimal policy π^*. This is because we no longer 'exploit' the reward, prioritising quick convergence, but are open to 'explore' the policy space. The larger the parameter ϵ, the broader the exploration, at the cost of higher energy consumption. It is stipulated, that the added adaptability in the form of ϵ, will make ϵ-Greedy better when leveraging efficiency and performance.

Softmax action selection differs from the above methods, in that sub-optimal choices will be weighted as a graded function of their estimated value. It is likely to reach the optimal policy quicker than Greedy or ϵ-Greedy, but at a cost of higher energy usage. Formally, it chooses action a, with probability [199]:

$$P_t = \frac{e^{Q_t(a)/\tau}}{\sum_{b=1}^{n} e^{Q_t(b)/\tau}} \tag{6.4}$$

In this study we will consider the above three selection methods: Greedy, ϵ-Greedy and Softmax. The usefulness of these methods, given our use case, will be judged by how well they perform in simulation and during validation.

6.3.2.3 Parameter Re-Estimation

When the system enters $S1$, it is allowed to access to labels from reliable 'oracle' sensors. The labels from each 'oracle' can be considered as the real descriptor of location. Each of these 'oracles' maps its output to a given location state. If the 'oracles' are activated at time t, the system can re-estimate the old emission and transition probabilities with the observations from this 'oracle', to which it currently has access. This is done with a single iteration of Expectation-Maximisation (EM) of the previous Gaussian distribution and a sample RSS_t. The weighting in EM specifies how much we trust the 'oracle' reading – in essence, it specifies how much of the old distribution should be retained. The optimal weights were found empirically for both the simulation and validation.

6.3.2.4 Proposed Algorithm

Algorithm 2 starts by initialising the HMM and SARSA parameters. Note, that for HMM, T represents the available state space, whereas $\hat{\boldsymbol{L}}$ is the inferred, most likely sequence of states. It runs as long as there is data coming from the sensors, shown here as $\mathcal{O}$. We

Input: $\{\lambda, T\}$ = HMM parameters, $\{\mathscr{S}, \mathscr{A}, \mathscr{P}, \mathscr{R}, \gamma, \alpha\}$ = SARSA parameters
while $\mathscr{O}$ *available* **do**
  $\mathscr{O} \leftarrow$ vector of sensor observations at t
  $\hat{\boldsymbol{L}} \leftarrow$ infer location $P(T|\mathscr{O}, \lambda)$
  if $s_t == S1$ **then**
    $\Gamma \leftarrow$ vector of weak oracle labels at t
    $\lambda^* \leftarrow$ estimate likelihood $\mathscr{L}(\lambda|\Gamma)$
    $e(t) \leftarrow$ compare T with Γ
  else
    if $s_t == S2$ **then**
      $\lambda^* \leftarrow \lambda$
      $e(t) \leftarrow e(t-1)$
    end
  end
  if $e(t) \geq e(t-1)$ **then**
    ψ_t = -1
  else
    if $e(t) < e(t-1)$ **then**
      ψ_t = 1
    end
  end
  $a_{t+1} \leftarrow$ next action based on Greedy, ϵ-Greedy or Softmax and dynamics $\mathscr{P}$
  $s_{t+1} \leftarrow a_t$
  $Q(s_t, a_t) \leftarrow Q(s_t, a_t) + \alpha[\psi_t + r(s_t, a_t) + \gamma Q(s_{t+1}, a_{t+1}) - Q(s_t, a_t)]$
  $s_t \leftarrow s_{t+1}$
  $a_t \leftarrow a_{t+1}$
  $\lambda \leftarrow \lambda^*$
end

Algorithm 2: Proposed Algorithm

assume that the incoming data stream is vectorised. Each iteration of time t specifies a new vector of incoming data, either collected from 'oracle' and RSS sensors, or just RSS. This is dependent upon the state in which the system resided at $t-1$. Inference is performed by running the Forward-Backward algorithm. Depending on the current state of the MDP, the output of this could be compared with the weak labels provided by the 'oracles', and the HMM parameters λ could be re-estimated. If not, the error is retained from the previous run. The reward boost assignment then follows, and is also dependent upon the current state. After choosing next action, with respect to the selection method, SARSA is used to calculate $Q(s_t, a_t)$.

The algorithm will be evaluated on a simulated environment and validated on SPHERE Challenge dataset. In the simulation, we aim to scrutinise the algorithm under comprehensive set of changes in the environment, in order to confirm its capabilities and demonstrate its effectiveness. The validation dataset will serve to verify its

usefulness under real-world conditions.

6.3.3 Evaluation

The simulation setup was created to closely resemble a real-life system. A state-space of varying size was created. Each state j is described in terms of arriving symbols RSS_t from all G APs. Both the size of the simulation space and the number of simulated APs were incremented. For the simulation space, this changed from 10 to 30, in increments of 10. The size of every state was 1m × 1m. For APs, the number ranged from 5 to 8. The distributions from each AP were simulated according to a BLE path loss model. The parameters of the model were appropriated from [139], which was calculated in the same test-bed environment as the SPHERE Challenge dataset. We also define 'oracles' in a simulation environment as states, which we observe directly at all time. The amount of 'oracle' coverage of the state space was also incremented in 10% intervals from 10% to 100%.

The 3 curves presented in Figs. 6.11, 6.12, 6.13, 6.15, 6.17, 6.19, are dubbed Control, Reinforced and Underlying. The Underlying curve shows the result of the fundamental distributions which were generated when the synthetic state space was created. They describe the underlying model of the simulated state space, and can be thought of as a localisation result under optimal policy π^*. The Control curve show the result of the the same fundamental distributions, albeit with 3dB of Additive White Gaussian Noise (AWGN) added. This simulates a noisy channel in the indoor environment. The Reinforced distribution is regulated by the presented method. The Control and Reinforced models begin as one and the same. The objective to observe is the Reinforced curve tending towards the Underlying curve as the number of plays is increased, effectively showing how close the algorithm is to the optimal model.

The metric used to show the dependence on energy-inefficient sensors is the total number of iterations where the system stayed in $S1$, divided by the total number of iterations. The normalisation of this metric allows us to represent the dependence as a variable between $[0,1)$. The closer to 1, the more dependent the system is on multiple sensors. The simulation MDP parameters of α and γ were set to 0.4 and 0.9 respectively, and the oracle weight during each re-estimation is 0.7. All of the above were chosen empirically, as they were found to provide best localisation results.

Considering the results of 'oracle' usage, the graphs in Figs. 6.11, 6.12, 6.13 show the average performance of the algorithm as a function of 'oracle' coverage. These graphs confirm that the algorithm is viable - the performance of the algorithm under

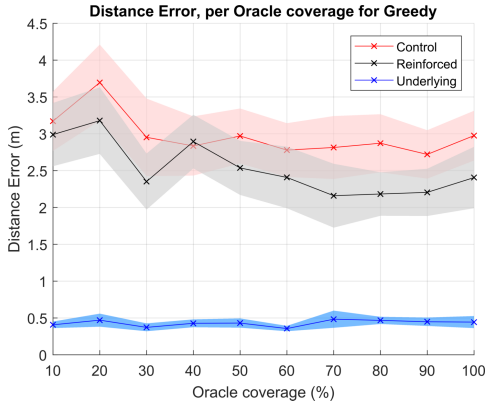

Figure 6.11: Distance error per oracle coverage under Greedy regime.

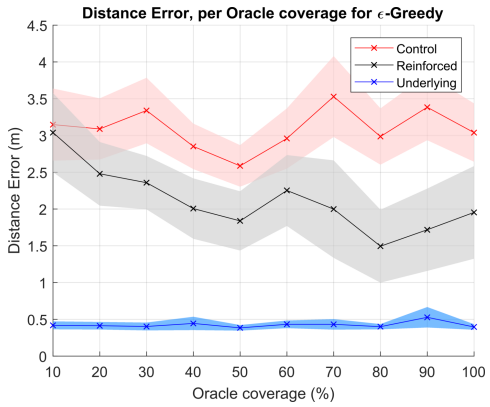

Figure 6.12: Distance error per oracle coverage under ϵ-Greedy regime.

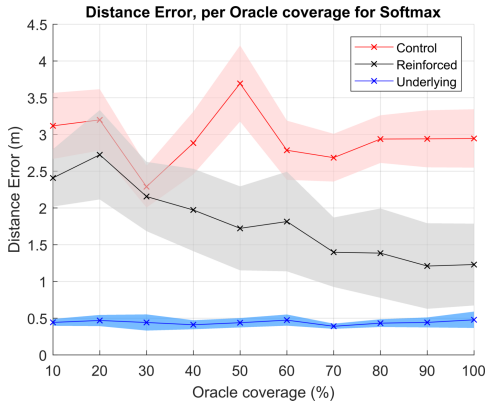

Figure 6.13: Distance error per oracle coverage under Softmax regime.

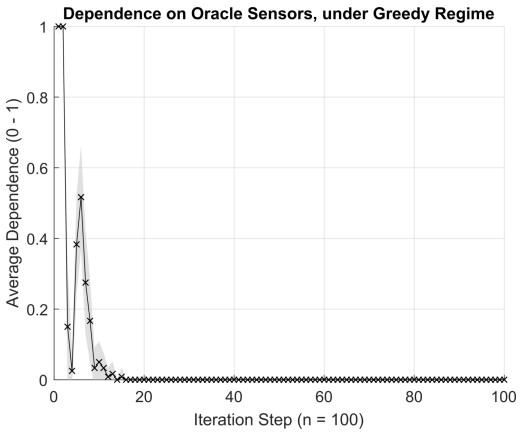

Figure 6.14: Oracle Dependence, Greedy.

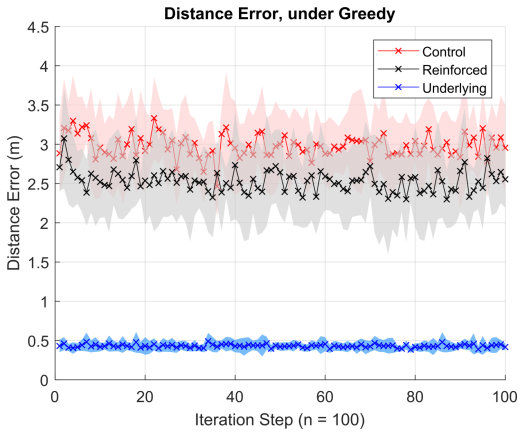

Figure 6.15: Distance error, Greedy.

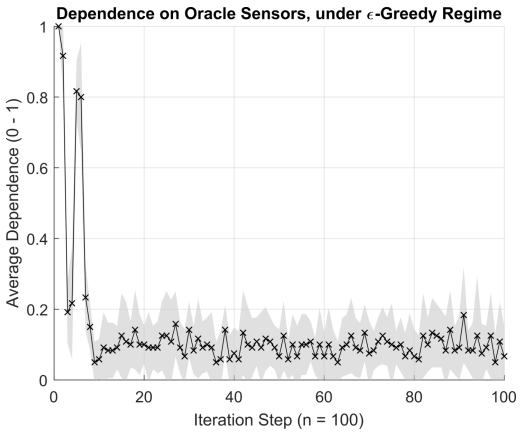

Figure 6.16: Oracle Dependence, ϵ-Greedy.

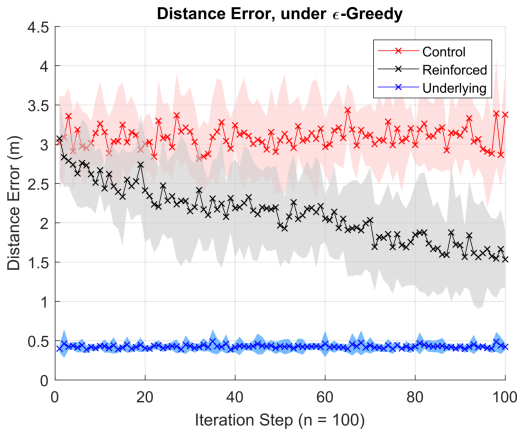

Figure 6.17: Distance error, ϵ-Greedy.

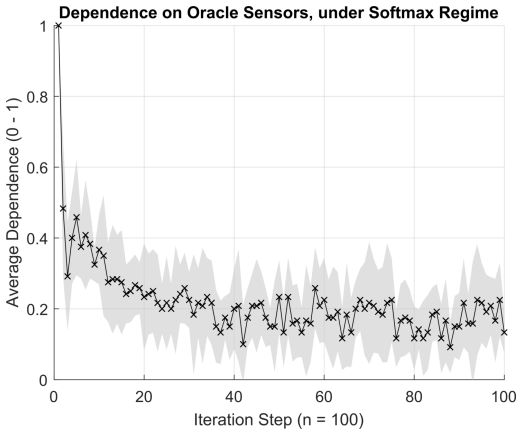

Figure 6.18: Oracle Dependence, Softmax.

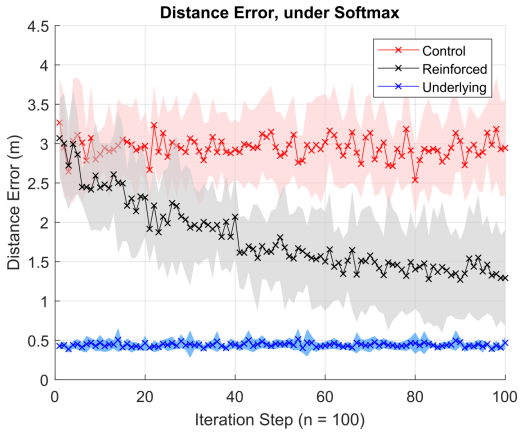

Figure 6.19: Distance error, Softmax.

different action selection regimes was compatible with the prediction. The improvement in performance is a function of how much state space is covered by 'oracles'. Depending upon which action selection method is chosen, the improvement varies between 0.5m for Greedy to 1.5m for Softmax.

We will now discuss the dependency results from the simulated environment. The graphs are consistent with the hypothesised effect of the action selection method. The 3 Figures, 6.14, 6.16 and 6.18 show the results of Greedy, ϵ-Greedy and Softmax selections respectively. Greedy selection exploits the rewards immediately, and converges to near 0 dependence on 'oracles'. This in turn shows, that the closer we are to 0, the faster the distance error converges in Fig. 6.15. The convergence here is sub-optimal, as the trajectory of the system could be improved. This is visible in Fig. 6.19. The Softmax method was used with a temperature of $\tau = 1$. This is displayed with a dependence graph in Fig. 6.18. A gradual roll-off improves the localisation performance. However, this results in higher energy usage, as the energy-heavy senor usage converges to 0.2.

Figures 6.16, 6.17, 6.18 and 6.19 show the optimal trade-off between energy efficiency and quickness of training. The ϵ-Greedy algorithm quickly reaches the mean of 0.1, which is consistent with the parameter ϵ, set to the same value. The Softmax regime provides less erratic reduction of the dependence, in turn providing a better localisation performance.

The above results are consistent with the theoretical hypothesis. Figs. 6.11, 6.12, 6.13 confirm, that as the number of oracles increases, so does the improvement in performance. The dependency in 6.14, 6.16 and 6.18 agree with the respective action selection methods. The graphs in Figs. 6.15, 6.17 and 6.19 also conform to their respective regimes. All of the methods will be tested on the SPHERE Challenge data for completeness – however only two, that is ϵ-Greedy and Softmax are in contention to see which one is optimal for the use with this algorithm.

6.3.4 Validation & Discussion

We use specific sensors, available in the SPHERE Challenge dataset to be treated as 'oracles'. These sensors include RGB-D video cameras and PIR sensors. The version of the dataset used in this study includes labels not available in public domain at the time of writing of this thesis.

Along with the RSS information available from 4-unique APs scattered around the house, we also have access to room-level location labels. The house includes a total of 9 labelled rooms. No cameras were placed in sensitive locations in the house which meant

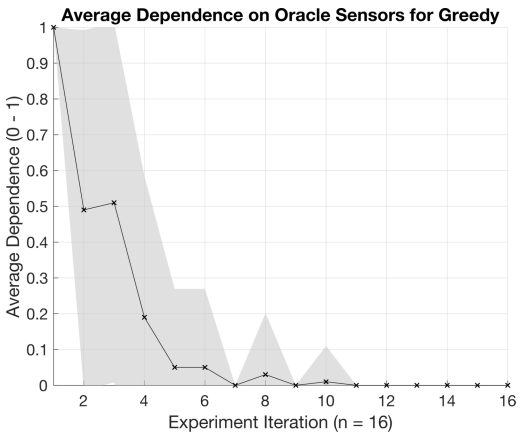

Figure 6.20: Oracle Sensors Dependence, Greedy regime

Figure 6.21: Distance error results, Greedy regime

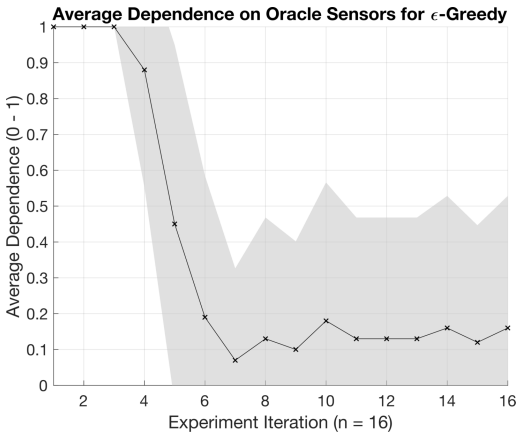

Figure 6.22: Oracle Sensors Dependence, ϵ-Greedy regime

Figure 6.23: Distance error results, ϵ-Greedy regime

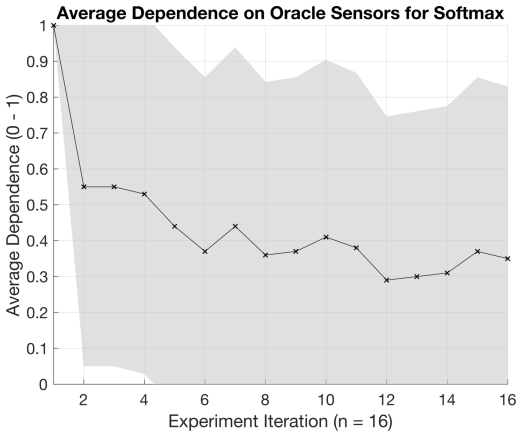

Figure 6.24: Oracle Sensors Dependence, Softmax regime

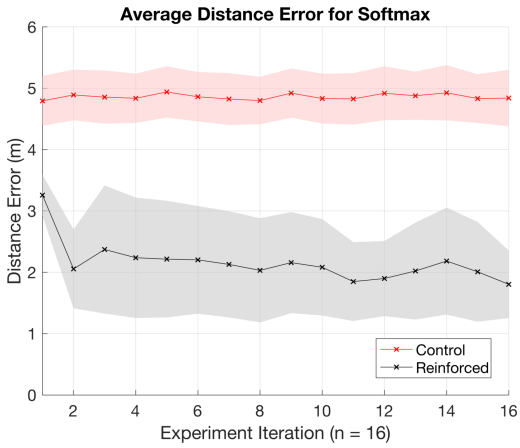

Figure 6.25: Distance error results, Softmax regime

that some states would lack descriptor 'oracles'. The rooms which did include 'oracles' are the kitchen, the living room and the downstairs hallway. The PIR sensors however are available in every room. Their usage was limited however, as their reliability was poor. They were used to re-estimate, but were omitted from localisation inference.

The method follows as before. After training a weak model, the energy usage and the relative performance are being scrutinised and leveraged. The data included 19 unique scripted and labelled experiments. In order to obtain a fair result, the training and test proportions were set at 15% to 85% respectively. At any one time, a uniform random selection of 3 experiments were chosen to train the model. Testing was performed by running the remainder of user data in a randomly permuted order. This method was repeated $n = 100$ times.

The system was set up such that in $S1$ the system uses a fusion of RSS and camera data. The fusion takes place using similar architecture to Model 1 from Fig. 6.2, albeit with extracted camera data instead of accelerometer signatures. Again, in this state, the parameters are re-estimated according to the labels provided by the 'oracles'. As was mentioned above, the PIR were used to re-estimate, but were omitted from location inference. In $S2$, the system relies only on the RSS, with no parameter mixing. The graphs again show the dependency on 'oracle' sensors, normalised to 1, and the localisation error convergence graph. The latter further diverges into the control distribution, which is the model trained on initial users and reinforced distribution, which is being continually re-estimated. The localisation labels are room-level.

The results are presented in Tables 6.5 and 6.6. They show, that the method holds when exposed to non-simulated data. Fig. 6.22 shows the dependency graph, with a steady decline in energy-inefficient sensor usage. This can very closely correlate to lower energy consumption. The variability of the dependence was likely caused by the dataset itself.

Table 6.5: SPHERE Challenge performance results

Selection	**Model**	**25% of Exp.(m)**	**50% of Exp.(m)**	**100% of Exp.(m)**
Greedy	Control	4.79 (± 0.41)	4.87 (± 0.43)	4.89 (± 0.43)
	Reinforced	2.34 (± 0.90)	2.67 (± 1.05)	2.54 (± 1.00)
ϵ-Greedy	Control	4.82 (± 0.45)	4.89 (± 0.42)	4.85 (± 0.41)
	Reinforced	1.77 (± 0.45)	2.09 (± 0.84)	2.11 (± 0.77)
Softmax	Control	4.83 (± 0.40)	4.80 (± 0.39)	4.84 (± 0.46)
	Reinforced	2.24 (± 0.98)	2.03(± 0.85)	1.80 (± 0.55)

Table 6.6: SPHERE Challenge dependence results

Selection	**25% Iterated**	**50% Iterated**	**100% Iterated**
Greedy	0.19 (± 0.39)	0.03 (± 0.17)	0 (± 0)
ϵ-Greedy	0.88 (± 0.33)	0.13 (± 0.34)	0.16 (± 0.37)
Softmax	0.53 (± 0.5)	0.36 (± 0.48)	0.35 (± 0.48)

The labels were room-level, which meant that even slight deviation would substantially increase the error. The performance in Fig. 6.23 also shows a steady performance increase from the control distribution, as the number of plays is being increased.

The data was also scrutinised under the other two action selection regimes. The results for Greedy and Softmax methods are shown in Figs. 6.21 and 6.25. The performance of these methods is consistent with the simulated results. For Greedy in Figs. 6.20 and 6.21, the system reaches the maximum reward and remains in the 'low-power' state. It is also for this method that the performance improvement, relative to the Control model, is the smallest.

Softmax in Figs. 6.24 and 6.25, shows a volatile convergence of the dependence. This however translates to a persistent improvement of localisation result. The dependence might be due to the fact that the data used was not as consistent as in the simulation. As it was noted in Section 6.3.1, training and calibration differs for each user. Since this difference was not encoded in the simulation, it could explain the reason for the behaviour of the Softmax method.

Due to this volatility, as well as higher relative sensor usage in Fig. 6.24, compared with 6.22, the ϵ-Greedy method is the superior method in terms of action selection. This selection method offers a good trade-off between the average sensor usage and the improvement of performance. The parameter ϵ was set to 0.1 again, but it can be changed depending on the need, allowing it to be more controllable than Greedy or Softmax.

Whilst ϵ-Greedy is the best method for this particular use, the other methods could be advantageous in the context of other sensor applications. Softmax could perform well when considering the amount of sensors used, as opposed to their type, in terms of indoor localisation. In this case, more exploration could translate to better performance, with less regard paid to energy efficiency [118]. On the other hand, applications where efficiency is critical, could benefit most from Greedy selection. These applications could include on-board feature extraction and activity recognition [50, 181] which would ideally run for a prolonged period of time without recharging.

6.4 Conclusions and Challenges

In this chapter, we considered novel techniques for robustification of residential indoor localisation result. The first study added contextual information about the user, in an attempt to make the result

This chapter proves that inferring the location of an individual in their own home could be improved by incorporating additional data sources. To that end, a specific accelerometer signature was associated with a specific location. By performing the same, or similar tasks, in the same places, the signatures are comparable enough between different free-living experiments, as to aid the RSS localisation technique. The results show that the localisation is robust even when noise is added to the system and if the sources of information are gradually being removed.

The second half of the chapter addressed a novel adaptive technique for energy-aware indoor localisation. A simulated environment was built and scrutinised against different methods of action selection. A widely available dataset was then used to validate the hypothesised performance under data collected in a real pervasive health test bed. This chapter shows that the algorithm can generalise well to non-simulated settings and environments, even when using a dataset which was not inherently collected with localisation in mind.

CHAPTER 7

Efficient Sensor Selection Methods for Indoor Localisation Measurement Scenarios

Having addressed indoor localisation with respect to novel techniques of robustness and energy efficiency, we will now concentrate upon the third, and final, over-arching theme of this thesis. In this chapter, we will concentrate upon sensor selection methods with respect to optimal accuracy performance. When it comes to WSN-based IPS, there exists a limit of useful information which the network can either handle or provide. This chapter proves, that in the domain of residential indoor localisation, there exists a finite number of sensor nodes, which can perform at least as well as the entire deployed set.

To motivate this problem further, we also consider a novel method of estimating greedy costs associated with sensor selection. It is dependent upon the inference method which is used in this thesis, and stipulates that discrete state spaces can offer special concessions, in terms of said inference, if appropriate sensors are chosen. The study will consider simulated results, aimed at confirming various sensor selection methods, before validating the results on real world measurements. As the validation will prove, the studies which consider sensor selection for indoor localisation seldom confirm their findings on data which was collected in real houses. What is even more convincing, is that the methods are exhaustively scrutinised on four different residential abodes, with data from chapter 3. The findings show, that the simulated results, even when following a rigorous procedure, rarely will uncover the imperfections faced by IPS in the real world.

7.1 Related Work and Contributions

Recent advances in low-power WSN, make it straightforward to design, prototype and deploy large number of low-cost sensors [98]. These sensors can be used to monitor human behaviours, actions and activities, for a prolonged period of time [225]. They can be placed on the user's body or within their living environment [225]. The data gathered can be later used by clinicians to monitor, for example, recovery of their patients from within their home [129].

With the increased ubiquity and pervasiveness of these devices come various considerations, such as environmental impact [101], privacy [137] and user accessibility [43]. To address these considerations, the main focus of indoor localisation literature is likely to shift, as lack of access to computational power and large number of sensor nodes no longer presents a viable challenge. In turn, methods are likely to consider optimal placement, selection and utilisation of the available modalities under various processing paradigms.

Indoor localisation has been cited as an important tool for recovery monitoring [206]. It provides clinicians with information on the exact locations in the house where, and how long for, the patients dwell. From this data, one can deduce the current status of the patient, the speed of recovery and even sound the alarm in case of abnormal behaviour [129].

The main contributions of this chapter are:

- We outline and propose a new sensor selection method, inspired by signal propagation in a discrete state spaces for indoor localisation.
- We scrutinise the above mentioned algorithm against other methods accepted in the literature, such as Mutual Information (MI) selection, and show that it is comparable when evaluated using a simulated signal propagation model.
- We compare the simulated validation against a unique measurement dataset with high resolution annotations form chapter 3.
- We reinforce this assertion by performing selection with respect to algorithms found in previous chapter 6, which include contextual accelerometer information.

This chapter is structured as follows: This section will further discuss the work related to this study, paying close attention to discrete sensor selection literature. In Section 7.2 we outline the methods used in this study and propose our own new algorithm.

Then, in Sections 7.3 and 7.4, the methods will be scrutinised and their performance subsequently investigated against real world measurements. This includes localisation based on simple RSS and a model which complements it using an accelerometer. Finally, we conclude in Section 7.5.

Sensor selection can be formulated as a convex optimisation problem [2, 90]. Placements can be estimated [246] with respect to utility score, such as coverage or information gain [29]. Sensors can also be selected from a larger superset [27, 90] from discrete and pre-defined locations. These approaches to sensor selection usually assign a utility coverage score, which is subsequently maximised. Methods which are used most often include submodular and supermodular set functions [17, 106]. One of their major shortcomings however, is the fact that sensor selection under certain supermodular constraints has been proven to be NP-hard [17, 90].

Considering the above methods, the utilities comprise of information theoretic metrics, such as conditional entropy [247] and MI [29]. The use of entropy constrains the system to information content of a specific sensor only in its immediate environment without the knowledge of its vicinity [106]. The extension of this formulation to MI showed, that while the selection under MI did not suffer from the same issues, its effective solution requires prior knowledge of joint distributions between variables [106].

There have been strides made in localisation-centric sensor placement and selection where the authors consider optimal sensor geometry [217]. The location is chosen based on minimisation of the difference between the received power and a path loss model, using Maximum Likelihood Estimation. Still, the experiment environment is not comparable to the environment in this thesis, as it does not resemble a residential setting. The validation environment in a laboratory is an open space with few obstacles. A study done by Ababneh [2] aimed to show the impact of sensor selection on RSS-based localisation. The author presented two novel selection algorithms, before confirming their viability through a simulation study.

In [242], the authors considered optimal sensor selection in the context of RSS-based target localisation. A closed-form solution to the problem was presented and tested on simulated $100m \times 100m$ environment. By analysing the geometric structure of the nearby environment, the authors were able to improve the simulated result error. Energy consumption and sensor parsimony are then discussed. The above work is related to our study, as we also perform localisation based on RSS. However, we consider our experiment test bed to be more challenging to analyse from an RF perspective due to relative volatility of the signals collected as part of our experiments, which would be

difficult to approximate using a closed form solution.

Some work has also been done in optimal selection based on visual sensor networks [118]. The target is tracked in a simulated and experiment environments using a number of cameras. They then use utility-based sensor selection method, which outperforms the baseline algorithm. The location error is minimised once the number of camera sensors increases. The localisation method in this study fundamentally differs from ours as it uses a different type of sensors, which require a direct line of sight. Selection methods, as opposed to placement, only consider a discrete number of already placed sensors [27, 90]. Instead of using the environment geometry and sensor output in order to obtain a definite place in space [217], selection only considers the response from already placed discrete sensors within that space [90]. In our study we will assume that the experiment environment is filled with an abundant amount of APs, which can then be easily removed.

7.2 Method

In this section we outline the method used to perform the selection of optimal subsets of sensor nodes. We will begin by outlining the basic principle behind submodular set functions and their utilities. We then describe the novel approach of sensor selection based on Kullback-Leibler divergence. To finish, we will summarise the baseline algorithms which we will use to scrutinise our performance.

7.2.1 Mutual Information approach

Utility scores used in discrete sensor selection problems comprise mostly of information theoretic approaches, such as Mutual Information (MI) [29]. MI is a popular entropy-based metric, which considers the measure of relative information 'gain' of one variable given another [106]. It is preferred over other metrics, such as conditional entropy, as it is able to account for the entire instrumentation space. The use of conditional entropy constrains the system to information content of a specific sensor only in its immediate environment without the knowledge of its vicinity [106]. In the context of sensor selection, MI can be used to estimate the amount of information presented to the system through the addition of an arbitrary sensor [106].

Formulation of MI for use with submodular functions showed, that while the selection under MI did not suffer from the same issues, its effective solution requires prior knowledge of joint distributions between variables [106]. The implementation in this

chapter aims to exploit this, as due to the nature of RSS fingerprinting localisation, the joint distributions are fully observable. This makes the MI approach directly applicable to our example.

The monotonic nature of submodular functions, especially when employing a simple greedy algorithm for its evaluation, can provide polynomial-time performance guarantees for near-optimal solutions [106]. Additionally, this metric does not require expensive computation of precise sensor positions, as it assumes that the sensor nodes are provided as discrete variables [106, 247]. Consider a finite set C. We define a set function, such that $F : 2^C \rightarrow \Re$ and assume $F(\emptyset) = 0$. This set function is considered submodular if it satisfies the property of diminishing returns [104]:

$$F(A \cup s) - F(A) \geq F(B \cup s) - F(B) \tag{7.1}$$

where s in both cases is an arbitrary addition to each set and $A \subseteq B \subseteq C$. This function is strictly monotonically decreasing if $F(A) \leq F(B)$.

MI can be defined as a metric of mutual dependence between two random variables F and D:

$$I(F;D) = H(F) - H(F|D) \tag{7.2}$$

where $H(F)$ is a marginal entropy of variable F and $H(F|D)$ is the conditional entropy between the variables. Consider a superset V containing all possible discrete sensor locations. We introduce B, which is defined as a subset of V, such that $B \subseteq V$. It provides the RSS information containing a selection of available APs. We also define variable RSS_B which specify the RSS symbols arriving from the APs contained in subset B. Recall RSS from Eq. 4.5. For clarity we will drop the index specifying the state locations, as we assume that given each subset B we observe the information from the entire state space given sensors included in B.

In the context of submodular maximisation, MI between two variables RSS_B and RSS_V aims to maximise the mutual dependence of information contained in subset B given the knowledge of the remainder set $V \setminus B$ [106]:

$$B^* = \underset{V \setminus B}{\arg\max} H(RSS_{V \setminus B}) - H(RSS_{V \setminus B}|RSS_B) \tag{7.3}$$

$$F(B) = I(RSS_B; RSS_{V \setminus B}) \tag{7.4}$$

where $H(RSS_{V \setminus B})$ specifies the entropy of variable RSS with sensor subset $V \setminus B$ and $H(RSS_{V \setminus B}|RSS_B)$ is the conditional entropy of $RSS_{V \setminus B}$ given RSS_B. Equation 7.4 specifies the utility function for a subset B.

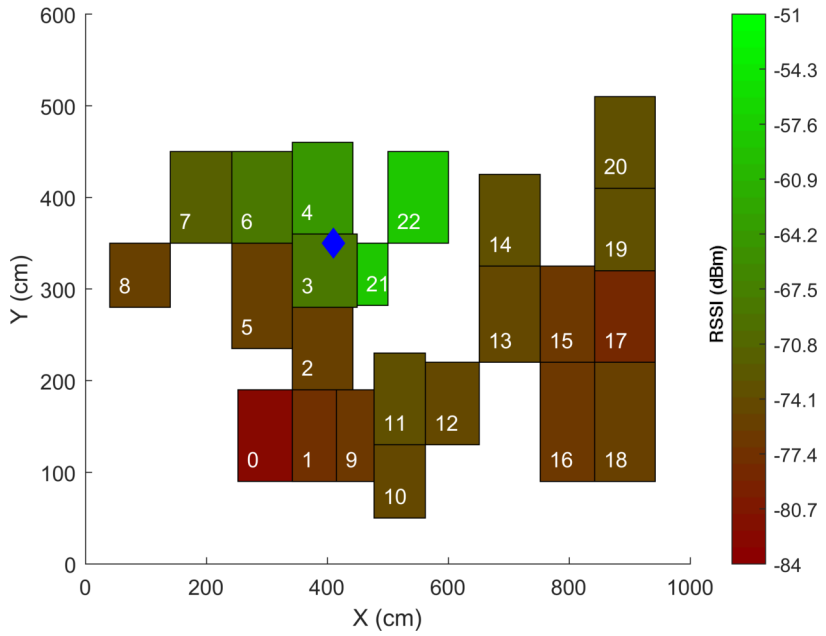

Figure 7.1: 2-dimensional state space of House 1 with an overlaid average RSS intensity heat map in dB for AP sensor 1. Blue diamond specifies the approximate position of the AP.

Despite the fact that MI approach is considered state-of-the-art, one of the major shortcomings in this implementation is lack of knowledge of signal diversity across adjoining states (spatial neighbours). The above utility in Eq. 7.4 calculates the step-wise information gain between sensors which, as it was the case in literature [90, 106, 247], will provide their optimal instrumentation.

7.2.2 Kullback-Leibler approach

Kullback-Leibler is a non-symmetric statistical distancing metric between two probability distributions, calculated as a measure of relative entropy. Its use has been established in the domain of localisation by RSS fingerprinting [16, 142, 143]. The authors in [16] suggested that KL as a metric of divergence between two physical locations, defined by RSS features, works well at leveraging the accuracy and latency of RSS symbols. This makes this particular method well equipped for our use. In our implementation we use KL as a metric which directly takes into account the above-mentioned signal diversity into account.

To motivate the need for KL in our implementation, consider the state space in Figs. 7.1 and 7.2. They represent the mean value of RSS in each state, given sensors

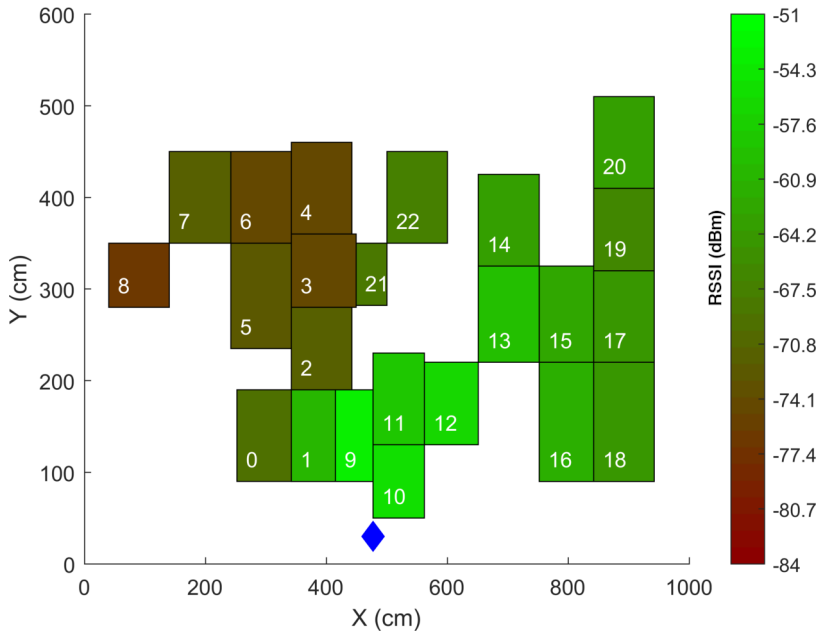

Figure 7.2: 2-dimensional state space of House 1 with an overlaid average RSS intensity heat map in dB for AP sensor 4. Blue diamond specifies the approximate position of the AP.

1 and 4 in House 1. The distribution of the received power from each state to each sensor follows, approximately, a Gaussian, as in Eq. 4.5. Each distribution provides some information about the user in each state. Due to the dynamics of radio propagation and multi-path fading however, it may come to pass that any two adjacent states will share information, making the distributions overlap. In the case of our inference, as in Eq. 4.14, the adjoining states would ideally share no information, i.e. the divergence between two distributions from the two sensors in the same state would be as large as possible.

The aim in turn, is to make the ambiguity between any two states as small as possible. In order to make the inference easier, the divergence between adjoining states will also have to be taken into account. In the case of Figs. 7.1 and 7.2, this ambiguity is best exemplified by observing the signal propagation across all states. Indeed, there are states, in which the intensity of the signal is very similar, especially in the case of Fig. 7.2.

We extend its formulation to the context of greedy sensor selection. Using two arbitrary distributions f and d, it is defined as [47, 142]:

$$D_{KL}(f||d) = \int_{\infty}^{\infty} f(x) log \frac{f(x)}{d(x)} dx \tag{7.5}$$

$$D_{KL}(f||d) = H(f,d) - H(f) \tag{7.6}$$

where $H(f,d)$ is the cross-entropy and $H(f)$ entropy of variable f. Thus, in a purely KL setting, the algorithm would seek to maximise the divergence as a cost function [128]:

$$B^* = \arg\max_{V \setminus B} \Big[\sum_B D_{KL}(RSS_B || RSS_{V \setminus B}) \Big] \tag{7.7}$$

The above equation will favour the sensors with most varied signal, as seen across all states in the environment. However, in order to make this method aware of the information gain at each sensor iteration step, we subtract the above equation from MI:

$$B^* = \arg\max_{V \setminus B} \Big[I(RSS_B; RSS_{V \setminus B}) - \sum_B (D_{KL}(RSS_B || RSS_{V \setminus B})) \Big] \tag{7.8}$$

where the first term $I(RSS_B; RSS_{V \setminus B})$ is the mutual information. It will henceforth be labelled as KL-MI.

7.3 Evaluation

7.3.1 Baselines

In order to test the two sensor selection approaches, we compare them against an exhaustive Brute Force (BF) approach as well as a Greedy Brute Force (GBF). The difference between the two is that BF searches through all possible permutations of sensors in order to find optimality, whereas GBF will select sensors based on their performance, given only the previously selected sensors.

BF exhaustively iterates through all possible combinations of sensors, calculating the accuracy and choosing the sensor set which yields the smallest error. After the set is chosen, the search space is again recalculated, and a new set is selected. This happens until no more sensors are available. This algorithm is used as a baseline, and as such we assume access to ground truth labels. This method is also considered optimal in this work and as such no other method will outperform it.

GBF calculates the performance given the set of available sensors, and at each time step, chooses the sensor which gives the best performance. This continues until no more APs are available. We expect this method to be worse than BF, but to take correspondingly less time. The GBF algorithm is outlined in Algorithm 3.

7.3.2 Simulation

A simulation system, previously outlined in chapter 3, was used to check the viability of the method in a basic, obstacle-free environment. We thoroughly expand on this simulation framework by implementing bespoke sensor selection mechanics. The implementation makes use of the Submodular Function Optimization toolbox [105]. For the simulation, the location state space varied between 50 to 250, $1m \times 1m$ states, in increments of 50. The number of APs was incremented from 1 to 10. Each state contained a probability distribution from every AP. The simulated distributions followed a BLE path loss model with parameters taken from [139]. These parameters are meant to resemble a residential environment. Results show the performance of the two algorithms, given increasing size of the experimental test bed, and increasing number of sensor APs. The metric used to measure the performance of the algorithms is the distance error. Distance error is defined as the Euclidean distance between predicted tile and groundtruth [127]. This metric has previously been outlined in chapter 4.

The simulated results are shown in Figs. 7.3 and 7.4. As expected, the exhaustive BF approach outperforms all of the proposed methods. This result can be considered as optimal in terms of performance. In addition, the simulation showed that the two methods, MI and KL-MI are comparable. This suggests, that the variability across states, in a discrete state space test-bed has little to no effect on the choice of the sensor. It is possible however, that the distinct divergences between states are simply too small to provide any meaningful improvement.

Additionally, Fig. 7.5 shows the relative computational cost with respect to number of information sources. As expected, the search for optimal solution increases exponentially in complexity. Additionally, we argue that the superior performance of BF is not enough to propose it as a viable method. Whilst both, MI and KL-MI exhibit higher relative error, this can be leveraged for lesser complexity and quicker turnaround times.

The simulation also highlights the need for near-optimal algorithms in localisation implementations much bigger than typical residential abodes. Understandably, indoor localisation techniques are also popular in industrial or medical applications [83, 94], where the spaces are much larger. Indeed, the methods contained therein are also much more suited for deployments even outside of residential domain due to the complexity associated with both, exhaustive and greedy brute force selection.

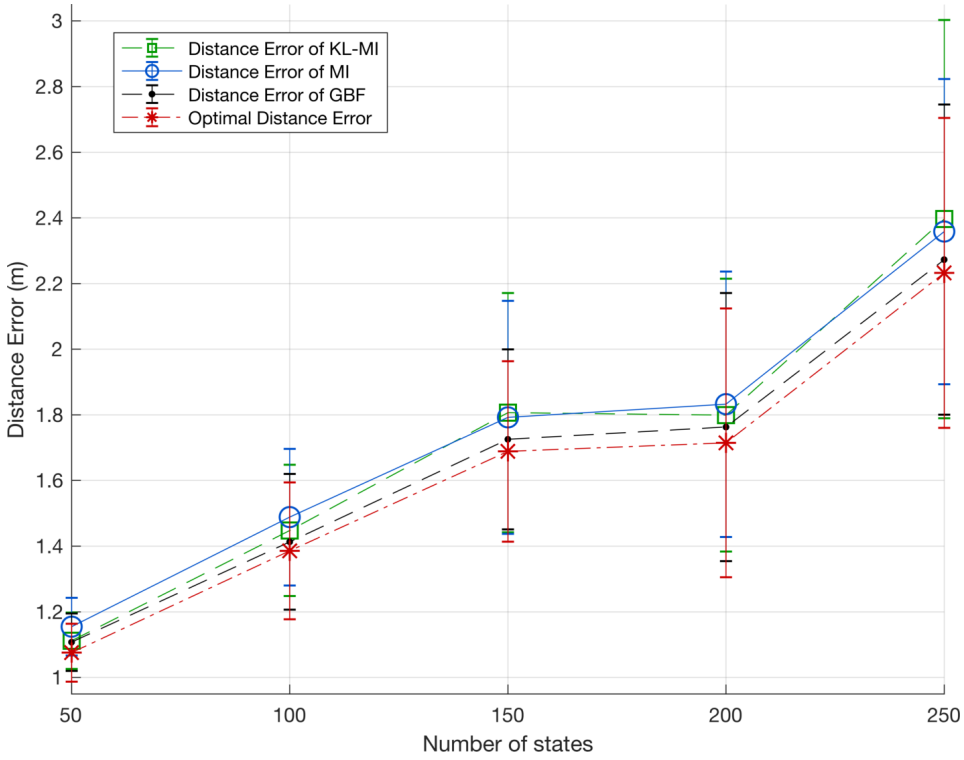

Figure 7.3: Error per growing state space.

House	APs	States	Experiments
House 1	8	23	living_1 living_2 living_3
House 2	11	76	living_1 living_2 living_3
House 3	11	52	living_1 living_2 living_3
House 4	11	45	living_1 living_2 living_3

Table 7.1: Table defining the experiments used in the validation and their parameters.

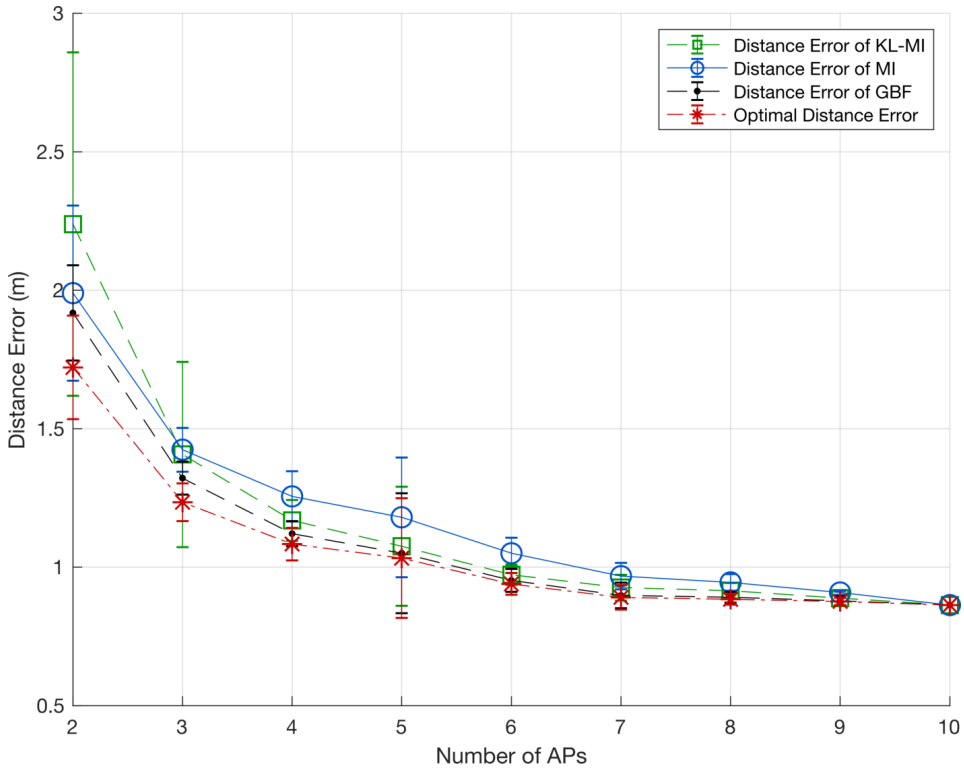

Figure 7.4: Error per increasing number of AP sensors.

7.4 Validation & Discussion

Recall from chapter 3, that the experiments included an RF-fingerprinting example where every node was visited in turn by the participant. The validation experiments are given in Table 7.1. There were at least 3 unique living experiments available for each house. The model was trained through three-fold cross validation across the experiments (so called leave-one-out). The results were then averaged over those three living experiments for each house. Since the algorithms rely on the information to be available about every state, it was deemed appropriate to select the optimal sets of sensors for MI and KL-MI using a thorough fingerprint, as described in chapter 3. This is due to the fingerprint containing every state available in the environment, as opposed to living experiments which could omit certain locations. In order to remain fair however, the BF and GBF were optimised over the living experiments. This is because these particular metrics are supposed to show the optimal or near-optimal performance of the available dataset.

The following discussion will evaluate the performance of the presented algorithms using the data from those 4 houses. Here we will also provide an overview of the improved localisation method outlined in chapter 6. Traces of data from accelerometer in each

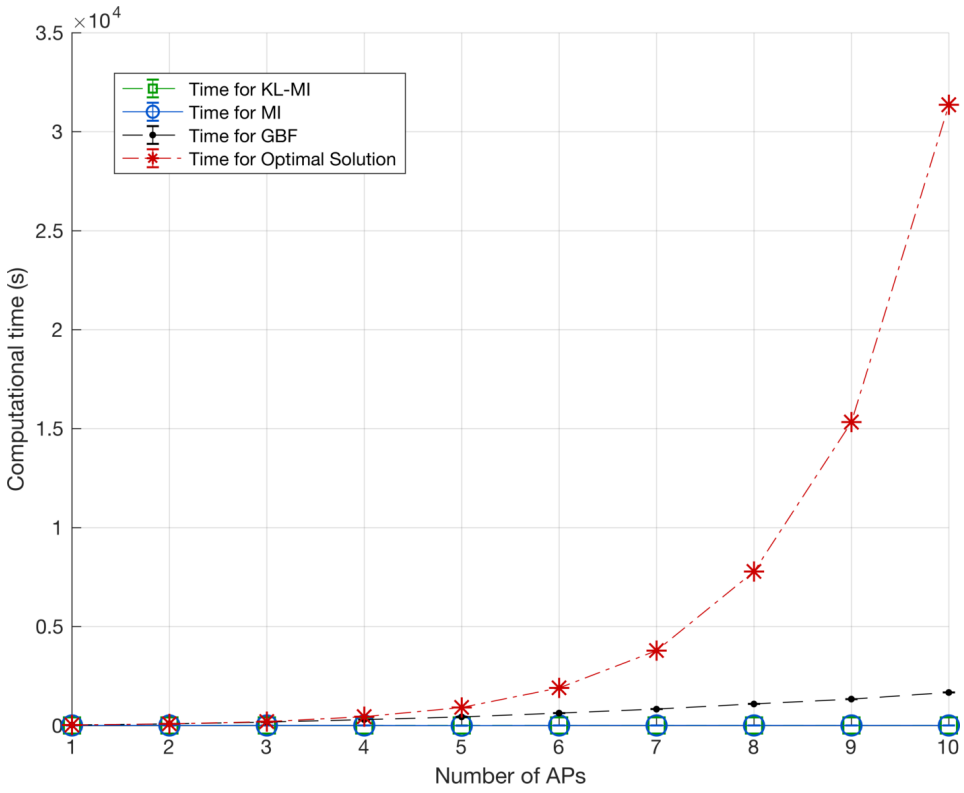

Figure 7.5: Time taken to calculate each method given number of AP sensors.

location state were recorded and their features extracted. These features can then be used in conjunction with RSS to locate the user within their home. The two methods are outlined in Figs. 6.1 and 6.2. We will describe the basic RSS location inference as Method 1 and the accelerometer-enriched as Method 2. We define the notation as follows: RSS are the RSS observation symbols at some time t from AP k at state j, Acc are the accelerometer feature observations and L is the location state inference. For further detail we refer to [100].

Let us firstly discuss the parallels between the simulated results and the validation. Indeed, the performance improves with each additional sensor, as expected. Moreover, BF again correctly shows the optimal sets at each iteration. Interestingly, the real life validation seems to converge to near-optimality much quicker than the simulation. This suggests, that for each unique abode there exists a certain amount of sensors, and their discrete positions, which could be considered optimal.

This can be further substantiated by looking at Fig. 7.6, which shows an example of selected sensors overlaid on the state space of House 1. Understandably, the selected sensors differ between methods. However, there are a number of 'dominant' sensors

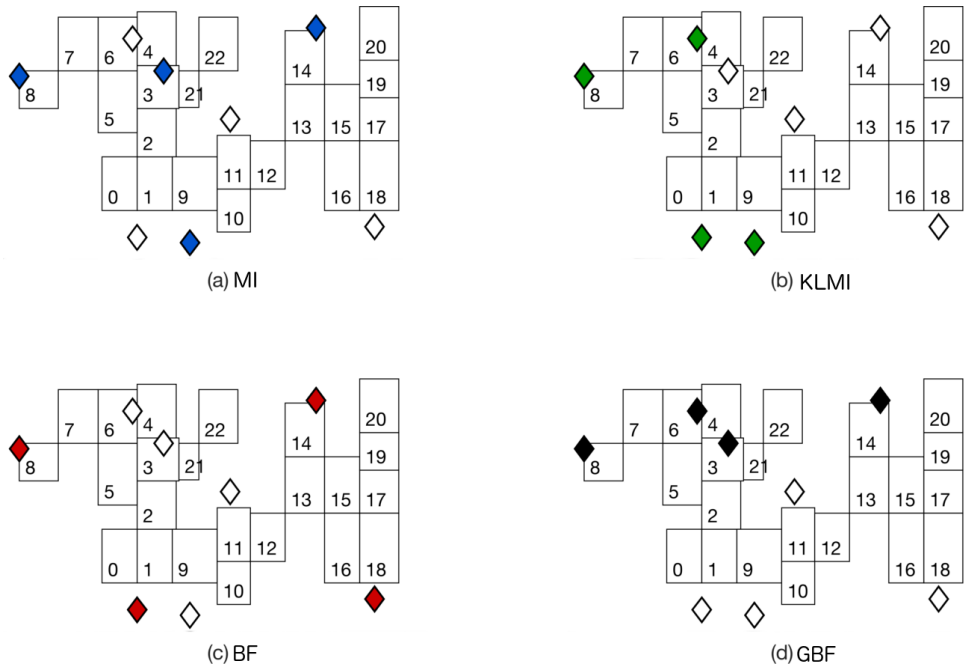

Figure 7.6: Example of the selection of half of all available sensors overlaid on state space of House 1 using each selection algorithm for Method 1. Diamonds specify AP sensors, coloured diamonds are the selections per algorithm.

which are selected by every algorithm, and correspondingly sensors which are omitted in each case. This, in conjunction with Fig. 7.7, suggests that there exist spaces in each residence, from which the signal strength could be construed as optimal in terms of state sequence inference. The remainder of the results of Method 1 are shown in Figs. 7.9, 7.11 and 7.13 for Houses 2, 3 and 4 respectively. They also confirm the quick sensor saturation, achieving near optimal performance, roughly with half of all APs available.

The results of Method 1 are shown in Figs. 7.7, 7.9, 7.11 and 7.13 for Houses 1, 2, 3 and 4 respectively. As is evident, the real-world environment rarely provides states with differing RSS signatures. Due to that fact, MI and KL-MI are comparable in nearly every house. It is also noteworthy, that each house reaches its 'sensor saturation' point relatively quickly. As it is shown in the graphs, near-optimal performance of the sensors could be achieved using fewer than a half of all APs available.

The graphs pertaining to Method 2, 7.8, 7.10, 7.12 and 7.14 show similar results. The accelerometer trace from living experiments is not a viable representation of a specific human participant due to relatively large space of possible interpretation between various users, as described in chapter 3. Gaits and living patterns have been found to differ between people [136]. This explains the large distance error of the initial AP choice

Input:
$\{\lambda, \mathscr{X}\}$ = HMM Parameters, $\{\Gamma\}$ = Labels,
$\{S\}$ = Ground truth sensor set
Begin:
$\mathbf{A}^* = \emptyset$
$n = |S|$
repeat
  $k \leftarrow (n - |\mathbf{A}^*|)$
  for *1 to* k **do**
    $\mathscr{T} \leftarrow P(V|\mathscr{X}_{\mathbf{A}}, \lambda)$
    $\mathrm{e}(k) \leftarrow (|\sqrt{\sum_{i=1}^{2}(\mathscr{T} - \Gamma)^2}|)$ // `Euclid error`
  end
  $s^* \leftarrow \arg\min_k \mathrm{e}(k)$
  $\mathbf{A}^* \leftarrow \mathbf{A}^* \cup \{s^*\}$
until $|\boldsymbol{A}^*|! = n$;
Output:
$\{\mathbf{A}^*\}$ = Optimal set

Algorithm 3: Greedy Brute Force Algorithm for Method 1

across all houses when using this method, as the living experiments were performed by various users, and that was not taken into account during selection. Models trained on specific users were unlikely to work optimally on others. The figures also show how the houses will 'saturate' at different numbers of APs depending on their size, confirming that size of the state space is proportional to the number of required APs to achieve well performing localisation.

7.5 Conclusions and Challenges

Two methods of discrete sensor selection were presented and scrutinised using simulated data. The simulation confirmed the viability of the methods as well as a baseline algorithm. We proposed a new sensor selection objective, taking into account the diversity of signal across states and inference mechanics. A unique dataset was then used to scrutinise these methods on data collected in a number of residential houses.

This chapter confirmed that these particular algorithms are capable of selecting a subset of sensors based on the quality of the signals from said sensors. It was shown that the diversity between states, which was the main motivation of this method, provides little to no improvement in sensor selection. The two algorithms were proven to be comparable, when considered in the context of our localisation infrastructure. Both of these methods were also investigated in relation to our previous work, through fusion to

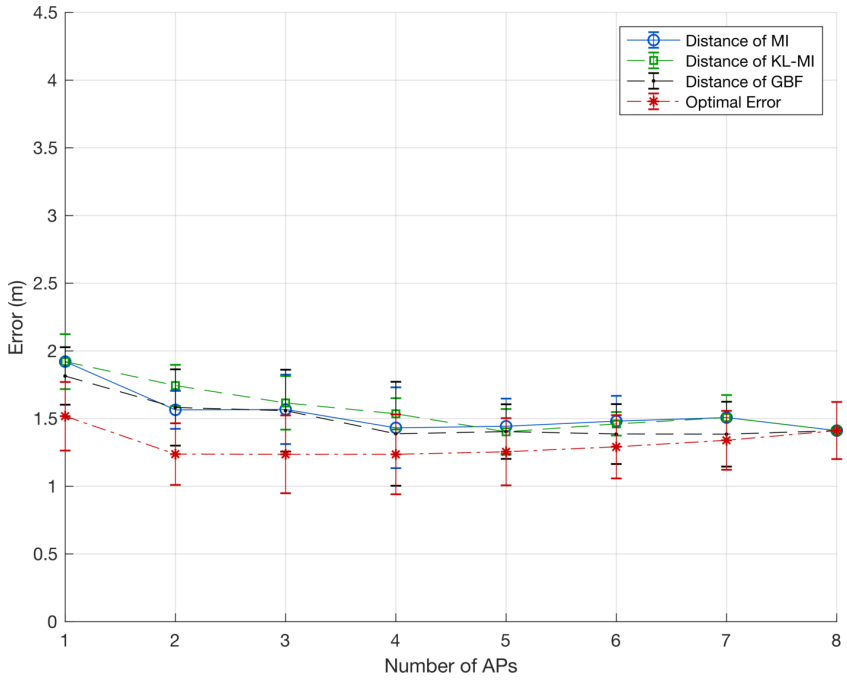

Figure 7.7: Error of Method 1 per increasing APs for House 1.

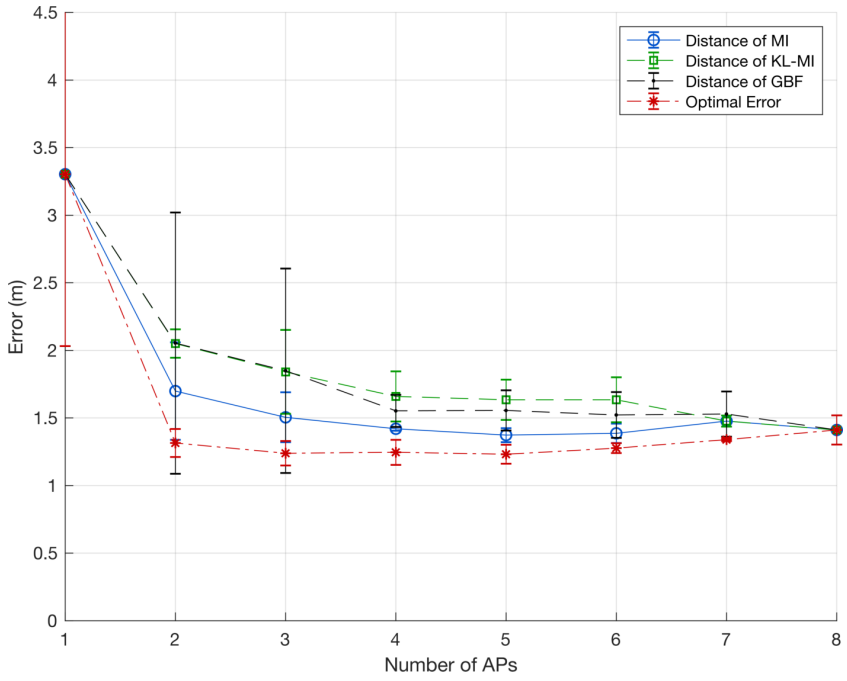

Figure 7.8: Error of Method 2 per increasing APs for House 1.

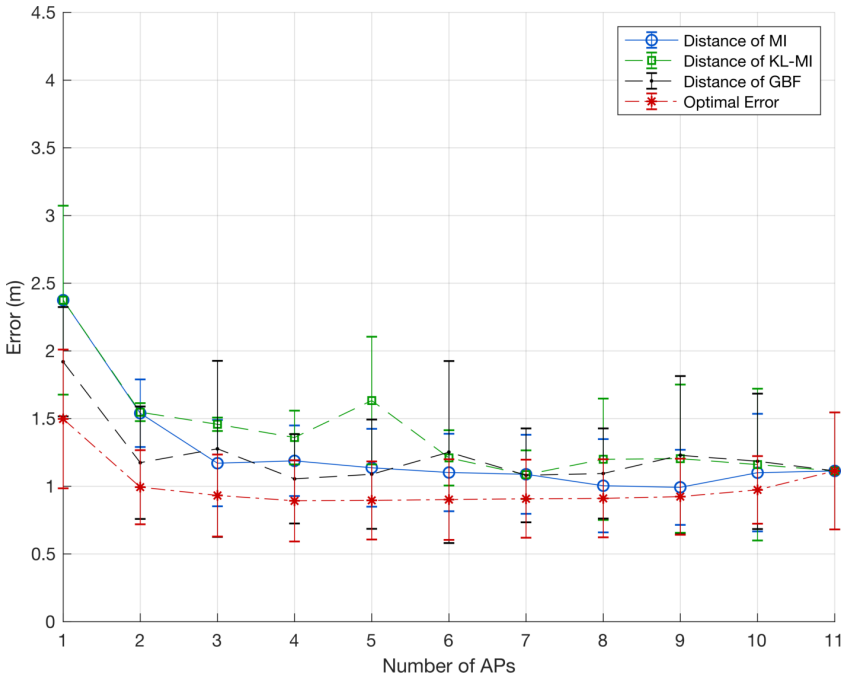

Figure 7.9: Error of Method 1 per increasing APs for House 2.

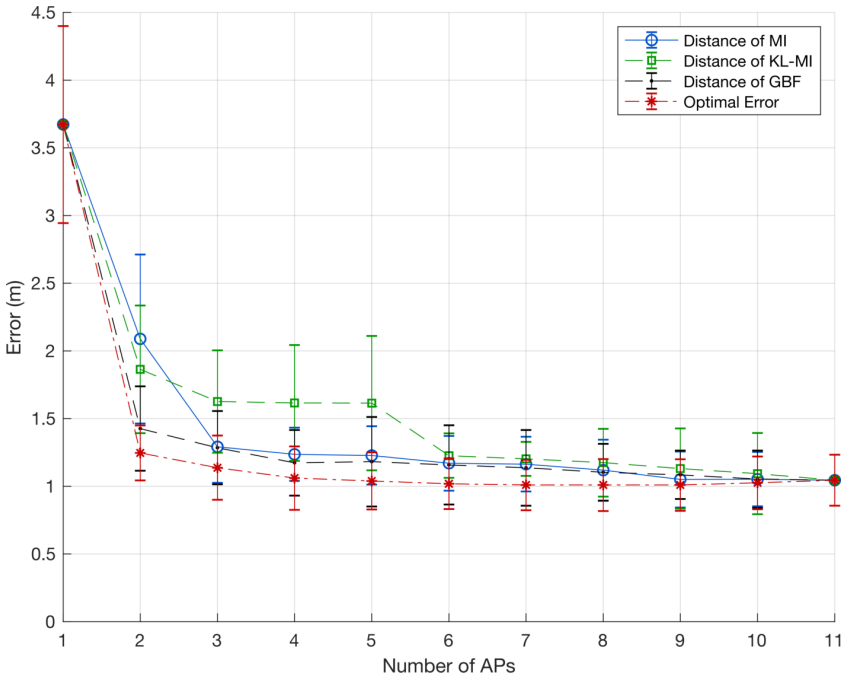

Figure 7.10: Error of Method 2 per increasing APs for House 2.

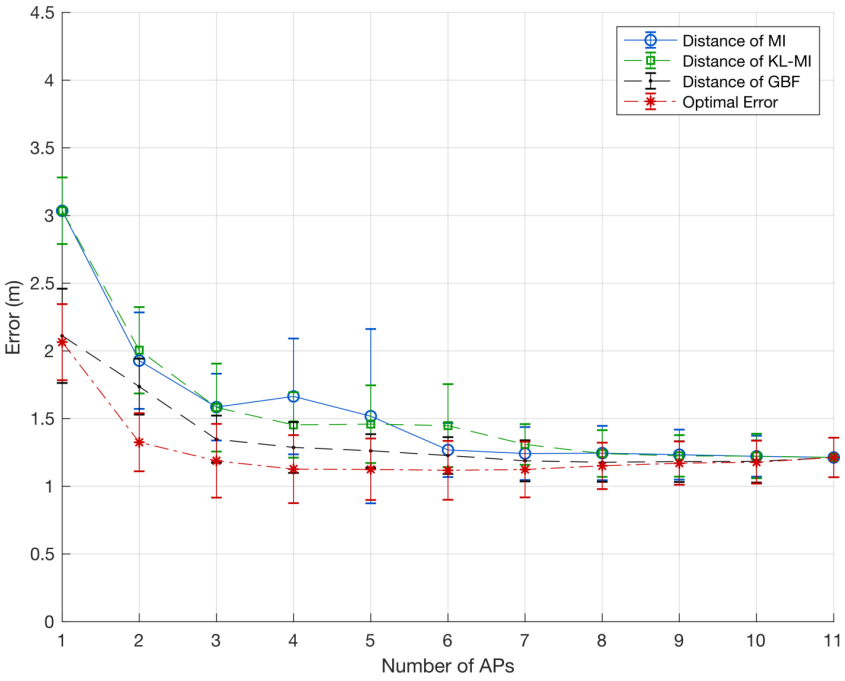

Figure 7.11: Error of Method 1 per increasing APs for House 3.

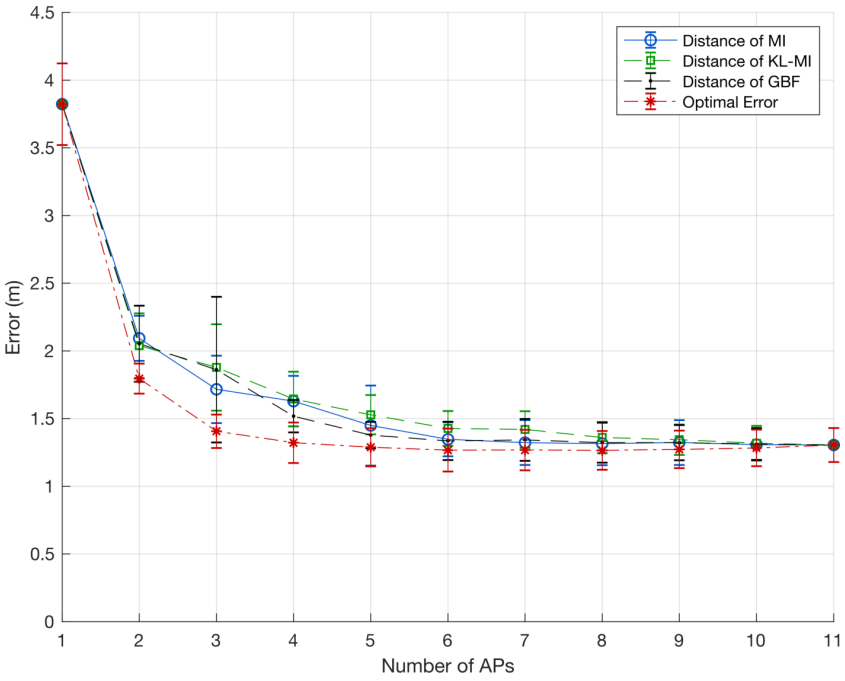

Figure 7.12: Error of Method 2 per increasing APs for House 3.

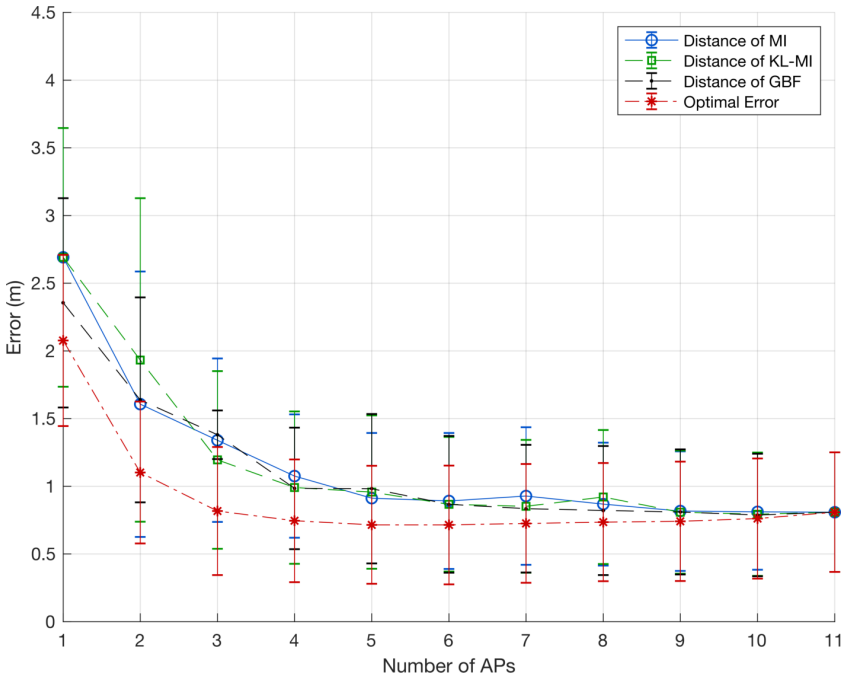

Figure 7.13: Error of Method 1 per increasing APs for House 4.

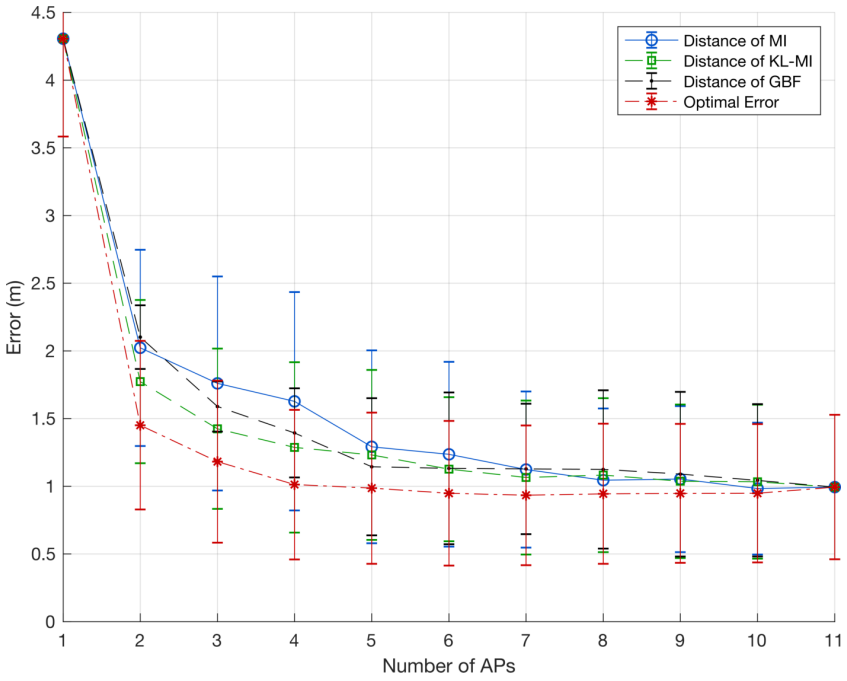

Figure 7.14: Error of Method 2 per increasing APs for House 4.

additional contextual sensors.

CHAPTER 8

CONCLUSIONS AND FUTURE WORK

This concluding chapter will serve to summarise all of the preceding work. Here, we aim to provide an evaluation of the thesis and its overall contribution to the field. We will also address various new avenues of investigation which were uncovered through this work, or made themselves apparent only after the said work has been performed. The latter point will also act as a platform for possible future endeavours which are believed to of interest to the field and the community.

This thesis was predominantly concerned with robust and efficient approaches to indoor localisation in residential environments. In this chapter we intend to continue with the overarching trend of health care, the motivation of which underpinned the incentive behind the novel data, methodologies and algorithms contained therein. However, that same objective also introduced a number of constraints which had to be taken into account. Here, we will describe the work carried out, evaluating it in terms of relative versatility, primarily (but not exclusively) with respect to the above use case. Additionally, we will consider the entire field of indoor localisation and attempt to install the contribution yielded by this thesis into existing field of research.

We will initially summarise all of the above chapters, focusing on the challenges which they set out to address. We will then consider the degree to which these challenges were addressed, specifically considering the use case of residential indoor localisation for health care. This use case will not be exclusive however, as we will also focus on the wider picture of the current state-of-the-art, and how it can be expanded. Finally, we will close this thesis by exposing the shortcomings which are yet to be addressed and provide

viable avenues for future research enquiries.

8.1 Thesis Summary

This thesis aimed to provide an clear picture of residential indoor localisation methodology in a context of health care monitoring. This work has covered the main aspects of the indoor localisation 'pipeline'. Initially, we provided a thorough, comprehensive outline of the popular sensors used in literature. The overview also presented modalities which could not be easily appropriated for use in residential indoor localisation, either due to them being still considered emerging or due to excessive infrastructure they demand. The thesis then narrowed the space of sensor selection by motivating the use of specific sensors in our own infrastructure, explaining their appropriateness for our purpose in terms of usability, robustness and efficiency. The above was demonstrated using novel data, collected in residential environments. This demonstration showed the possible ways to model the sensory output, produced during data collection. Additionally, the data collection has uncovered various deficiencies associated with training and collecting thorough high-resolution data. This was later improved upon using an automated system for localisation and mapping. Finally, the thesis addressed various over-arching themes of sensor-based fusion and localisation like efficiency, robustness and accuracy in two technical chapters.

The novel contribution of this thesis began with a survey of the existing literature. This chapter explored the space of currently popular sensor modalities, as used for various indoor localisation applications. These modalities were found to offer unique advantages and disadvantages in terms of tracking and positioning performance. They were later evaluated using a framework, which scrutinised their relative usefulness and value in said domain. This framework exposed their shortcomings and helped to provide a clear picture of sensors deemed most appropriate for use in this thesis. Later, the chapter explored important fusion paradigms and provided literature-based patterns of sensor combinations in various application areas. After explaining the theory behind popular fusion methods, as well as preliminary background for this work, the chapter closed by exposing various unexplored avenues for future research.

The above chapter has tackled a topic seldom addressed by the wider localisation community. Whilst the literature concentrates on algorithms, methods and standards used for indoor localisation, there is a gap when considering the perspective of popularly utilized sensor modalities and their fusion. This manuscript aimed to close this gap by

taking thorough account of sensor utilisation and fusion taxonomy, with comprehensive overview of seminal papers and existing data sets.

Chapter 3 concentrated on technical details the data collection methods, from the choice of infrastructure, through to testing and validation. First, the chapter explained the need for WSN in the space of residential healthcare monitoring. This included describing the advantages and disadvantages provided by residential environments in terms of radio signal propagation and their modelling. Later, it considered the WSN infrastructure hardware, which was utilised to gather the data contained therein. The example of the typical pervasive health care residential data then followed. This chapter has also outlined novel collection of high resolution localisation data, which served as basis for majority of the algorithms included in this thesis. Here, we additionally included signal modelling techniques which this thesis has used throughout. This chapter has closed by outlining the predominant challenges faced during the collection of said data and possible countermeasures which are likely to alleviate them.

Th contribution of the above chapter is two-fold: Firstly, it presents an example of a viable, low-cost, pervasive monitoring system. This system, including the sensors contained therein, as motivated by the previous chapter, is explained, using an example of data it produced. This data showed, that pervasive monitoring of a user in their own environment is possible. Secondly, a larger collection of novel residential house data was presented. This data has been used throughout this thesis, in order to confirm the viability of various algorithms and methods. Since this data set spans various houses and users, it sets a precedent which all of the algorithms have to follow to be proven feasible.

In chapter 4, the methods and metrics, which were used in this thesis, have been addressed. It firstly outlined all of the metrics which were used to validate the work contained in this thesis, giving their mathematical formulations. Then, the chapter continued to describe the modelling of the signals (and lack thereof), as well as the temporal structure prediction methods which form the foundation of all of the novel algorithms in this thesis.

The main objective of chapter 5 was to address the aforementioned challenges set out in the previous chapter. It described a novel system for gathering data, which removes the need for arduous labour experienced with the above mentioned collection. Furthermore, this method proposes the user-based measuring to be ejected 'from-the-loop', helping to reduce bias and human error. The chapter begun with explaining the theory behind SLAM, which simultaneously provided a motivation of its usage in

this context. The chapter then explained an another data collection which took place, specifically to validate the method contained in this chapter. The crucial contribution was the confirmation of this new method of data collection and mapping.

The aim of this chapter was to prove that the 'pipeline' of data collection and training outlined in the previous chapter can be substantially streamlined. This streamlining came from presenting novel hardware, designed with data collection and training in mind. Then, through the utilisation of localisation and mapping techniques, it was able to match the performance of the method explained in the previous chapter. The contribution of this chapter is self-evident, in that the labour required to perform fingerprinting training in residential areas has been facilitated through automation.

The following chapter provided a concrete examples of improvement of indoor localisation through various novel studies and methods. Initially, a study of data fusion was provided, which explored how best to connect the model of causal relationships between contextual data and localisation performance. After providing various data flow models and confirming them on an adapted pervasive health dataset, the chapter confirmed their viability by evaluating these models on the novel collected data. Additionally, it considered a study of robustness, and showed that contextual information from additional sensors was advantageous in the face of usual adversity found in WSNs. Later, the same chapter explored how the WSNs can be made aware of their energy efficiency. Through the use of RL, a new method was devised, which explored the space of sensor utilisation under energy constraints. This method was also used to perform life-long model training. After validating the hypothesis using a novel simulator, the same pervasive health dataset from the previous study was used to confirm the findings. The main contributions of this chapter included the two studies, and their relative impact on residential indoor localisation. This chapter has also addressed two of the three over-arching themes of sensor fusion applications in this thesis, namely fusion for robustness and fusion for energy efficiency. It should be, however, reiterated, that the energy efficiency in this work is understood purely on the basis of sensor utilisation. This is a deliberate choice, as to make the methods here easy to generalise to a variety of problems, even extending outside of the indoor localisation use case. No explicit power measurements were made.

The addition of this chapter includes various novel methods of indoor localisation. The viability of these methods has been shown, by constraining the algorithms by typical impositions found in residential environments, health care monitoring and WSN. By considering sensor fusion, adaptability and resilience, this chapter has shown that indoor localisation, as well as health monitoring can be improved through contextual

information, such as activity, and that the topology of acceleration sensors can guard against network outages and service issues. Additionally, localisation systems can be improved through more dependent sensors, such as cameras. This allowed the system to perform weak training across time, as well as maintain energy-awareness. The findings of this chapter have shown that indoor localisation systems, especially ones with access to accelerometer data and other sensor modalities will have to maintain a degree of adaptability and energy efficiency in the future.

The final technical chapter of this thesis explained a novel senor selection method for residential indoor localisation. Initially, it explored the space of sensor selection in WSN, before embarking on outlining the theory behind most common selection algorithms. Then, it motivated the use of a new utilisation cost metric, inspired by signal propagation and inference methods from our previous work. The algorithms were checked against base line algorithms, and later confirmed on our own pervasive health care dataset. The main contribution of this chapter was, in addition to providing an outline of selection in WSN for residential indoor localisation, thorough validation study, which helped narrow the gap in sensor selection literature. This chapter showed, that the selection algorithms based on information theoretic and quantitative methods cannot simply be evaluated using simulated results, and should additionally be scrutinised using real life measurements.

Interestingly, practical sensor selection remains seldom featured in the literature of residential indoor localisation using WSN, instead remaining the staple of more theoretical contributions. The motivation behind this section is largely similar to the previous chapter – it professes the need for adaptability and efficiency in WSN. By proving that the localisation algorithms are able to maintain comparable performance, whilst using a fraction of the sensor space, the contribution of this chapter is clear. Furthermore, by examining the viability of these algorithms when applied to real data, the chapter shows that practical sensor selection can be advantageous in relation to residential indoor localisation.

8.2 Objectives for Further Research

8.2.1 Future Technologies for Indoor Localisation

It is important to note, that indoor localisation sensing through the paradigm of BLE RSSI is not the exclusive way of solving this challenge. Whilst featured prominently in the

literature, the new incoming communication technologies have the potential of disrupting the current indoor localisation consensus, and bring the community closer to evermore accurate positioning strategies. Currently, there exists a community preference to include new localisation systems based on novel standards in communications including 5G, mmWave, multiple-input multiple-output (MIMO) , Massive MIMO (MMIMO) and UWB.

There exist some work on indoor localisation approaches which use MMIMO [221]. Widmaier et al. showed that the use of CSI of a MMIMO system when feed to an ANN is a practical method of achieving sub-meter accuracy. Indeed, there exist further examples of utilising CSI for indoor localisation [234] and even activity recognition [200]. Interestingly, Wu et al. [229] provided a novel paradigm based on Time Reversal (TR) , and obtained reasonable accuracy in controlled environments.

Work from Mendrzik et al. [140] showed the viability of using mmWave MIMO for localisation and mapping. In this work, the authors attempted a radio SLAM technique, whereby the location of the user and the corresponding radio map was extracted simultaneously. Whilst the notion of context-specific semantic SLAM is not a novel concept, here the authors exploit the 5G PHY layer, being able to estimate ToA, angle-of-departure (AoD) and AoA and subsequently use it for SLAM. Similar approach was taken by Shahmansoori et al. [185]. We feel this work to be of interest here, mainly as it combines the notion of indoor localisation and environment mapping, effectively performing training online. This, along with the fact that these methods can be utilised to optimise some of the work outlined in previously in this thesis, most notably chapters 5 and 7, can be thought of as the starting point for future work.

8.2.2 Novel Methods of Localisation

Let us first address the possible space for future sensor fusion implementations, as followed up from chapter 2. Figure 8.1 shows the fusion combinations and popular approaches in sensor-driven indoor localisation in the last decade. This particular figure is not exhaustive, and as it was noted before, is only attached as a starting point for further investigation of a particular fusion combination. Indeed, there is an evident community preference towards sensors which, either have a broad foundation on which to build the algorithms such as RF, or are based on modalities which are easy to come by, such as IMUs and magnetometers. While magnetometers have seen extensive use as part of PDR applications where they usually establish direction, there is lack of recent, comprehensive study of its viability with RF sensors. Both types utilise fingerprinting as

part of its training phase. This type of data could be collected simultaneously, and can often reuse already existing IMU chipsets reported in various studies.

Cameras have seen a large body of literature dedicated to localisation, mainly due to the rise of camera-enabled smartphones. With easy access to smartphone sensor clusters, and their processing plants, researchers can perform more in-depth fusion of the sensors and collect more resolute data. Additionally, phones have good connectivity capabilities making them well suited for applications with quick-transfer requirements such as databases and for range-based RF localisation tasks. Interestingly, due to the recent trend in smartphone photography, where in order to obtain more resolute images the devices include two cameras, it could technically be possible to perform structure-from-motion mapping using a single smartphone with two or more camera sensors.

In terms of modality fusion, Ultrasound and VLC could both be considered relatively unexplored. Most of the literature, for both of these modalities, present implementations in a sterile environment of a laboratory, reporting sub-meter accuracy. That would suggest that these types of modalities are still in the proof of concept stage of research. There is yet to be study which would use these modalities in a wide-scale positioning infrastructure or fusion campaign. On the other hand, the fusion of RF and Inertia/Magnetometers is very widely explored, in both performance studies and their appearance in various data sets. The aforementioned Ultrasound and VLC-based approaches are, however, again underrepresented in this domain. This is not surprising due to the relatively large infrastructures demanded by these modalities. Additionally, there exists space for localisation-specific data set encompassing human-borne LiDAR for fingerprinting applications. This could be used with AMF or RF.

Fusion methodologies are also likely to shift. Recent proliferation of DNN techniques and ANN in general, is likely to drive the fusion into the deep learning domain. Indeed, chapter 2 has shown that there have been strides made in that direction. Deep Learning has, in particular, began to permeate the space of indoor localisation. With an increased number of objective-specific hardware accelerators and portable networks, such as NVIDIA Jetson [152] or Coral Accelerator [65] it would soon become easier to run real-time, tailored networks allowing for precise localisation estimation. However, when compared to Bayesian location estimation methods, this particular domain is still lacking, in both proper theoretical formulation and exhausting comparison studies. This is not to say, that the current state-of-the-art Bayesian methods will be completely ousted. A more likely prediction is one of the two systems working together, either in unison, or as compliments of each other, in order to make the prediction more accurate.

With respect to the data collection methods and models, the majority of the proposed challenges and issues have already been addressed by chapter 5. However, there exist many other challenges which still remain overlooked. These are specifically related to the topology of the training method. Fingerprinting, even if automated, still remains a precarious exercise. Collecting 'one-off' data, using only a snapshot of possible model parameters, at a high labour cost, still prohibits this technique from finding a good industrial application and is so far confined to research implementations. However, relatively little research have been done on improving this training technique.

Additionally, since the space of WSN is sensitive to radio propagation, the novel training methods should focus on an added component of environment dynamics. So far, there have not been a great lot of research in a way of a robust implementation which would perform periodical re-training as to establish the most likely picture of the signal propagation characteristics, in a given residence over long periods of time. This is understandably difficult to obtain, but would open a new avenue of efficient model re-estimation research. An interesting field of CSI-based estimation could also be thoroughly expanded. There exist possibility of utilising passive radio signals, the disturbance of which can be used to track users in the environment. This alleviates the need for intrusive wearable sensors, theoretically allowing the users to traverse the environment free of any unnecessary hindrance. Whilst it precludes the use of typical on-body sensors, such as accelerometers, it could help popularise the field of indoor localisation, as the algorithms would no longer be reliant on extensive infrastructures.

The chapter 5, outlining the 'H4LO' system, could be used for early work on such re-estimation. It is equipped to perform quick fingerprinting, and it relies on the sequential map gathering to estimate its position. This problem can also be relaxed, in that if a residence was mapped already and initial position is known, extracting pose estimates is only the matter of matching current point cloud with already existing maps. This reduces the overhead of having to perform careful fingerprinting, as the signals and spatial features could be correlated to existing fingerprint maps of the environment, updating it in the process, without the need for costly SLAM computation. In terms of actual system, the future work would concentrate on improving the accuracy of the results. Using the extensive IMU data, it is possible to distinguish and classify between floors and improve on the quality of the maps, reducing the effects of obstacles, such as laser reflections. Additionally, this dataset can help with interpretability of RSS data with regard to spatial features, and vice versa.

The study of sensor fusion in chapter 6 could be improved in terms of performance

and scale. The future work would involve incorporating additional sensors, including gyroscope and magnetometer, together with complementing information pertaining to the layout of the house. This would serve to explore how the layout complexity relates to packet drop and the location accuracy. Additionally, implementing a more elaborate accelerometer processing, such as a PDR implementation, would improve the quality of future studies on this topic. Instead of relying on a purely RF setting localisation, having a PDR as a back up implementation could also solve various 'null point' problems with existing RF localisation, such as floor ambiguity.

In relation to the energy efficiency study, further work would include generalising this method to a different dataset, not necessarily concentrating on the localisation performance. Whilst localisation offered advantages, such as predictable dynamics, studying the effect of activity recognition, scrutinised under energy efficiency could offer new routes of obtaining efficiency in a WSN. Additionally, a better simulation model for these particular problems could also be developed - one which includes dynamic AP selections and 'oracles' which are to some degree fallible.

Chapter 7 could be improved by including other metrics over which the sensor selection will be optimised. These can include specific on-body and off-body sensors and combination thereof, as opposed to simple RF data quality metrics. In addition to quality of information, the optimisation could include a metric of energy efficiency or accessibility to utilities, such as power sockets. There could also be a study which determines whether the sensor selection problem is user-invariant, especially in relation to digital health applications. Interestingly, the energy efficiency and sensor selection studies could also be complimented by a combination of the two together. Considering the space of adaptive sensor selection, the energy efficiency metric could be explored in terms of optimal selection of sensors given the location in the house. Simply put, finding an optimal set of sensors for every location in the house, and updating this selection in terms of energy efficiency and/or localisation performance.

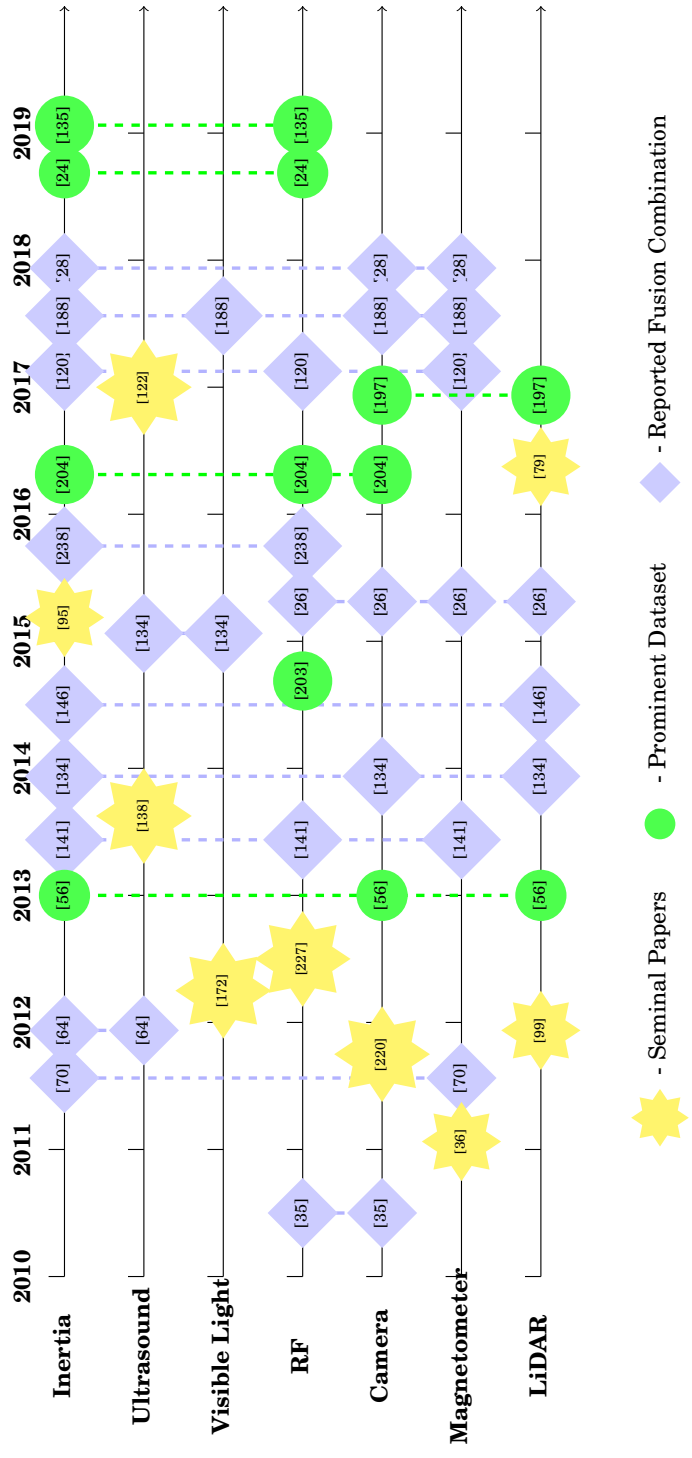

Figure 8.1: Outline of reported fusion combinations, data sets and seminal papers in the literature of sensors and their fusion for indoor localisation in the past decade. The data sets and fusion combinations include dashed lines, signifying that the study encompassed respective selected modalities.

BIBLIOGRAPHY

[1] *ELAN (Version 4.9.3)*, Feb. 2016.

[2] A. A. ABABNEH, *Density-based sensor selection for rss target localization*, IEEE Sensors Journal, (2018).

[3] W. A. ABDULHAFIZ AND A. KHAMIS, *Bayesian approach to multisensor data fusion with pre-and post-filtering*, in Networking, Sensing and Control (ICNSC), 2013 10th IEEE International Conference on, IEEE, 2013, pp. 373–378.

[4] A. M. ABU-MAHFOUZ AND G. P. HANCKE, *ALWadHA Localization Algorithm: Yet More Energy Efficient*, IEEE Access, 5 (2017), pp. 6661–6667.

[5] D. B. AHMED AND E. M. DIAZ, *3d Loose-Coupled Fusion of Inertial Sensors for Pedestrian Localization*, in 2018 (IPIN), Sept. 2018, pp. 206–212.

[6] T. AKIYAMA, H. OHASHI, A. SATO, G. NAKAHARA, AND K. YAMASAKI, *Pedestrian dead reckoning using adaptive particle filter to human moving mode*, in Indoor Positioning and Indoor Navigation (IPIN), 2013, IEEE, 2013, pp. 1–7.

[7] M. B. ALATISE AND G. P. HANCKE, *Pose Estimation of a Mobile Robot Based on Fusion of IMU Data and Vision Data Using an Extended Kalman Filter*, Sensors, 17 (2017), p. 2164.

[8] J. ARMSTRONG, Y. SEKERCIOGLU, AND A. NEILD, *Visible light positioning: a roadmap for international standardization*, IEEE Communications Magazine, 51 (2013), pp. 68–73.

[9] M. S. ARULAMPALAM, S. MASKELL, N. GORDON, AND T. CLAPP, *A tutorial on particle filters for online nonlinear/non-gaussian bayesian tracking*, IEEE Transactions on signal processing, 50 (2002), pp. 174–188.

[10] S. BAHADORI, L. IOCCHI, G. LEONE, D. NARDI, AND L. SCOZZAFAVA, *Real-time people localization and tracking through fixed stereo vision*, Applied Intelligence, 26 (2007), pp. 83–97.

[11] P. BAHL AND V. N. PADMANABHAN, *RADAR: an in-building RF-based user location and tracking system*, in Proceedings IEEE INFOCOM 2000. Conference on Computer Communications. Nineteenth Annual Joint Conference of the IEEE Computer and Communications Societies (Cat. No.00CH37064), vol. 2, 2000, pp. 775–784 vol.2.

[12] S. S. BANERJEE AND R. R. DHOLAKIA, *Mobile advertising: Does location based advertising work?*, (2008).

[13] L. BAO AND S. S. INTILLE, *Activity Recognition from User-Annotated Acceleration Data*, in Pervasive Computing, A. Ferscha and F. Mattern, eds., Springer Berlin Heidelberg, Apr. 2004, pp. 1–17.

[14] D. BARBER, *Bayesian reasoning and machine learning*, Cambridge University Press, 2012.

[15] P. BARSOCCHI, S. LENZI, S. CHESSA, AND G. GIUNTA, *A Novel Approach to Indoor RSSI Localization by Automatic Calibration of the Wireless Propagation Model*, in Vehicular Technology Conference, 2009. VTC Spring 2009. IEEE 69th, Apr. 2009, pp. 1–5.

[16] A. BEHBOODI, F. LEMIC, AND A. WOLISZ, *A mathematical model for fingerprinting-based localization algorithms*, CoRR, (2016).

[17] F. BIAN, D. KEMPE, AND R. GOVINDAN, *Utility Based Sensor Selection*, in Proceedings of the 5th International Conference on Information Processing in Sensor Networks, IPSN '06, New York, NY, USA, 2006, ACM, pp. 11–18.

[18] P. BIBER AND W. STRASSER, *The normal distributions transform: a new approach to laser scan matching*, in 2003 IEEE/RSJ International Conference on Intelligent Robots and Systems, 2003. (IROS 2003). Proceedings, vol. 3, Oct. 2003, pp. 2743–2748 vol.3.

[19] BOSCH SENSORTEC, *BNO055, Intelligent 9-axis absolute orientation sensor*, 11 2014.

[20] A. BOSE AND C. H. FOH, *A practical path loss model for indoor WiFi positioning enhancement*, in 2007 6th International Conference on Information, Communications Signal Processing, Dec. 2007, pp. 1–5.

[21] S. BOSE, A. K. GUPTA, AND P. HANDEL, *On the noise and power performance of a shoe-mounted multi-IMU inertial positioning system*, in 2017 (IPIN), Sept. 2017, pp. 1–8.

[22] M. N. K. BOULOS AND G. BERRY, *Real-time locating systems (rtls) in healthcare: a condensed primer*, International journal of health geographics, 11 (2012), p. 25.

[23] Y. BOUSSEMART, J. LAS FARGEAS, M. L. CUMMINGS, AND N. ROY, *Comparing learning techniques for hidden markov models of human supervisory control behavior*, in AIAA Infotech@ Aerospace Conference and AIAA Unmanned... Unlimited Conference, 2009, p. 1842.

[24] D. BYRNE, M. KOZLOWSKI, R. SANTOS-RODRIGUEZ, R. PIECHOCKI, AND I. CRADDOCK, *Residential Wearable RSSI and Accelerometer Measurements with Detailed Annotations*, Scientific Data 5, 2018, (2018).

[25] M. CAMPLANI, A. PAIEMENT, M. MIRMEHDI, D. DAMEN, S. HANNUNA, T. BURGHARDT, AND L. TAO, *Multiple human tracking in rgb-depth data: a survey*, IET computer vision, 11 (2016), pp. 265–285.

[26] A. CANEDO-RODRÍGUEZ, V. ALVAREZ-SANTOS, C. V. REGUEIRO, R. IGLESIAS, S. BARRO, AND J. PRESEDO, *Particle filter robot localisation through robust fusion of laser, wifi, compass, and a network of external cameras*, Information Fusion, 27 (2016), pp. 170–188.

[27] A. CARMI AND P. GURFIL, *Sensor Selection via Compressed Sensing*, Automatica, 49 (2013), pp. 3304–3314.

[28] D. CARUSO, A. EUDES, M. SANFOURCHE, D. VISSIÈRE, AND G. LE BESNERAIS, *A Robust Indoor/Outdoor Navigation Filter Fusing Data from Vision and Magneto-Inertial Measurement Unit*, Sensors, 17 (2017), p. 2795.

[29] W. F. CASELTON AND J. V. ZIDEK, *Optimal monitoring network designs*, Statistics & Probability Letters, 2 (1984), pp. 223–227.

[30] M. CASTILLO-CARA, J. LOVÓN-MELGAREJO, G. BRAVO-ROCCA, L. OROZCO-BARBOSA, AND I. GARCÍA-VAREA, *An Empirical Study of the Transmission Power Setting for Bluetooth-Based Indoor Localization Mechanisms*, Sensors, 17 (2017), p. 1318.

[31] K. CHACCOUR, R. DARAZI, A. H. EL HASSANS, AND E. ANDRES, *Smart carpet using differential piezoresistive pressure sensors for elderly fall detection*, in Wireless and Mobile Computing, Networking and Communications (WiMob), 2015 IEEE 11th International Conference on, IEEE, 2015, pp. 225–229.

[32] Z. CHEN, Q. ZHU, H. JIANG, H. ZOU, Y. C. SOH, L. XIE, R. JIA, AND S. COSTAS, *An iBeacon Assisted Indoor Localization and Tracking System*, Microsoft Indoor Localization Competition, (2015).

[33] Z. CHEN, H. ZOU, H. JIANG, Q. ZHU, Y. C. SOH, AND L. XIE, *Fusion of wifi, smartphone sensors and landmarks using the kalman filter for indoor localization*, Sensors, 15 (2015), pp. 715–732.

[34] B. CHMELAŘ, L. PŘEUČIL, AND P. ŠTĚPÁN, *Range-data based position localization and refinement for a mobile robot*, IFAC Proceedings Volumes, 33 (2000), pp. 369–374.

[35] B.-S. CHOI AND J.-J. LEE, *Sensor network based localization algorithm using fusion sensor-agent for indoor service robot*, IEEE Transactions on Consumer Electronics, 56 (2010).

[36] J. CHUNG, M. DONAHOE, C. SCHMANDT, I.-J. KIM, P. RAZAVAI, AND M. WISEMAN, *Indoor location sensing using geo-magnetism*, in Proceedings of the 9th international conference on Mobile systems, applications, and services, ACM, 2011, pp. 141–154.

[37] M. CILIBERTO, L. WANG, D. ROGGEN, AND R. ZILLMER, *A case study for human gesture recognition from poorly annotated data*, in Proceedings of the 2018 ACM International Joint Conference and 2018 International Symposium on Pervasive and Ubiquitous Computing and Wearable Computers, ACM, 2018, pp. 1434–1443.

[38] M. CONTIGIANI, E. FRONTONI, A. MANCINI, AND A. GATTO, *Indoor people localization and tracking using an energy harvesting smart floor*, in Mechatronic

and Embedded Systems and Applications (MESA), 2014 IEEE/ASME 10th International Conference on, IEEE, 2014, pp. 1–5.

[39] A. P. CRACKNELL, *Introduction to remote sensing*, CRC press, 2007.

[40] L. D'ALFONSO, A. GRIFFO, P. MURACA, AND P. PUGLIESE, *A slam algorithm for indoor mobile robot localization using an extended kalman filter and a segment based environment mapping*, in Advanced Robotics (ICAR), 2013 16th International Conference on, IEEE, 2013, pp. 1–6.

[41] D. C. DANG AND Y. S. SUH, *Walking Distance Estimation Using Walking Canes with Inertial Sensors*, Sensors, 18 (2018), p. 230.

[42] G. DEAK, K. CURRAN, AND J. CONDELL, *A survey of active and passive indoor localisation systems*, Computer Communications, 35 (2012), pp. 1939–1954.

[43] T. DIETHE, M. HOLMES, M. KULL, M. PERELLO NIETO, K. SOKOL, H. SONG, E. TONKIN, N. TWOMEY, AND P. FLACH, *Releasing ehealth analytics into the wild: Lessons learnt from the sphere project*, in Proceedings of the 24th ACM SIGKDD International Conference on Knowledge Discovery & Data Mining, ACM, 2018, pp. 243–252.

[44] T. DIETHE, N. TWOMEY, AND P. FLACH, *Bdl. net: Bayesian dictionary learning in infer. net*, in Machine Learning for Signal Processing (MLSP), 2016 IEEE 26th International Workshop on, IEEE, 2016, pp. 1–6.

[45] E. W. DIJKSTRA, *A note on two problems in connexion with graphs*, Numerische mathematik, 1 (1959), pp. 269–271.

[46] C. DOUKAS AND I. MAGLOGIANNIS, *Bringing iot and cloud computing towards pervasive healthcare*, in Innovative Mobile and Internet Services in Ubiquitous Computing (IMIS), 2012 Sixth International Conference on, IEEE, 2012, pp. 922–926.

[47] R. O. DUDA, P. E. HART, AND D. G. STORK, *Pattern Classification (2Nd Edition)*, Wiley-Interscience, 2000.

[48] H. DURRANT-WHYTE AND T. C. HENDERSON, *Multisensor data fusion*, in Springer handbook of robotics, Springer, 2008, pp. 585–610.

[49] R. ELBAKLY, M. ELHAMSHARY, AND M. YOUSSEF, *Hyrise: A robust and ubiquitous multi-sensor fusion-based floor localization system*, Proceedings of the ACM on Interactive, Mobile, Wearable and Ubiquitous Technologies, 2 (2018), p. 104.

[50] A. ELSTS, R. MCCONVILLE, X. FAFOUTIS, N. TWOMEY, R. PIECHOCKI, R. SANTOS-RODRIGUEZ, AND I. CRADDOCK, *On-board feature extraction from acceleration data for activity recognition*, in Proceedings of the 2018 International Conference on Embedded Wireless Systems and Networks, 2018, pp. 163–168.

[51] F. ENDRES, J. HESS, N. ENGELHARD, J. STURM, D. CREMERS, AND W. BURGARD, *An evaluation of the rgb-d slam system*, in Robotics and Automation (ICRA), 2012 IEEE International Conference on, IEEE, 2012, pp. 1691–1696.

[52] X. FAFOUTIS, A. ELSTS, R. PIECHOCKI, AND I. CRADDOCK, *Experiences and Lessons Learned From Making IoT Sensing Platforms for Large-Scale Deployments*, IEEE Access, 6 (2018), pp. 3140–3148.

[53] X. FAFOUTIS, A. ELSTS, A. VAFEAS, G. OIKONOMOU, AND R. PIECHOCKI, *On predicting the battery lifetime of iot devices: Experiences from the sphere deployments*, in Proceedings of the 7th International Workshop on Real-World Embedded Wireless Systems and Networks, ACM, 2018, pp. 7–12.

[54] X. FAFOUTIS, B. JANKO, E. MELLIOS, G. HILTON, R. S. SHERRATT, R. PIECHOCKI, AND I. CRADDOCK, *A Low-Maintenance Wearable Activity Tracker for Residential Monitoring and Healthcare Applications*, In Proceedings of the International Conference on Wearables in Healthcare (HealthWear), (2016).

[55] X. FAFOUTIS, A. VAFEAS, B. JANKO, R. S. SHERRATT, J. POPE, A. ELSTS, E. MELLIOS, G. HILTON, G. OIKONOMOU, R. PIECHOCKI, AND I. CRADDOCK, *Designing Wearable Sensing Platforms for Healthcare in a Residential Environment*, EAI Endorsed Transactions on Pervasive Health and Technology, "3" (2017).

[56] M. FALLON, H. JOHANNSSON, M. KAESS, AND J. J. LEONARD, *The mit stata center dataset*, The International Journal of Robotics Research, 32 (2013), pp. 1695–1699.

[57] B. FERRIS, D. FOX, AND N. LAWRENCE, *WiFi-SLAM Using Gaussian Process Latent Variable Models*, in Proceedings of the 20th International Joint Conference on Artifical Intelligence, IJCAI'07, San Francisco, CA, USA, 2007, Morgan Kaufmann Publishers Inc., pp. 2480–2485.

[58] A. FILIPPESCHI, N. SCHMITZ, M. MIEZAL, G. BLESER, E. RUFFALDI, AND D. STRICKER, *Survey of motion tracking methods based on inertial sensors: a focus on upper limb human motion*, Sensors, 17 (2017), p. 1257.

[59] E. R. FOSSUM, *Cmos image sensors: Electronic camera-on-a-chip*, IEEE transactions on electron devices, 44 (1997), pp. 1689–1698.

[60] E. FOXLIN, *Pedestrian tracking with shoe-mounted inertial sensors*, IEEE Computer graphics and applications, 25 (2005), pp. 38–46.

[61] M. L. FUNG, M. Z. CHEN, AND Y. H. CHEN, *Sensor fusion: A review of methods and applications*, in Control And Decision Conference (CCDC), 2017 29th Chinese, IEEE, 2017, pp. 3853–3860.

[62] S. GARRIDO-JURADO, R. MUÑOZ-SALINAS, F. MADRID-CUEVAS, AND M. MARÍN-JIMÉNEZ, *Automatic generation and detection of highly reliable fiducial markers under occlusion*, Pattern Recognition, 47 (2014), p. 2280–2292.

[63] C. GENTNER AND M. ULMSCHNEIDER, *Simultaneous localization and mapping for pedestrians using low-cost ultra-wideband system and gyroscope*, in 2017 (IPIN), Sept. 2017, pp. 1–8.

[64] G. GIRARD, S. CÔTÉ, S. ZLATANOVA, Y. BARETTE, J. ST-PIERRE, AND P. VAN OOSTEROM, *Indoor pedestrian navigation using foot-mounted imu and portable ultrasound range sensors*, Sensors, 11 (2011), pp. 7606–7624.

[65] GOOGLE LLC, *Coral USB Accelerator datasheet*, 05 2019.

[66] G. GRISETTI, R. KUMMERLE, C. STACHNISS, AND W. BURGARD, *A Tutorial on Graph-Based SLAM*, IEEE Intelligent Transportation Systems Magazine, 2 (2010), pp. 31–43.

[67] T. GU, Z. WU, X. TAO, H. K. PUNG, AND J. LU, *epsicar: An emerging patterns based approach to sequential, interleaved and concurrent activity recognition*, in Pervasive Computing and Communications, 2009. PerCom 2009. IEEE International Conference on, IEEE, 2009, pp. 1–9.

[68] I. GUVENC AND Z. SAHINOGLU, *Threshold-based TOA estimation for impulse radio UWB systems*, in 2005 IEEE International Conference on Ultra-Wideband, Sept. 2005, pp. 420–425.

[69] D. HAN, S.-H. JUNG, AND S. LEE, *A sensor fusion method for wi-fi-based indoor positioning*, ICT Express, 2 (2016), pp. 71–74.

[70] S. HAN AND J. WANG, *A novel method to integrate imu and magnetometers in attitude and heading reference systems*, The Journal of Navigation, 64 (2011), pp. 727–738.

[71] D. HANLEY, X. ZHANG, A. S. D. D. OLIVEIRA, D. STEINBERG, AND T. BRETL, *Experimental Evaluation of the Planar Assumption in Magnetic Positioning*, in 2018 (IPIN), Sept. 2018, pp. 1–8.

[72] S. HANNUNA, M. CAMPLANI, J. HALL, M. MIRMEHDI, D. DAMEN, T. BURGHARDT, A. PAIEMENT, AND L. TAO, *Ds-kcf: a real-time tracker for rgb-d data*, Journal of Real-Time Image Processing, (2016), pp. 1–20.

[73] R. HARLE, *A Survey of Indoor Inertial Positioning Systems for Pedestrians*, IEEE Communications Surveys Tutorials, 15 (2013), pp. 1281–1293.

[74] J. HAVERINEN AND A. KEMPPAINEN, *Global indoor self-localization based on the ambient magnetic field*, Robotics and Autonomous Systems, 57 (2009), pp. 1028–1035.

[75] M. HAZAS AND A. HOPPER, *Broadband ultrasonic location systems for improved indoor positioning*, IEEE Transactions on mobile Computing, (2006), pp. 536–547.

[76] X. HE, D. N. ALOI, AND J. LI, *Probabilistic multi-sensor fusion based indoor positioning system on a mobile device*, Sensors, 15 (2015), pp. 31464–31481.

[77] A. HERRERA-MAY, L. AGUILERA-CORTÉS, P. GARCÍA-RAMÍREZ, AND E. MANJARREZ, *Resonant magnetic field sensors based on mems technology*, Sensors, 9 (2009), pp. 7785–7813.

[78] A. HERRERA-MAY, J. SOLER-BALCAZAR, H. VÁZQUEZ-LEAL, J. MARTÍNEZ-CASTILLO, M. VIGUERAS-ZUÑIGA, AND L. AGUILERA-CORTÉS, *Recent advances of mems resonators for lorentz force based magnetic field sensors: Design, applications and challenges*, Sensors, 16 (2016), p. 1359.

[79] W. HESS, D. KOHLER, H. RAPP, AND D. ANDOR, *Real-time loop closure in 2d lidar slam*, in Robotics and Automation (ICRA), 2016 IEEE International Conference on, IEEE, 2016, pp. 1271–1278.

[80] M. HIMMELSBACH, A. MUELLER, T. LÜTTEL, AND H.-J. WÜNSCHE, *Lidar-based 3d object perception*, in Proceedings of 1st international workshop on cognition for technical systems, vol. 1, 2008.

[81] M. K. HOANG, J. SCHMALENSTROEER, C. DRUEKE, D. H. T. VU, AND R. HAEB-UMBACH, *A hidden Markov model for indoor user tracking based on WiFi fingerprinting and step detection*, in 21st European Signal Processing Conference (EUSIPCO 2013), Sept. 2013, pp. 1–5.

[82] Y. HONG, J. CHEN, Z. WANG, AND C. YU, *Performance of a precoding mimo system for decentralized multiuser indoor visible light communications*, IEEE Photonics journal, 5 (2013), pp. 7800211–7800211.

[83] Y. HOU, X. YANG, AND Q. ABBASI, *Efficient aoa-based wireless indoor localization for hospital outpatients using mobile devices*, Sensors, 18 (2018), p. 3698.

[84] H.-H. HSU, J.-K. CHANG, W.-J. PENG, T. K. SHIH, T.-W. PAI, AND K. L. MAN, *Indoor localization and navigation using smartphone sensory data*, Annals of Operations Research, 265 (2018), pp. 187–204.

[85] Y.-L. HSU, Y.-J. CHEN, AND S.-W. SHIH, *A particle filter approach for pedestrian dead reckoning using wearable sensors*, in Innovative Mobile and Internet Services in Ubiquitous Computing (IMIS), 2016 10th International Conference on, IEEE, 2016, pp. 26–32.

[86] C. HUANG, Z. LIAO, AND L. ZHAO, *Synergism of INS and PDR in self-contained pedestrian tracking with a miniature sensor module*, IEEE Sensors Journal, (2010), pp. 1349–1359.

[87] A. A. HUSSEIN, C. Y. LEOW, AND T. A. RAHMAN, *Robust multiple frequency multiple power localization schemes in the presence of multiple jamming attacks*, PloS one, 12 (2017), p. e0177326.

[88] A. A. HUSSEIN, T. A. RAHMAN, AND C. Y. LEOW, *Performance Evaluation of Localization Accuracy for a Log-Normal Shadow Fading Wireless Sensor Net-*

work under Physical Barrier Attacks, Sensors (Basel, Switzerland), 15 (2015), pp. 30545–30570.

[89] Z. JIAO, B. ZHANG, M. LIU, AND C. LI, *Visible light communication based indoor positioning techniques*, IEEE Network, 31 (2017).

[90] S. JOSHI AND S. BOYD, *Sensor Selection via Convex Optimization*, IEEE Transactions on Signal Processing, 57 (2009), pp. 451–462.

[91] T. JUDD, *A personal dead reckoning module*, in ION GPS, vol. 97, 1997, pp. 1–5.

[92] M. JUNG AND J.-B. SONG, *Graph slam for agv using geometrical arrangement based on lamp and surf features in a factory environment*, in Control, Automation and Systems (ICCAS), 2016 16th International Conference on, IEEE, 2016, pp. 844–848.

[93] O. KALTIOKALLIO, R. HOSTETTLER, N. PATWARI, AND R. JÄNTTI, *Recursive Bayesian Filters for RSS-Based Device-Free Localization and Tracking*, in 2018 (IPIN), Sept. 2018, pp. 1–8.

[94] S. M. KAMRUZZAMAN, M. JASEEMUDDIN, X. FERNANDO, AND P. MOEINI, *Wireless positioning sensor network integrated with cloud for industrial automation*, in Local Computer Networks (LCN), 2017 IEEE 42nd Conference on, IEEE, 2017, pp. 543–546.

[95] W. KANG AND Y. HAN, *Smartpdr: Smartphone-based pedestrian dead reckoning for indoor localization*, IEEE Sensors journal, 15 (2015), pp. 2906–2916.

[96] M. O. KHYAM, S. S. GE, X. LI, AND M. PICKERING, *Orthogonal Chirp-Based Ultrasonic Positioning*, Sensors, 17 (2017), p. 976.

[97] S. KNAUTH, *Smartphone PDR positioning in large environments employing WiFi, particle filter, and backward optimization*, in 2017 (IPIN), Sept. 2017, pp. 1–6.

[98] J. KO, C. LU, M. B. SRIVASTAVA, J. A. STANKOVIC, A. TERZIS, AND M. WELSH, *Wireless Sensor Networks for Healthcare*, Proceedings of the IEEE, 98 (2010), pp. 1947–1960.

[99] S. KOHLBRECHER, O. V. STRYK, J. MEYER, AND U. KLINGAUF, *A flexible and scalable SLAM system with full 3d motion estimation*, in 2011 IEEE International Symposium on Safety, Security, and Rescue Robotics, Nov. 2011, pp. 155–160.

[100] M. KOZLOWSKI, D. BYRNE, R. SANTOS-RODRIGUEZ, AND R. J. PIECHOCKI, *Data Fusion for Robust Indoor Localisation in Digital Health*, in 2018 IEEE Wireless Communications and Networking Conference Workshops (WCNCW): IoT-Health 2018: IRACON Workshop on IoT Enabling Technologies in Healthcare (IEEE WCNCW IoT-Health 2018), Barcelona, Spain, Apr. 2018.

[101] M. KOZLOWSKI, R. MCCONVILLE, R. SANTOS-RODRIGUEZ, AND R. J. PIECHOCKI, *Energy Efficiency in Reinforcement Learning for Wireless Sensor Networks*, in Proceedings of the European Conference on Machine Learning and Principles and Practice of Knowledge Discovery in Databases (ECML-PKDD 2018), Green Data Mining Workshop, Sept. 2018.

[102] M. KOZŁOWSKI, R. SANTOS-RODRÍGUEZ, AND R. PIECHOCKI, *Sensor modalities and fusion for robust indoor localisation*, EAI Endorsed Transactions on Ambient Systems, 6 (2019).

[103] M. KOZLOWSKI, N. TWOMEY, D. BYRNE, J. POPE, R. SANTOS-RODRIGUEZ, AND R. PIECHOCKI, *H4lo: Automation platform for efficient rf fingerprinting using slam-derived map and poses*, IET Radar, Sonar & Navigation, (2020).

[104] A. KRAUSE, *Optimizing sensing: Theory and applications*, tech. rep., 2008.

[105] A. KRAUSE, *Sfo: A toolbox for submodular function optimization*, Journal of Machine Learning Research, 11 (2010), pp. 1141–1144.

[106] A. KRAUSE, A. SINGH, AND C. GUESTRIN, *Near-Optimal Sensor Placements in Gaussian Processes: Theory, Efficient Algorithms and Empirical Studies*, J. Mach. Learn. Res., 9 (2008), pp. 235–284.

[107] J. KUANG, X. NIU, AND X. CHEN, *Robust pedestrian dead reckoning based on mems-imu for smartphones*, Sensors (Basel, Switzerland), 18 (2018).

[108] G. A. KUMAR, A. K. PATIL, R. PATIL, S. S. PARK, AND Y. H. CHAI, *A LiDAR and IMU Integrated Indoor Navigation System for UAVs and Its Application in Real-Time Pipeline Classification*, Sensors, 17 (2017), p. 1268.

[109] Y.-S. KUO, P. PANNUTO, K.-J. HSIAO, AND P. DUTTA, *Luxapose: Indoor positioning with mobile phones and visible light*, in Proceedings of the 20th annual international conference on Mobile computing and networking, ACM, 2014, pp. 447–458.

[110] M. KWAK, Y. PARK, J. KIM, J. HAN, AND T. KWON, *An energy-efficient and lightweight indoor localization system for internet-of-things (iot) environments*, Proceedings of the ACM on Interactive, Mobile, Wearable and Ubiquitous Technologies, 2 (2018), p. 17.

[111] N. LEE AND D. HAN, *Magnetic indoor positioning system using deep neural network*, in Indoor Positioning and Indoor Navigation (IPIN), 2017, IEEE, 2017, pp. 1–8.

[112] S. LEE, D. HAR, AND D. KUM, *Drone-assisted disaster management: Finding victims via infrared camera and lidar sensor fusion*, in Computer Science and Engineering (APWC on CSE), 2016 3rd Asia-Pacific World Congress on, IEEE, 2016, pp. 84–89.

[113] T.-J. LEE, C.-H. KIM, AND D.-I. D. CHO, *A monocular vision sensor-based efficient slam method for indoor service robots*, IEEE Transactions on Industrial Electronics, 66 (2019), pp. 318–328.

[114] Y.-C. LEE AND S.-H. PARK, *Rssi-based fingerprint map building for indoor localization*, in 2013 10th International Conference on Ubiquitous Robots and Ambient Intelligence (URAI), IEEE, 2013, pp. 292–293.

[115] C. LI, Q. XU, Z. GONG, AND R. ZHENG, *TuRF: Fast Data Collection for Fingerprint-based Indoor Localization*, arXiv:1705.07483 [cs], (2017).
arXiv: 1705.07483.

[116] L. LI, P. HU, C. PENG, G. SHEN, AND F. ZHAO, *Epsilon: A visible light based positioning system.*, in NSDI, vol. 14, 2014, pp. 331–343.

[117] M. LI, V. T. ROUF, M. J. THOMPSON, AND D. A. HORSLEY, *Three-axis lorentz-force magnetic sensor for electronic compass applications*, Journal of Microelectromechanical Systems, 21 (2012), pp. 1002–1010.

[118] W. LI AND W. ZHANG, *Sensor selection for improving accuracy of target localisation in wireless visual sensor networks*, IET Wireless Sensor Systems, 2 (2012), pp. 293–301.

[119] X. LI, Y. WANG, AND K. KHOSHELHAM, *A robust and adaptive complementary kalman filter based on mahalanobis distance for ultra wideband/inertial measurement unit fusion positioning*, Sensors, 18 (2018), p. 3435.

[120] Y. LI, Y. ZHUANG, P. ZHANG, H. LAN, X. NIU, AND N. EL-SHEIMY, *An improved inertial/wifi/magnetic fusion structure for indoor navigation*, Information Fusion, 34 (2017), pp. 101–119.

[121] H. LIU, H. DARABI, P. BANERJEE, AND J. LIU, *Survey of Wireless Indoor Positioning Techniques and Systems*, IEEE Transactions on Systems, Man, and Cybernetics, Part C (Applications and Reviews), 37 (2007), pp. 1067–1080.

[122] H. LIU, F. SUN, B. FANG, AND X. ZHANG, *Robotic room-level localization using multiple sets of sonar measurements*, IEEE Transactions on Instrumentation and Measurement, 66 (2017), pp. 2–13.

[123] M. LIU, R. CHEN, D. LI, Y. CHEN, G. GUO, Z. CAO, AND Y. PAN, *Scene Recognition for Indoor Localization Using a Multi-Sensor Fusion Approach*, Sensors, 17 (2017), p. 2847.

[124] Q. LIU, J. WILLIAMSON, K. LI, W. MOHRMAN, Q. LV, R. P. DICK, AND L. SHANG, *Gazelle: Energy-efficient wearable analysis for running*, IEEE Transactions on Mobile Computing, (2017), pp. 2531–2544.

[125] T. LOWE, S. KIM, AND M. COX, *Complementary perception for handheld slam*, IEEE Robotics and Automation Letters, 3 (2018), pp. 1104–1111.

[126] X. LUO, Q. GUAN, H. TAN, L. GAO, Z. WANG, AND X. LUO, *Simultaneous indoor tracking and activity recognition using pyroelectric infrared sensors*, Sensors, 17 (2017), p. 1738.

[127] D. LYMBEROPOULOS AND J. LIU, *The Microsoft Indoor Localization Competition: Experiences and Lessons Learned*, IEEE Signal Processing Magazine, 34 (2017), pp. 125–140.

[128] L. V. D. MAATEN AND G. HINTON, *Visualizing data using t-sne*, Journal of machine learning research, 9 (2008), pp. 2579–2605.

[129] P. MAGAÑA-ESPINOZA, R. AQUINO-SANTOS, N. CÁRDENAS-BENÍTEZ, J. AGUILAR-VELASCO, C. BUENROSTRO-SEGURA, A. EDWARDS-BLOCK, AND A. MEDINA-CASS, *WiSPH: a wireless sensor network-based home care monitoring system*, Sensors (Basel, Switzerland), 14 (2014), pp. 7096–7119.

[130] E. R. MAGSINO, I. W.-H. HO, AND Z. SITU, *The effects of dynamic environment on channel frequency response-based indoor positioning*, in Personal, Indoor, and Mobile Radio Communications (PIMRC), 2017 IEEE 28th Annual International Symposium on, IEEE, 2017, pp. 1–6.

[131] A. MALLIOS, P. RIDAO, D. RIBAS, M. CARRERAS, AND R. CAMILLI, *Toward autonomous exploration in confined underwater environments*, Journal of Field Robotics, 33 (2016), pp. 994–1012.

[132] A. MANNINI, S. S. INTILLE, M. ROSENBERGER, A. M. SABATINI, AND W. HASKELL, *Activity recognition using a single accelerometer placed at the wrist or ankle*, Medicine and science in sports and exercise, 45 (2013), pp. 2193–2203.

[133] A. MANOS, I. KLEIN, AND T. HAZAN, *Gravity Direction Estimation and Heading Determination for Pedestrian Navigation*, in 2018 (IPIN), Sept. 2018, pp. 206–212.

[134] I. MARIN-GARCIA, P. CHAVEZ-BURBANO, A. MUÑOZ-ARCENTLES, V. CALERO-BRAVO, AND R. PEREZ-JIMENEZ, *Indoor location technique based on visible light communications and ultrasound emitters*, in 2015 IEEE International Conference on Consumer Electronics (ICCE), IEEE, 2015, pp. 297–298.

[135] R. MCCONVILLE, D. BYRNE, I. CRADDOCK, R. PIECHOCKI, J. POPE, AND R. SANTOS-RODRIGUEZ, *A dataset for room level indoor localization using a smart home in a box*, in Data in Brief, 2019.

[136] R. MCCONVILLE, D. BYRNE, I. CRADDOCK, R. PIECHOCKI, R. SANTOS-RODRIGUEZ, AND J. POPE, *Understanding the Quality of Calibrations for Indoor Localisation*, in 2018 IEEE 4th World Forum on Internet of Things (WF-IoT 2018), Institute of Electrical and Electronics Engineers (IEEE), 2018.

[137] R. MCCONVILLE, R. SANTOS-RODRIGUEZ, AND N. TWOMEY, *Person identification and discovery with wrist worn accelerometer data*, in Proceedings of the European Symposium on Artificial Neural Networks, Computational Intelligence and Machine Learning, 2018, Jan. 2018.

[138] C. MEDINA, J. C. SEGURA, AND A. DE LA TORRE, *Ultrasound indoor positioning system based on a low-power wireless sensor network providing sub-centimeter accuracy*, Sensors, 13 (2013), pp. 3501–3526.

[139] E. MELLIOS, A. GOULIANOS, S. DUMANLI, G. HILTON, R. PIECHOCKI, AND I. CRADDOCK, *Off-body Channel Measurements at 2.4 GHz and 868 MHz in an Indoor Environment*, ICST, 2014.

[140] R. MENDRZIK, H. WYMEERSCH, AND G. BAUCH, *Joint localization and mapping through millimeter wave mimo in 5g systems*, in 2018 IEEE Global Communications Conference (GLOBECOM), IEEE, 2018, pp. 1–6.

[141] P. MIROWSKI, T. K. HO, S. YI, AND M. MACDONALD, *Signalslam: Simultaneous localization and mapping with mixed wifi, bluetooth, lte and magnetic signals*, in Indoor Positioning and Indoor Navigation (IPIN), 2013 International Conference on, IEEE, 2013, pp. 1–10.

[142] P. MIROWSKI, H. STECK, P. WHITING, R. PALANIAPPAN, M. MACDONALD, AND T. HO, *Kl-divergence kernel regression for non-gaussian fingerprint based localization*, in IPIN 2011, United States, 2011, IEEE, pp. 1–10.

[143] P. MIROWSKI, P. WHITING, H. STECK, R. PALANIAPPAN, M. MACDONALD, D. HARTMANN, AND T. K. HO, *Probability kernel regression for wifi localisation*, Journal of Location Based Services, 6 (2012), pp. 81–100.

[144] R. MIYAGUSUKU, A. YAMASHITA, AND H. ASAMA, *Data information fusion from multiple access points for wifi-based self-localization*, IEEE Robotics and Automation Letters, 4 (2019), pp. 269–276.

[145] M. MONTEMERLO, S. THRUN, AND W. WHITTAKER, *Conditional particle filters for simultaneous mobile robot localization and people-tracking*, in Robotics and Automation, 2002. Proceedings. ICRA'02. IEEE International Conference on, vol. 1, IEEE, 2002, pp. 695–701.

[146] N. MOSTOFI, M. ELHABIBY, AND N. EL-SHEIMY, *Indoor localization and mapping using camera and inertial measurement unit (imu)*, in Position, Location and Navigation Symposium-PLANS 2014, 2014 IEEE/ION, IEEE, 2014, pp. 1329–1335.

[147] R. MUÑOZ-SALINAS, M. J. MARÍN-JIMENEZ, AND R. MEDINA-CARNICER, *Spm-slam: Simultaneous localization and mapping with squared planar markers*, Pattern Recognition, 86 (2019), pp. 156–171.

[148] H. MURAKAMI, M. NAKAMURA, S. YAMASAKI, H. HASHIZUME, AND M. SUGIMOTO, *Smartphone Localization Using Active-Passive Acoustic Sensing*, in 2018 (IPIN), Sept. 2018, pp. 206–212.

[149] D. NAVARRO AND G. BENET, *Magnetic map building for mobile robot localization purpose*, in Emerging Technologies & Factory Automation, 2009. ETFA 2009. IEEE Conference on, IEEE, 2009, pp. 1–4.

[150] Y. NI, J. LIU, S. LIU, AND Y. BAI, *An Indoor Pedestrian Positioning Method Using HMM with a Fuzzy Pattern Recognition Algorithm in a WLAN Fingerprint System*, Sensors (Basel, Switzerland), 16 (2016).

[151] K. NIRMAL, A. SREEJITH, J. MATHEW, M. SARPOTDAR, A. SURESH, A. PRAKASH, M. SAFONOVA, AND J. MURTHY, *Noise modeling and analysis of an imu-based attitude sensor: improvement of performance by filtering and sensor fusion*, in Advances in Optical and Mechanical Technologies for Telescopes and Instrumentation II, vol. 9912, International Society for Optics and Photonics, 2016, p. 99126W.

[152] NVIDIA, *NVIDIA Jetson TX1 System-On-Chip*, 10 2016.

[153] S. OGISO, K. MIZUTANI, N. WAKATSUKI, AND T. EBIHARA, *Robust Localization of Mobile Robot in Reverberant Rooms Using Acoustic Beacons with Iterative Bayesian Filtering*, in 2018 (IPIN), Sept. 2018, pp. 1–6.

[154] D. O. OLGUIN, P. A. GLOOR, AND A. PENTLAND, *Wearable sensors for pervasive healthcare management*, in Pervasive Computing Technologies for Healthcare, 2009. PervasiveHealth 2009. 3rd International Conference on, IEEE, 2009, pp. 1–4.

[155] J. PANSIOT, D. STOYANOV, D. MCILWRAITH, B. P. LO, AND G.-Z. YANG, *Ambient and wearable sensor fusion for activity recognition in healthcare monitoring systems*, in 4th international workshop on wearable and implantable body sensor networks (BSN 2007), Springer, 2007, pp. 208–212.

[156] J. A. PAREDES, F. J. ÁLVAREZ, T. AGUILERA, AND J. M. VILLADANGOS, *3d Indoor Positioning of UAVs with Spread Spectrum Ultrasound and Time-of-Flight Cameras*, Sensors, 18 (2018), p. 89.

[157] A. K. PAUL AND T. SATO, *Localization in Wireless Sensor Networks: A Survey on Algorithms, Measurement Techniques, Applications and Challenges*, Journal of Sensor and Actuator Networks, 6 (2017), p. 24.

[158] C.-C. PENG, Y.-T. WANG, AND C.-L. CHEN, *Lidar based scan matching for indoor localization*, in System Integration (SII), 2017 IEEE/SICE International Symposium on, IEEE, 2017, pp. 139–144.

[159] H. PENG, F. LONG, AND C. DING, *Feature selection based on mutual information criteria of max-dependency, max-relevance, and min-redundancy*, IEEE Transactions on Pattern Analysis and Machine Intelligence, 27 (2005), pp. 1226–1238.

[160] J. POPE, R. MCCONVILLE, M. KOZLOWSKI, X. FAFOUTIS, R. SANTOS-RODRIGUEZ, R. PIECHOCKI, AND I. CRADDOCK, *SPHERE in a Box: Practical and Scalable EurValve Activity Monitoring Smart Home Kit*, Oct. 2017.

[161] J. POPE, R. MCCONVILLE, M. KOZLOWSKI, X. FAFOUTIS, R. SANTOS-RODRIGUEZ, R. J. PIECHOCKI, AND I. CRADDOCK, *Sphere in a box: Practical and scalable eurvalve activity monitoring smart home kit*, in (LCN Workshops), 2017 IEEE 42nd Conference on, IEEE, 2017, pp. 128–135.

[162] A. POPLETEEV, *Ambiloc: A year-long dataset of fm, tv and gsm fingerprints for ambient indoor localization*, in 8th International Conference on Indoor Positioning and Indoor Navigation (IPIN-2017), 2017.

[163] R. POSSAS, S. PINTO CACERES, AND F. RAMOS, *Egocentric activity recognition on a budget*, in Proceedings of the IEEE Conference on Computer Vision and Pattern Recognition, 2018, pp. 5967–5976.

[164] S. J. PREECE, J. Y. GOULERMAS, L. P. J. KENNEY, AND D. HOWARD, *A Comparison of Feature Extraction Methods for the Classification of Dynamic Activities From Accelerometer Data*, IEEE Transactions on Biomedical Engineering, 56 (2009), pp. 871–879.

[165] N. B. PRIYANTHA, A. CHAKRABORTY, AND H. BALAKRISHNAN, *The cricket location-support system*, in Proceedings of the 6th annual international conference on Mobile computing and networking, ACM, 2000, pp. 32–43.

[166] N. B. PRIYANTHA, A. K. MIU, H. BALAKRISHNAN, AND S. TELLER, *The cricket compass for context-aware mobile applications*, in Proceedings of the 7th annual international conference on Mobile computing and networking, ACM, 2001, pp. 1–14.

[167] J. QI AND G.-P. LIU, *A Robust High-Accuracy Ultrasound Indoor Positioning System Based on a Wireless Sensor Network*, Sensors, 17 (2017), p. 2554.

[168] K. QIU, F. ZHANG, AND M. LIU, *Visible light communication-based indoor localization using gaussian process*, in Intelligent Robots and Systems (IROS), 2015 IEEE/RSJ International Conference on, IEEE, 2015, pp. 3125–3130.

[169] L. RABINER AND B. JUANG, *Fundamentals of speech recognition*, PTR Prentice Hall, Apr. 1993.

[170] K. K. RACHURI, M. MUSOLESI, AND C. MASCOLO, *Energy-accuracy trade-offs in querying sensor data for continuous sensing mobile systems*, in Proc. of Mobile Context-Awareness Workshop, vol. 10, 2010.

[171] J. RACKO, P. BRIDA, A. PERTTULA, J. PARVIAINEN, AND J. COLLIN, *Pedestrian dead reckoning with particle filter for handheld smartphone*, in Indoor Positioning and Indoor Navigation (IPIN), 2016, IEEE, 2016, pp. 1–7.

[172] S. RAJAGOPAL, R. D. ROBERTS, AND S.-K. LIM, *Ieee 802.15. 7 visible light communication: modulation schemes and dimming support*, IEEE Communications Magazine, 50 (2012).

[173] P. RAO, X. WANG, AND A. THEUWISSEN, *Ccd structures implemented in standard 0.18 μm cmos technology*, Electronics Letters, 44 (2008), pp. 548–549.

[174] T. S. RAPPAPORT ET AL., *Wireless communications: principles and practice*, vol. 2, prentice hall PTR New Jersey, 1996.

[175] N. RAVI, N. DANDEKAR, P. MYSORE, AND M. L. LITTMAN, *Activity Recognition from Accelerometer Data.*, in ResearchGate, vol. 3, Jan. 2005, pp. 1541–1546.

[176] I. REKLEITIS, G. DUDEK, AND E. MILIOS, *Experiments in free-space triangulation using cooperative localization*, in Intelligent Robots and Systems, 2003.(IROS 2003). Proceedings. 2003 IEEE/RSJ International Conference on, vol. 2, IEEE, 2003, pp. 1777–1782.

[177] P. RICHTER, M. VALKAMA, AND E. S. LOHAN, *Attack tolerance of rss-based fingerprinting*, in Wireless Communications and Networking Conference (WCNC), 2018 IEEE, IEEE, 2018, pp. 1–6.

[178] M. RÁTOSI AND G. SIMON, *Real-Time Localization and Tracking Using Visible Light Communication*, in 2018 (IPIN), Sept. 2018, pp. 1–8.

[179] P. P. SALIAN, S. PRABHU, P. AMIN, S. K. NAIK, AND M. PARASHURAM, *Visible light communication*, in 2013 Texas Instruments India Educators, IEEE, 2013, pp. 379–383.

[180] G. SAMMARTANO AND A. SPANÒ, *Point clouds by slam-based mobile mapping systems: accuracy and geometric content validation in multisensor survey and stand-alone acquisition*, Applied Geomatics, 10 (2018), pp. 317–339.

[181] R. SANTOS-RODRIGUEZ AND N. TWOMEY, *Efficient approximate representations of computationally expensive features*, in European Symposium on Artificial Neural Networks (ESANN), 2018, 1 2018.

[182] B. SCHMITZ, A. GYÖRKÖS, AND T. ERTL, *Combination of map-supported particle filters with activity recognition for blind navigation*, in International Conference on Computers for Handicapped Persons, Springer, 2012, pp. 529–535.

[183] W. SEO AND K.-R. BAEK, *Indoor Dead Reckoning Localization Using Ultrasonic Anemometer with IMU*, 2017.

[184] D. K. SHAEFFER, *Mems inertial sensors: A tutorial overview*, IEEE Communications Magazine, 51 (2013), pp. 100–109.

[185] A. SHAHMANSOORI, G. E. GARCIA, G. DESTINO, G. SECO-GRANADOS, AND H. WYMEERSCH, *5g position and orientation estimation through millimeter wave mimo*, in 2015 IEEE Globecom Workshops (GC Wkshps), IEEE, 2015, pp. 1–6.

[186] SHANGHAI SLAMTEC.CO. LTD, *RPLIDAR A1, Low Cost 360 Degree Laser Range Scanner*, 07 2016.

[187] Y. SHI, W. ZHANG, Z. YAO, M. LI, Z. LIANG, Z. CAO, H. ZHANG, AND Q. HUANG, *Design of a hybrid indoor location system based on multi-sensor fusion for robot navigation*, Sensors, 18 (2018), p. 3581.

[188] G. SIMON, G. ZACHÁR, AND G. VAKULYA, *Lookup: Robust and accurate indoor localization using visible light communication*, IEEE Transactions on Instrumentation and Measurement, 66 (2017), pp. 2337–2348.

[189] SLAMTEC, *RPLIDAR A1 Low Cost 360 Degree Laser Range Scanner Introduction and Datasheet*, May 2016.

[190] C. SMAILI, M. E. EL NAJJAR, AND F. CHARPILLET, *Multi-sensor fusion method using dynamic bayesian network for precise vehicle localization and road matching*, in Tools with Artificial Intelligence, 2007. ICTAI 2007. 19th IEEE International Conference on, vol. 1, IEEE, 2007, pp. 146–151.

[191] S. SONG AND J. XIAO, *Tracking revisited using rgbd camera: Unified benchmark and baselines*, in Proceedings of the IEEE international conference on computer vision, 2013, pp. 233–240.

[192] N. STROZZI, F. PARISI, AND G. FERRARI, *A Novel Step Detection and Step Length Estimation Algorithm for Hand-held Smartphones*, in 2018 (IPIN), Sept. 2018, pp. 1–7.

[193] J. STURM, N. ENGELHARD, F. ENDRES, W. BURGARD, AND D. CREMERS, *A benchmark for the evaluation of rgb-d slam systems*, in Intelligent Robots and Systems (IROS), 2012 IEEE/RSJ International Conference on, IEEE, 2012, pp. 573–580.

[194] K. P. SUBBU, B. GOZICK, AND R. DANTU, *Locateme: Magnetic-fields-based indoor localization using smartphones*, ACM Transactions on Intelligent Systems and Technology (TIST), 4 (2013), p. 73.

[195] M. SUGANO, *Indoor localization system using rssi measurement of wireless sensor network based on zigbee standard*, in Wireless and Optical Communications, IASTED/ACTA Press, 2006, pp. 1–6.

[196] W. SUN, M. XUE, H. YU, H. TANG, AND A. LIN, *Augmentation of fingerprints for indoor wifi localization based on gaussian process regression*, IEEE Transactions on Vehicular Technology, 67 (2018), pp. 10896–10905.

[197] X. SUN, Y. XIE, P. LUO, AND L. WANG, *A dataset for benchmarking image-based localization*, in Proc. CVPR, vol. 1, 2017, p. 3.

[198] K. SUNG, D. K. LEE, AND H. KIM, *Indoor pedestrian localization using ibeacon and improved kalman filter*, Sensors, 18 (2018), p. 1722.

[199] R. SUTTON, *Reinforcement Learning: An Introduction*, MIT Press, Cambridge, Mass, second edition edition ed., May 1998.

[200] B. TAN, Q. CHEN, K. CHETTY, K. WOODBRIDGE, W. LI, AND R. PIECHOCKI, *Exploiting wifi channel state information for residential healthcare informatics*, IEEE Communications Magazine, 56 (2018), pp. 130–137.

[201] H. TANG, M. HASEGAWA-JOHNSON, AND T. S. HUANG, *Toward robust learning of the Gaussian mixture state emission densities for hidden Markov models*, in 2010 IEEE International Conference on Acoustics, Speech and Signal Processing, Mar. 2010, pp. 5242–5245.

[202] S. THRUN, W. BURGARD, AND D. FOX, *Probabilistic Robotics (Intelligent Robotics and Autonomous Agents)*, The MIT Press, 2005.

[203] J. TORRES-SOSPEDRA, R. MONTOLIU, A. MARTÍNEZ-USÓ, J. P. AVARIENTO, T. J. ARNAU, M. BENEDITO-BORDONAU, AND J. HUERTA, *Ujiindoorloc: A new multi-building and multi-floor database for wlan fingerprint-based indoor localization problems*, in (IPIN), 2014, IEEE, 2014, pp. 261–270.

[204] N. TWOMEY, T. DIETHE, M. KULL, H. SONG, M. CAMPLANI, S. HANNUNA, X. FAFOUTIS, N. ZHU, P. WOZNOWSKI, P. FLACH, AND I. CRADDOCK, *The SPHERE Challenge: Activity Recognition with Multimodal Sensor Data*, (2016). arXiv: 1603.00797.

[205] J. W. VAN DAM, B. J. KRÖSE, AND F. C. GROEN, *Neural network applications in sensor fusion for an autonomous mobile robot*, in Reasoning with uncertainty in Robotics, Springer, 1996, pp. 263–278.

[206] T. VAN HAUTE, E. DE POORTER, P. CROMBEZ, F. LEMIC, V. HANDZISKI, N. WIRSTRÖM, A. WOLISZ, T. VOIGT, AND I. MOERMAN, *Performance analysis of multiple Indoor Positioning Systems in a healthcare environment*, International Journal of Health Geographics, 15 (2016), p. 7.

[207] D. VAN OPDENBOSCH, G. SCHROTH, R. HUITL, S. HILSENBECK, A. GARCEA, AND E. STEINBACH, *Camera-based indoor positioning using scalable streaming*

of compressed binary image signatures, in Image Processing (ICIP), 2014 IEEE International Conference on, IEEE, 2014, pp. 2804–2808.

[208] L. VARGAS-MELÉNDEZ, B. L. BOADA, M. J. L. BOADA, A. GAUCHÍA, AND V. DÍAZ, *A sensor fusion method based on an integrated neural network and kalman filter for vehicle roll angle estimation*, Sensors, 16 (2016), p. 1400.

[209] L. VARGAS-MELENDEZ, B. L. BOADA, M. J. L. BOADA, A. GAUCHIA, AND V. DIAZ, *Sensor fusion based on an integrated neural network and probability density function (pdf) dual kalman filter for on-line estimation of vehicle parameters and states*, Sensors, 17 (2017), p. 987.

[210] U. VARSHNEY, *Pervasive healthcare and wireless health monitoring*, Mobile Networks and Applications, 12 (2007), pp. 113–127.

[211] R. T. VIEIRA, L. CAIXETA, S. MACHADO, A. C. SILVA, A. E. NARDI, O. ARIAS-CARRIÓN, AND M. G. CARTA, *Epidemiology of early-onset dementia: a review of the literature*, Clinical practice and epidemiology in mental health: CP & EMH, 9 (2013), p. 88.

[212] D. VIVET, P. CHECCHIN, AND R. CHAPUIS, *Line-based SLAM with slow rotating range sensors: Results and evaluations*, in 2010 11th International Conference on Control Automation Robotics Vision (ICARCV), Dec. 2010, pp. 423–430.

[213] B. WANG, X. LIU, B. YU, R. JIA, AND X. GAN, *Pedestrian dead reckoning based on motion mode recognition using a smartphone*, Sensors, 18 (2018), p. 1811.

[214] H. WANG, S. SEN, A. ELGOHARY, M. FARID, M. YOUSSEF, AND R. R. CHOUDHURY, *No need to war-drive: Unsupervised indoor localization*, in Proceedings of the 10th international conference on Mobile systems, applications, and services, ACM, 2012, pp. 197–210.

[215] Q. WANG, H. LUO, A. MEN, F. ZHAO, X. GAO, J. WEI, Y. ZHANG, AND Y. HUANG, *Light positioning: A high-accuracy visible light indoor positioning system based on attitude identification and propagation model*, International Journal of Distributed Sensor Networks, 14 (2018), p. 1550147718758263.

[216] Q. WANG, H. LUO, A. MEN, F. ZHAO, AND Y. HUANG, *An infrastructure-free indoor localization algorithm for smartphones*, Sensors, 18 (2018), p. 3317.

[217] R. WANG, B. SHEN, AND Y. LIU, *Optimization of sensor deployment for localization accuracy improvement*, in 2016 IEEE International Conference on Consumer Electronics-China (ICCE-China), Dec. 2016, pp. 1–4.

[218] X. WANG, L. GAO, S. MAO, AND S. PANDEY, *Csi-based fingerprinting for indoor localization: A deep learning approach*, IEEE Transactions on Vehicular Technology, 66 (2017), pp. 763–776.

[219] Y.-T. WANG, C.-C. PENG, A. A. RAVANKAR, AND A. RAVANKAR, *A single lidar-based feature fusion indoor localization algorithm*, Sensors, 18 (2018), p. 1294.

[220] M. WERNER, M. KESSEL, AND C. MAROUANE, *Indoor positioning using smartphone camera*, in Indoor Positioning and Indoor Navigation (IPIN), 2011, IEEE, 2011, pp. 1–6.

[221] M. WIDMAIER, M. ARNOLD, S. DÖRNER, S. CAMMERER, AND S. T. BRINK, *Towards practical indoor positioning based on massive mimo systems*, arXiv preprint arXiv:1905.11858, (2019).

[222] S. WIELANDT AND L. D. STRYCKER, *Indoor Multipath Assisted Angle of Arrival Localization*, Sensors, 17 (2017), p. 2522.

[223] J. WILLIAMSON, Q. LIU, F. LU, W. MOHRMAN, K. LI, R. DICK, AND L. SHANG, *Data sensing and analysis: Challenges for wearables*, in IEEE ASP-DAC, 2015, pp. 136–141.

[224] O. J. WOODMAN, *An introduction to inertial navigation*, tech. rep., University of Cambridge, Computer Laboratory, 2007.

[225] P. WOZNOWSKI, A. BURROWS, T. DIETHE, X. FAFOUTIS, J. HALL, S. HANNUNA, M. CAMPLANI, N. TWOMEY, M. KOZLOWSKI, B. TAN, N. ZHU, A. ELSTS, A. VAFEAS, A. PAIEMENT, L. TAO, M. MIRMEHDI, T. BURGHARDT, D. DAMEN, P. FLACH, R. PIECHOCKI, I. CRADDOCK, AND G. OIKONOMOU, *SPHERE: A Sensor Platform for Healthcare in a Residential Environment*, in Designing, Developing, and Facilitating Smart Cities, V. Angelakis, E. Tragos, H. C. Pöhls, A. Kapovits, and A. Bassi, eds., Springer International Publishing, 2017, pp. 315–333.

[226] P. WOZNOWSKI, X. FAFOUTIS, T. SONG, S. HANNUNA, M. CAMPLANI, L. TAO, A. PAIEMENT, E. MELLIOS, M. HAGHIGHI, N. ZHU, G. HILTON, D. DAMEN,

T. BURGHARDT, M. MIRMEHDI, R. PIECHOCKI, D. KALESHI, AND I. CRADDOCK, *A multi-modal sensor infrastructure for healthcare in a residential environment*, in 2015 IEEE International Conference on Communication Workshop (ICCW), June 2015, pp. 271–277.

[227] C. WU, Z. YANG, Y. LIU, AND W. XI, *Will: Wireless indoor localization without site survey*, IEEE Transactions on Parallel and Distributed Systems, 24 (2013), pp. 839–848.

[228] M. WU, H. MA, M. FU, AND C. YANG, *Particle filter based simultaneous localization and mapping using landmarks with rplidar*, in International Conference on Intelligent Robotics and Applications, Springer, 2015, pp. 592–603.

[229] Z.-H. WU, Y. HAN, Y. CHEN, AND K. R. LIU, *A time-reversal paradigm for indoor positioning system*, IEEE Transactions on Vehicular Technology, 64 (2015), pp. 1331–1339.

[230] J. XIAO, Z. ZHOU, Y. YI, AND L. M. NI, *A Survey on Wireless Indoor Localization from the Device Perspective*, ACM Computing Surveys, 49 (2016), pp. 25:1–25:31.

[231] B. XING, Q. ZHU, F. PAN, AND X. FENG, *Marker-based multi-sensor fusion indoor localization system for micro air vehicles*, Sensors, 18 (2018), p. 1706.

[232] K. YAMAZAKI, K. KATO, K. ONO, H. SAEGUSA, K. TOKUNAGA, Y. IIDA, S. YAMAMOTO, K. ASHIHO, K. FUJIWARA, AND N. TAKAHASHI, *Analysis of magnetic disturbance due to buildings*, IEEE Transactions on Magnetics, 39 (2003), pp. 3226–3228.

[233] J. YANG, Y. LI, W. CHENG, Y. LIU, AND C. LIU, *EKF–GPR-Based Fingerprint Renovation for Subset-Based Indoor Localization with Adjusted Cosine Similarity*, Sensors, 18 (2018), p. 318.

[234] Z. YANG, Z. ZHOU, AND Y. LIU, *From rssi to csi: Indoor localization via channel response*, ACM Computing Surveys (CSUR), 46 (2013), p. 25.

[235] J. YIM, S. UDPA, L. UDPA, M. MINA, AND W. LORD, *Neural network approaches to data fusion*, in Review of Progress in Quantitative Nondestructive Evaluation, Springer, 1995, pp. 819–826.

[236] X. YIN, W. SHEN, J. SAMARABANDU, AND X. WANG, *Human activity detection based on multiple smart phone sensors and machine learning algorithms*, in 2015 IEEE 19th International Conference on Computer Supported Cooperative Work in Design (CSCWD), May 2015, pp. 582–587.

[237] S. YIU, M. DASHTI, H. CLAUSSEN, AND F. PEREZ-CRUZ, *Wireless RSSI fingerprinting localization*, Signal Processing, 131 (2017), pp. 235–244.

[238] P. K. YOON, S. ZIHAJEHZADEH, B.-S. KANG, AND E. J. PARK, *Adaptive kalman filter for indoor localization using bluetooth low energy and inertial measurement unit*, in Engineering in Medicine and Biology Society (EMBC), 2015 37th Annual International Conference of the IEEE, IEEE, 2015, pp. 825–828.

[239] F. ZAFARI, A. GKELIAS, AND K. LEUNG, *A Survey of Indoor Localization Systems and Technologies*, (2017).
arXiv: 1709.01015.

[240] S. ZHANG, A. V. ROWLANDS, P. MURRAY, AND T. L. HURST, *Physical Activity Classification Using the Genea Wrist-worn Accelerometer*, Medicine & Science in Sports & Exercise, 44 (2012), pp. 742–748.

[241] W. ZHANG, X. LI, D. WEI, X. JI, AND H. YUAN, *A foot-mounted PDR system based on IMU/EKF+HMM+ZUPT+ZARU+HDR+compass algorithm*, in 2017 (IPIN), Sept. 2017, pp. 1–5.

[242] B. ZHAO, X. GUAN, L. XIE, AND W. XIAO, *Sensor selection for received signal strength-based source localization in wireless sensor networks*, Journal of Control Theory and Applications, 9 (2011), pp. 51–57.

[243] Y. ZHAO, W. WONG, H. K. GARG, AND T. FENG, *Pedestrian Dead Reckoning with Turn-Based Correction*, in 2018 (IPIN), Sept. 2018, pp. 1–8.

[244] K. ZHENG, H. WANG, H. LI, W. XIANG, L. LEI, J. QIAO, AND X. S. SHEN, *Energy-Efficient Localization and Tracking of Mobile Devices in Wireless Sensor Networks*, IEEE Transactions on Vehicular Technology, 66 (2017), pp. 2714–2726.

[245] B. ZHOU, M. ELBADRY, R. GAO, AND F. YE, *Batmapper: acoustic sensing based indoor floor plan construction using smartphones*, in Proceedings of the 15th An-

nual International Conference on Mobile Systems, Applications, and Services, ACM, 2017, pp. 42–55.

[246] J. ZHOU, J. SHI, AND X. QU, *Landmark Placement for Wireless Localization in Rectangular-Shaped Industrial Facilities*, IEEE Transactions on Vehicular Technology, 59 (2010), pp. 3081–3090.

[247] J. V. ZIDEK, W. SUN, AND N. D. LE, *Designing and integrating composite networks for monitoring multivariate gaussian pollution fields*, Journal of the Royal Statistical Society: Series C (Applied Statistics), 49 (2000), pp. 63–79.

[248] Q. ZOU, W. XIA, Y. ZHU, J. ZHANG, B. HUANG, F. YAN, AND L. SHEN, *A vlc and imu integration indoor positioning algorithm with weighted unscented kalman filter*, in Computer and Communications (ICCC), 2017 3rd IEEE International Conference on, IEEE, 2017, pp. 887–891.